

CTI Journal

The Official Publication of the Cooling Technology Institute



www.cti.org - Log On

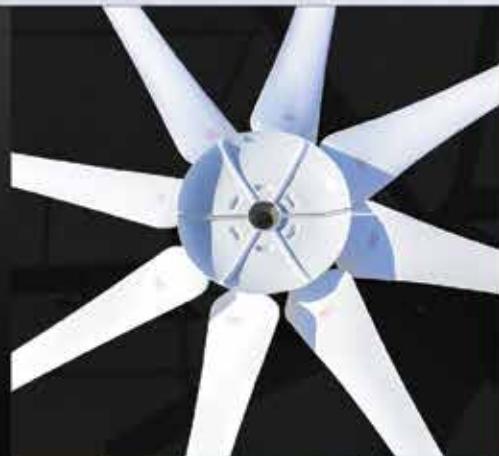
Winter 2018
Volume 39, No. 1

Tuf-Lite III
with Tuf-Edges
HUDSON
Products

ON THE LEADING EDGE OF AXIAL FAN DESIGN

Tuf-Lite III

- Hudson's one-piece FRP aerodynamic blade
- Most efficient blade in industry
- Highest quality and reliability
- Individually balanced and interchangeable
- Fatigue resistant vinyl-ester resin with Tuf-Edge® ceramic leading edge erosion protection
- Ultraviolet resistant
- Erosion and chemical resistant
- High temperature and static capabilities
- Sizes range from 6ft. to 33 ft. in diameter
- Manufactured in the United States
- Fastest delivery in market
- Unsurpassed customer service



**High Quality. Durable. Reliable. Efficient.
Continuous Innovation.**

HUDSON

MISSION STATEMENT

It is CTI's objective to: 1) Maintain and expand a broad base membership of individuals and organizations interested in Evaporative Heat Transfer Systems (EHTS), 2) Identify and address emerging and evolving issues concerning EHTS, 3) Encourage and support educational programs in various formats to enhance the capabilities and competence of the industry to realize the maximum benefit of EHTS, 4) Encourage and support cooperative research to improve EHTS Technology and efficiency for the long-term benefit of the environment, 5) Assure acceptable minimum quality levels and performance of EHTS and their components by establishing standard specifications, guidelines, and certification programs, 6) Establish standard testing and performance analysis systems and procedures for EHTS, 7) Communicate with and influence governmental entities regarding the environmentally responsible technologies, benefits, and issues associated with EHTS, and 8) Encourage and support forums and methods for exchanging technical information on EHTS.

LETTERS/MANUSCRIPTS

Letters to the editor and manuscripts for publication should be sent to: The Cooling Technology Institute, PO Box # 681807 Houston, TX 77268.

SUBSCRIPTIONS

The CTI Journal is published in January and June. Complimentary subscriptions mailed to individuals in the USA. Library subscriptions \$45/yr. Subscriptions mailed to individuals outside the USA are \$45/yr.

CHANGE OF ADDRESS

Request must be received at subscription office eight weeks before effective date. Send both old and new addresses for the change. You may fax your change to 281.537.1721 or email: vmanser@cti.org.

PUBLICATION DISCLAIMER

CTI has compiled this publication with care, but CTI has not Investigated, and CTI expressly disclaims any duty to investigate, any product, service process, procedure, design, or the like that may be described herein. The appearance of any technical data, editorial material, or advertisement in this publication does not constitute endorsement, warranty, or guarantee by CTI of any product, service process, procedure, design, or the like. CTI does not warranty that the information in this publication is free of errors, and CTI does not necessarily agree with any statement or opinion in this publication. The entire risk of the use of any information in this publication is assumed by the user. Copyright 2018 by the CTI Journal. All rights reserved.

Contents

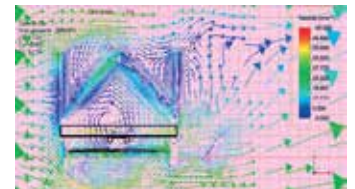


Feature Articles

- 8 Blade Dynamics**
Nicola Romano
- 16 Time and Temperature Dependent Deformation Behavior of PP Fills**
Nina Woicke, Daniel Dierenfeld
- 24 Simplifying Corrosion Control With A Safer Choice Inhibitor**
Eric C. Ward, Emily M. Crane and Gregory J. Koniges
- 34 Wet-Dry Technology to Abate the Visible Plume From An Existing Cooling Tower**
Mark Scholl, Jean-Pierre Libert and Darin Baugher
- 44 Modeling Scale Inhibitor Upper Limits: In Search of Synergy**
Robert J. Ferguson
- 52 Distribution – Distribution – Distribution**
James L. Willa
- 58 A Fresh Perspective on Controlling Yellow Metal Corrosion**
Jon Cohen, Jeff O'brien and Ray Post

Special Sections

- 27 CTI STD - 202 Custom Cooling Towers
- 62-63 CTI ToolKit
- 64-65 CTI Licensed Testing Agencies
- 66-71 CTI Certified Towers



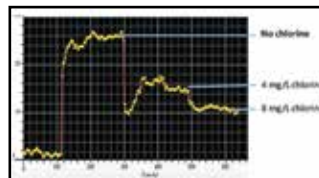
...see page 8

Departments

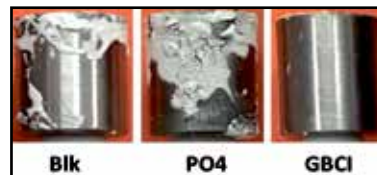
- 2 Multi Agency Press Release
- 2 Meeting Calendar
- 4 President Elect – 2018-2020
- 4 View From the Tower
- 6 Administrator's Corner



...see page 20



...see page 59



...see page 30



...see page 35

Journal Committee

Paul Lindahl, Editor-in-Chief
Virginia Manser, Managing Director/Advertising Manager
Donna Jones, Administrative Assistant
Andrew Manser, Administrative Assistant
Angie Montes, Administrative Assistant
Graphics by Sarita Graphics

Board of Directors

Bill Howard, President
Helen Cerra, President Elect
Brian Hanel, Vice President
Brandon Rees, Secretary
F.L. (Frank) Michell, Treasurer
Peter G. Elliott, Director
Narendra Gosain, Director
Thomas Kline, Director Elect
Chris Lazenby, Director Elect
Jean-Pierre Libert, Director
Kent Martens, Director
Frank Morrison, Director Elect
Janet Stout, Director
Helene Troncin, Director

Address all communications to:

Virginia A. Manser, CTI Administrator
Cooling Technology Institute
PO Box #681807
Houston, Texas 77268
281.583.4087
281.537.1721 (Fax)

Internet Address:

<http://www.cti.org>

E-mail:

vmanser@cti.org

For Immediate Release

Contact: Chairman, CTI Multi-Agency Testing Committee

**Houston, Texas
2-November-2017**

Cooling Technology Institute, PO Box 681807, Houston, Texas 77268 – The cooling Technology Institute announces its annual invitation for interested thermal testing agencies to apply for potential Licensing as CTI Thermal Testing Agencies. CTI provides an independent third party thermal testing program to service the industry. Interested agencies are required to declare their interest by March 1, 2018, at the CTI address listed..

Future Meeting Dates

Annual Conference

February 4-8, 2018
Hilton Houston North
Houston, TX

February 5-9, 2019
Sheraton New Orleans
New Orleans, LA

February 9-13, 2020
The Westin Galleria
Houston, TX

Committee Workshop

July 15-18, 2018
La Cantera
San Antonio, TX

July 7-10, 2019
The Peabody
Memphis, TN

TBA



RESEARCH COTTRELL COOLING, INC.

A subsidiary of Hamon Corporation



Doing Big Things

Contact us for your custom
engineered cooling solution.

Keith Silverman
908-333-2049
keith.silverman@rc-cooling.com

Jennifer Kellogg, *spare parts*
908-333-2004
jennifer.kellogg@rc-cooling.com



Post Office Box 1500, Somerville, NJ 08876
www.rc-cooling.com



Real experts, real results

Proven Treatment Technologies For:

Cooling Systems
Pretreatment
Boilers
Wastewater
Membranes & RO
Automation & Control

The Best People

Experienced service engineers who live in your community

Results That Last

Extending asset life while minimizing chemical and water usage

Continuous Innovation

Delivering customized products with a full-service analytical lab and R&D group

Environmental Protection & Safety

Protecting your people, your brand, and the environment with our innovative solutions

Phone number: 804-935-2000
Website: www.chemtreat.com



View From The Tower

All good things must come to an end ~ I have very much enjoyed being the President for the past two years at CTI and it has certainly been an honor and privilege serving as your CTI President. I cannot fathom how we used to have Presidential terms for only one year, there is so much to learn in the first six to nine months and then three months later your term is complete? Two year terms began back in early 2000 and have been advantageous for the President, the Board of Directors (BOD) and especially the CTI staff ever since! It allows for more continuity and success in the endeavor for all concerned. The CTI staff has done an exceptional job as CTI continues to grow both domestically as well as internationally. The BOD that served under me deserves recognition as well, the extra time and effort by all these individuals should not go unnoticed. Beyond these individuals, there are many additional CTI members that are committed to advancing CTI into the coming years, my hat is off to the many dedicated experts within CTI that put in countless volunteer hours to better our organization!

The thermal certification program and STD-201 began back in the early 1960's and tower certification has been occurring since the early 1980's and has been one of the most recognized means of certifying package towers throughout the world. There are over 60 participating manufacturers in this program and it continues to grow! Mike Womack, the Thermal Certification Administrator took over this task from Tom Weast over the past several years and has done a fabulous job. This program is recognized throughout the world as the leading certification program for package towers.



Material/Products Certification is building momentum now as well and CTI anticipates the same great success in this program that Thermal Certification has had. Denny Shea, Material/Product Certification Administrator is heading up this program. Materials that meet specific criteria called out in specifications, and having CTI material certification called out within these specifications, will ensure that owner operators will get exactly what they specify. Having CTI certification will help to protect this as well since additional testing and protocol will be required to be met prior to obtaining this CTI certification. This certification will also be monitored annually to verify the integrity and acceptance of the Material/ Product. Please help me to embrace this new CTI feature and look for good things in the near future regarding this Material/Product Certification!

It is a changing world we live in now and CTI continues to grow and address these changes. We now have the first female President taking the office of CTI!! It is with great pleasure that I will be relinquishing my Presidency to Helen Cerra of ChemTreat as she will be taking office in February 2018. Please welcome her and her BOD with open arms as CTI maintains its well established dominance in the Cooling Technology Industry! As always never forget to ask not what CTI can do for you, rather ask what you can do for CTI and by all means, join in, get involved, learn, educate others, participate and thrive!

Sincerely and respectfully,
Bill W. Howard, P.E.
CTI President

Cooling Technology Institute's 2018-2019 President Elect Helen Cerra

Helen is a Technical Staff Consultant with ChemTreat, Inc. located in Richmond, Virginia. She has over thirty years of professional experience in all aspects of water treatment, including boiler, cooling, waste treatment and environmental/regulatory affairs.

She has authored/co-authored papers for and made presentations at various trade organizations including, American Society of Heating, Refrigerating, and Air-Conditioning Engineers (ASHRAE), Cooling Technology Institute (CTI), Electric Utility Chemistry Workshop (EUCW), International Water Conference (IWC), Virginia Society of Healthcare Engineers (VSHE) and National Association of Corrosion Engineers (NACE).



With a concentration on *Legionella* minimization, Helen is Secretary of the ASHRAE Standing Standard Project Committee 188 as well as Chair of the ASHRAE Technical Committee 3.6, Water Treatment. In addition, she is active on the Water Treating and Program Committees with Cooling Technology Institute (CTI), having been a past member of their Board of Directors. She is currently Chair of GDL-159, the task group expanding CTI Guidelines for Control of *Legionella*. Helen holds a B.S. in Chemical Engineering from Lehigh University and is a member of American Institute of Chemical Engineers (AIChE) and ASHRAE.

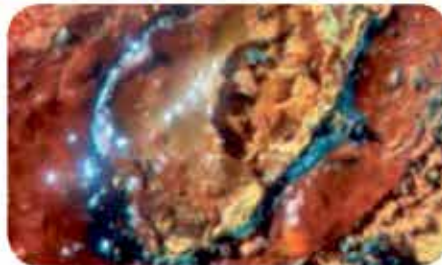


Do you see any of these issues in **cooling towers** at your **accounts**?

Cooling systems with inadequate biofouling control generally have problems with poor heat transfer efficiency, under-deposit corrosion, and *Legionella* bacteria control.



Biofilm on a heat exchanger tube sheet



Microbiologically Influenced Corrosion (MIC)



Scale embedded in biofilm on tower pack

Use **AMSA BCP™** chemistry with an oxidizing or non-oxidizing biocide to achieve clean industrial water cooling systems that run closer to design and require less down-time for maintenance.

How a Biofilm Control Program Works

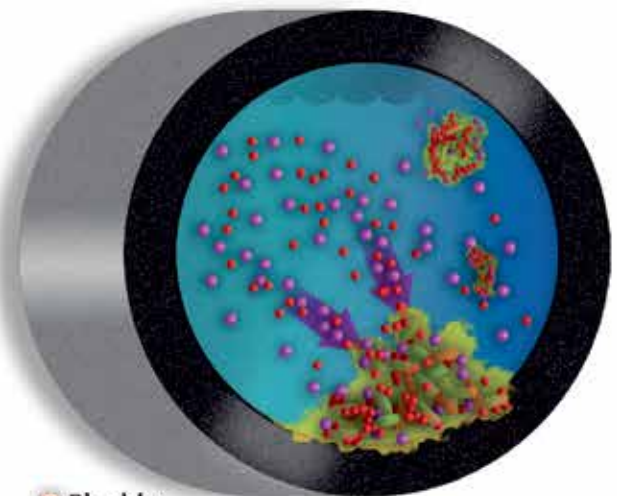
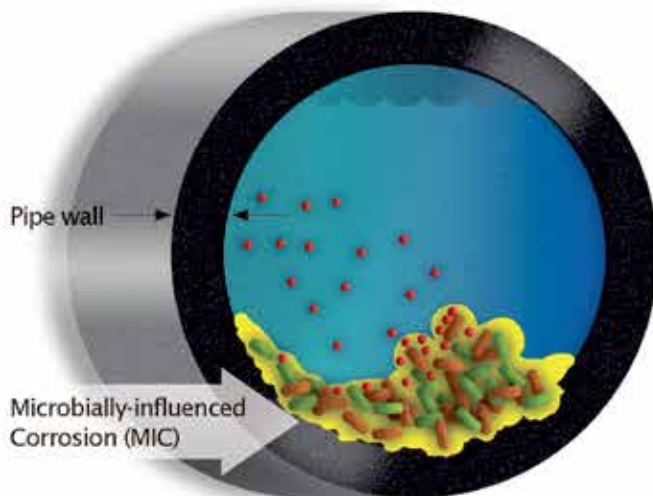
Without **BCP™** chemistry (DTEA II™)

- Oxidizing and non-oxidizing biocides have limited penetration into biofilm.
- The metal pipe wall shows evidence of MIC beneath biofouling deposits.

With **BCP™** chemistry (DTEA II™)

The penetration/dispersion/cleaning properties result in:

- Deeper penetration of biocides into biofilm allowing better bacteria kill
- Destabilized biofouling deposits removed from surfaces
- Cleaner surfaces with less MIC & better heat transfer



- Biocide
- AMSA BCP™ Chemistry

Copyright © 2016 by AMSA, Inc.



AMSA, Inc.™
4714 S. Garfield Rd. • Auburn, Michigan, USA • 48611
Tel: (989) 662-0377 Fax: (989) 662-6461
sales@amsainc.com
www.amsainc.com

Call Us Today! **888 739-0377**

Administrator's Corner

What is CTI's Mission Statement?

Our Mission



Vicky Manser
CTI Administrator

As a broad based industry association, our mission is to advocate and promote, for the benefit of the public, the use of all environmentally responsible cooling technologies. This includes wet cooling towers, air-cooled condensers, dry coolers, indirect cooling, and hybrid systems. We accomplish encouraging:

- ◆ Education on these technologies
- ◆ Development of codes, standards, and guidelines
- ◆ Development, use, and oversight of independent performance verification and certification programs
- ◆ Research to improve these technologies
- ◆ Advocacy and dialog on the benefits of cooling technologies with Government Agencies and other organizations with shared interests
- ◆ Technical information exchange

Help CTI help you!!!!!!

The best sheaves for the worst environments!

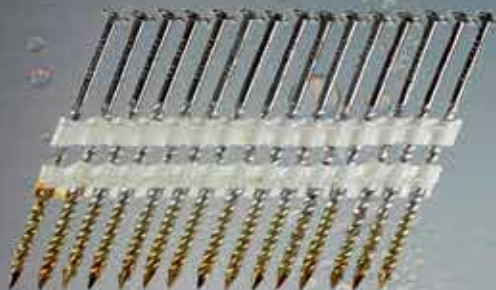
Ideally suited for the most aggressive atmospheres, unusual conditions, such as weight requirements and installation problems, Bailsco lightweight all-aluminum cast V-belt sheaves have been in the field for over 20 years.

Full range of sizes available up to 38" diameter, larger sizes available upon request. Special designs to meet OEM requirements.

Design, 3D scanning, molding, casting, machining, heat treating, and balancing are all done "in-house".

BAILSCO
POWER TRANSMISSION PRODUCTS

BAILSCO BLADES AND CASTINGS, INC.
Box 6093, Shreveport, LA 71136-6093 U.S.A.
Phone 318.861.2137 FAX 318.861.2953
www.bailsco.com
email: bailsco@bailsco.com



**20° - 22° Plastic Strip
Full Round Head, Screw-Shank Nails**
Type 304 and 316 stainless steel



Truss-Head Screws
Type 305 stainless steel



Self-Drilling Hex-Washer Head Screw
Type 305 and 316 stainless steel
with EPDM sealing washer

Your stainless-steel fastener source.



Common Annular-Ring-Shank Nails
Type 304 and 316 stainless steel



Spiral-Shank Nails
Type 304 and 316 stainless steel
with EPDM sealing washer



Self-Drilling Hex-Washer Head Screws
Type 305 and 316 stainless steel



Ring-Shank Nails
Type 304 and 316 stainless steel
with EPDM sealing washer



Common Spiral-Shank Nails
Type 304 stainless steel



Bugle-Head Wood Screws
Type 305 and 316 stainless steel



Hog Rings
Type 304 stainless steel



Fencing Staples
Type 304 stainless steel



EPDM Sealing Washers
Type 304 and 316 stainless steel



Simpson Strong-Tie is your source for fasteners for building and repairing cooling towers. Our wide selection of stainless-steel bulk and collated nails, screw/nail washer assemblies, and self-drilling screws are easy to install and provide superior results in wood, fiberglass and corrosive environments. Fasteners are available in 304, 305 and 316 stainless steel.

To learn more about the entire line of Simpson Strong-Tie® fasteners for cooling tower construction and repair, visit strongtie.com/fasten or call (800) 999-5099.



Blade Dynamics

Nicola Romano, COFIMCO Srl

Introduction

Scope of this paper is to study how the mechanical and aerodynamic properties of the blades affect the vibration transmitted to the hub by the blades itself and, consequently, to the structure.

Vibration is the consequence of variable loads acting on the blades and of their response: the root connection to the hub transfers the blade dynamic behavior to it and, consequently, to the supporting structure causing vibration. The variable loads are of aerodynamic nature. The other main loads, blade weight and centrifugal force, are steady.

This paper will focus on the blade's response. Investigating on the supporting structure's behavior is not in the scope of this study.

The main parameters that determinate the blade's response are:

- Blade's stiffness and mass distribution
- Blade's aerodynamic features
- Mechanical and aerodynamic dissipation
- Load's shape, amplitude and frequency

The above parameters combine among them resulting in the following quantities, all influencing the blade's dynamic behavior:

- Ratio Pulse Duration to Blade Natural Period
- Blade's deflection and Centrifugal Force
- Aerodynamic Damping
- Mechanical Damping

The mentioned elements will be studied separately.

References

- HARRIS' SHOCK AND VIBRATION HANDBOOK, 5th EDITION, Chapter 8.11
- CTI 2015 Paper n. TP15-17

Loads

Extensive CFD simulations have been carried out in order to evaluate the loads acting on the blades, both with calm environmental conditions (Wind Speed WS=0) and with high wind. Those simulations were focused on different blades' sizes and count. In particular, 3 different blades are shown in this study, with the following features, see Fig. 2.1:

	Blade A	Blade B	Blade C
Chord at root	890 mm - 2.9 ft	500 mm - 1.64 ft	500 mm - 1.64 ft
Chord at tip	730 mm - 2.4 ft	448 mm - 1.47 ft	448 mm - 1.47 ft
Blade mass	102.6 Kg - 226 lbs	89 Kg - 196 lbs	49.2 Kg - 108 lbs
Nominal Aerodynamic Load	2601 N - 585 lbs	1598 N - 359 lbs	1598 N - 359 lbs
Blade count	6	10	10
BOF (*), modes 1 & 2	6.9 Hz, 39.5 Hz	4.5 Hz, 15.7 Hz	2.8 Hz, 14.2 Hz
Main features	Heavy, stiff, high BOF (*)	Lighter than A, stiff, medium BOF (*)	Very light, low BOF (*)

Table 2.1

An important difference needs to be highlighted when considering loads arising from wind (or from the presence of other fans running nearby) and the ones coming from structural obstacles: the former is characterized by a relatively longer duration due to different flow areas; the latter has a relatively lower duration defined by the actual obstacle width and the fan's RPM.



Nicola Romano

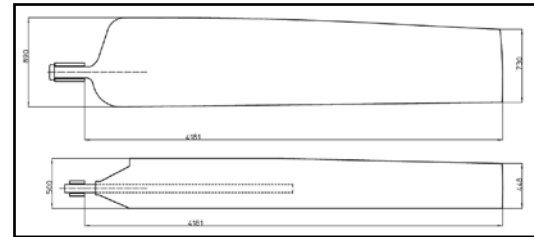


Fig. 2.1: Blades' dimensions
(*) BOF: Blade Operating Frequency

The aerodynamic load is time-dependent because of localized variations of the air flow encountered by the blade during its path. Those flow perturbations find their origin in two main reasons:

- Physical obstacles in the flow
- Flow asymmetry due to wind or other fans, see Fig. 2.2

The aerodynamic load is time-dependent because of localized variations of the air flow encountered by the blade during its path. Those flow perturbations find their origin in two main reasons:

- Physical obstacles in the flow
- Flow asymmetry due to wind or other fans, see Fig. 2.2

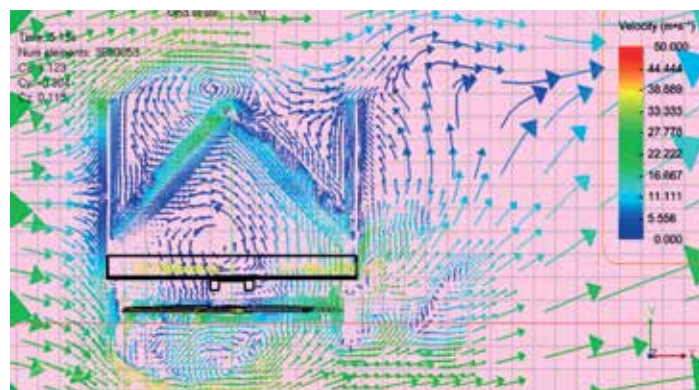


Fig. 2.2a: Flow from wind

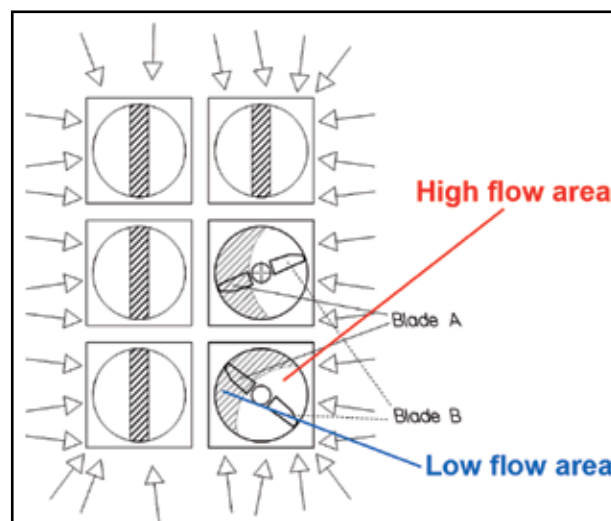


Fig. 2.2b: Flow from adjacent fans

An important difference needs to be highlighted when considering loads arising from wind (or from the presence of other fans running nearby) and the ones coming from structural obstacles: the former is characterized by a relatively longer duration due to different flow areas; the latter has a relatively lower duration defined by the actual obstacle width and the fan's RPM.

The two different load conditions are related to the different Angle of Coverage (AoC) of the low-flow and high-flow areas. The following figure 2.3 explains this aspect: generally, structural obstacles (beams, driving shafts, etc.) have an AoC quite narrower and independent from the working conditions or external factors.

On the contrary, flow asymmetries due to wind or other fans can be much wider and depend on wind speed, fan position in the bay, etc.

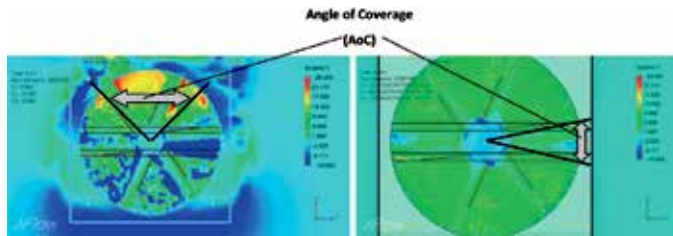


Fig.2.3a: Large flow asymmetry due to wind

Fig. 2.3b: Narrow flow perturbation

The result of such a difference can be seen in the load's time history acting on the blade, see fig. 2.4:

- Long, irregular pulses of high amplitude in the first case
- Short, regular pulses of lower amplitude in the second case.

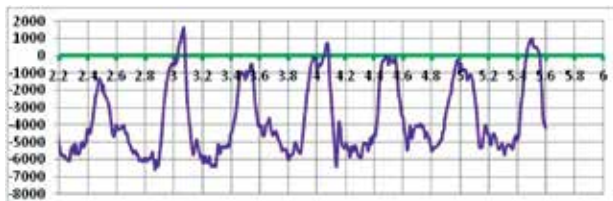


Fig. 2.4a: Load from high speed wind (Blade A)

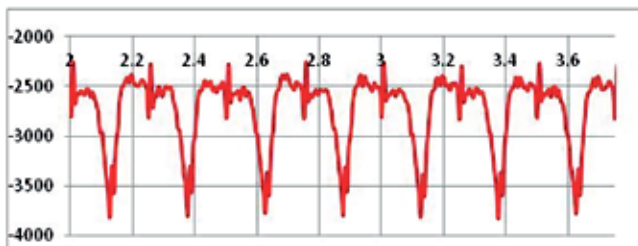


Fig. 2.4b: Load from ACC bridge (Blade A)

The most proper way of studying blade's dynamic is by means of modal analysis. Usually, the first 2 modes (fig. 2.5) are enough for a good response accuracy.

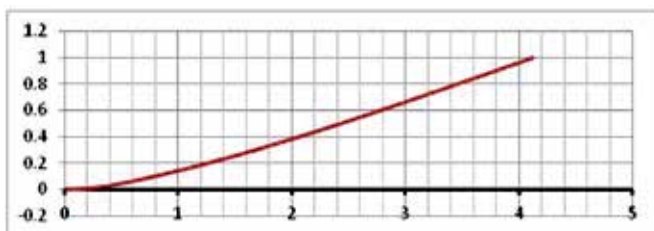


Fig. 2.5a: First mode's shape

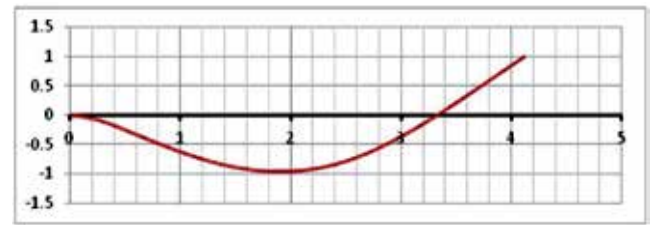


Fig. 2.5b: Second mode's shape

The said approach would allow the evaluation of the blade's response to any time-dependant load, see fig. 2.6, but wouldn't be very helpful in understanding the influence of the several parameters on the blade's behavior. A simpler model will therefore be used.

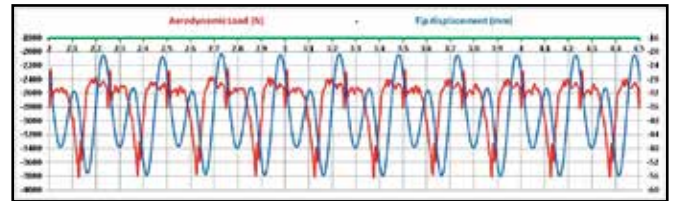


Fig. 2.6: Aerodynamic load and blade's response (tip displacement - time history)

Simplified Blade Model

In order to ease the understanding of the blade's dynamic, the three blades of table 2.1 are converted into three more simple spring-lumped mass systems (Fig. 3,1) hinged at the root. Each system has the same mass distribution as the blade it is simulating. A spring of proper stiffness K is added at the root in order to provide the system with the same Natural Frequency f_n of the related blade. Therefore, with the same natural period $T_n = 1 / f_n$.

The system is subjected to the following loads:

- an aerodynamic force $F_a(t) = \Sigma F_{ai}(t)$,
- its own weight $W = \Sigma W_i$,
- a centrifugal force $CF = \Sigma CF_i$ and
- an elastic action due to the connection to the hub $M_{el} = -K * (\theta - \theta_0)$.

All the above loads have a moment around the hinge. As long as all the forces are steady, the system lays in a static equilibrium where the resultant of the moment of all the loads around the hinge is zero. The elastic action is the one that gets transferred to the hub and can be measured by means of strain gages applied on the elastic component. In the following it will be referred to as Root Bending Moment (RBM).

For a fan blade, the forces W_i and CF_i are steady while the force $F_a(t)$ is time dependant. For the purpose of this study, it is of interest to evaluate the response of the blade to F_a variations. When the aerodynamic force changes, the system moves from its steady position. In this situation, from the above equations it can be seen that two main things happen:

1. the Root Bending Moment (RBM) changes according to the rule $RBM = -K * (\theta - \theta_0) \rightarrow \Delta RBM = -K * \Delta \theta$
2. the moment of the Centrifugal Force (MCF) changes as well according to the rule $MCF = -\Sigma F_{ci} * Z_i * \sin \theta \rightarrow \Delta MCF = -\Sigma F_{ci} * Z_i * \Delta(\sin \theta)$

It is evident that the value of K defines how stiff or soft the blade is. Both RBM and MCF have a stabilizing effect, reacting to the change from the equilibrium position. The RBM variation is the main factor responsible for the vibration transmitted to the hub.

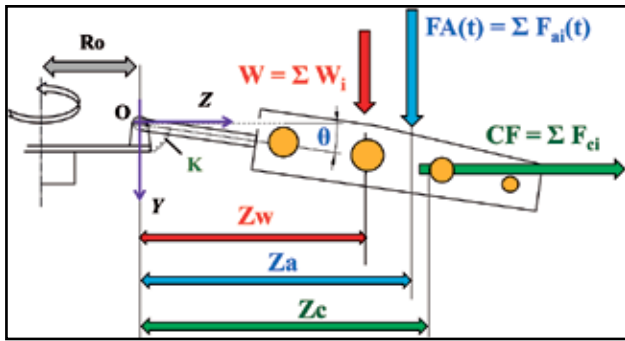


Fig. 3.1: Simplified Blade model and loads

Therefore, a simple way for reducing the vibration is to reduce the amount of stabilizing reaction due to the RBM and leaving most of the stabilizing job to the centrifugal force. This can be obtained reducing significantly the value of the stiffness (K) and allowing a relatively large displacement variation ($\Delta\theta$).

For a better understanding, the spring-mass system's response to two different dynamic load situations will be studied:

- single pulse
- periodic pulses

Single Pulse

The response of a linearly elastic system to a single pulse depends on:

- the amplitude of the load pulse,
- the pulse's shape and duration and
- the blade's frequency.

More precisely, on the ratio between the pulse's duration τ and the system's natural period

$$T_n = 1 / f_n$$

For the scope of this study, a rectangular step pulse will be considered, see fig. 4.1 and reference (a). Different pulse's shapes wouldn't change the result of a relevant amount for the purpose of this study.

It is a known fact that, see ref. (a), for an un-damped SDOF system, the spectrum of the maxima response to a step pulse is of the form shown in the following fig. 4.1 in terms of ratio Dynamic Response to Static Response (DR / SR). It can be seen that the higher the ratio Ψ of pulse duration (τ) to Blade Natural Period (T_n), the higher the maxima response.

The maxima response spectrum shows that, for a value of $\Psi > 0.5$, the system's maximum response is not affected by the ratio anymore while the Residual Response depends largely on it.

In order to evaluate the response of our simplified model, some damping is introduced (see chapter 6) and numerical integration of the dynamic equation is carried out.

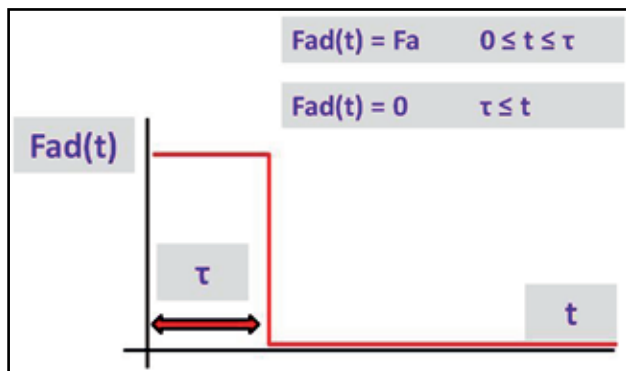


Fig. 4.1a: Rectangular step pulse

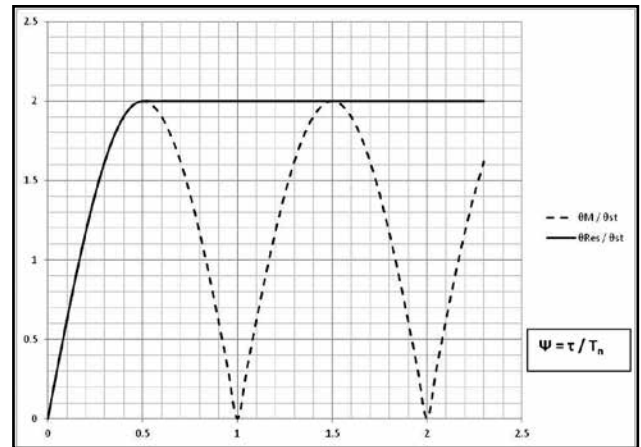


Fig. 4.1b: Maxima and Residual response spectrum of an un-damped SDOF system.

As a reference system, a 34 ft fan running at 100 RPM will be considered. Three different obstacle widths (defined by the "Angle of Coverage – AoC") will be taken in to account:

- Structural obstacle type 1 (10° AoC – CT driving shaft)
- Structural obstacle type 2 (30° AoC – ACC bridge)
- Low flow – High flow areas (90° AoC – High Wind)

Therefore, considering the fan's RPM, the pulse's durations will be, respectively:

$$\tau_1 = 0.017 \text{ s}; \quad \tau_2 = 0.05 \text{ s}; \quad \tau_3 = 0.15 \text{ s}.$$

The pulse's amplitude F_a has been chosen equal to 40% of the nominal aerodynamic load.

Numerical simulations lead to the system's response shown in Fig. 4.2 for the 3 blades under investigation in terms of

$$\text{RBM} = -K * (\theta - \theta_0)$$

It can be seen that the blades' response gets larger with larger AoC for all blades.

The response of Blade A is the largest, not only because of the higher nominal load acting on it compared with the one acting on the other blades (see Table 2.1), but mostly because of its ratio

$$\Psi = \tau / T_n$$

much closer (or above) to the value of 0.5 where the DR reaches its maximum value (see Fig. 4.1b).

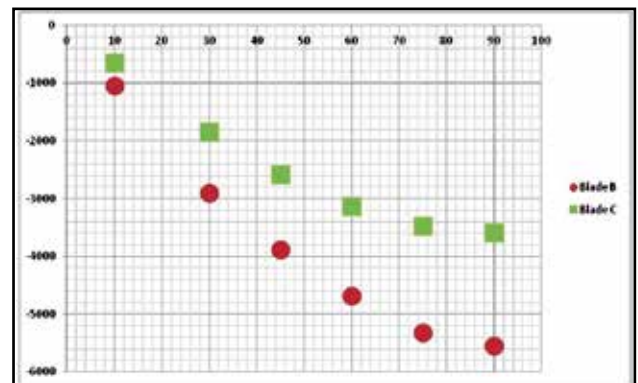


Fig. 4.2: Blades' response to single pulse (RBM – N*m)

AoC	10	30	90
▲	0.116	0.35	1.05
●	0.076	0.228	0.68
■	0.047	0.14	0.42

Table 4.1

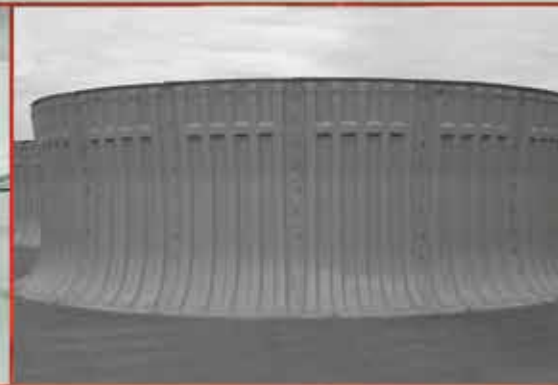
The Industry's Most Trusted Source in Components!

Dynamic Fabricators

We are known for providing dynamic solutions resulting in quality advantages and competitive pricing. Providing excellent customer service is our #1 priority. It's what keeps our customers coming back.

Your Complete Cooling Tower Supply Source with Locations in Wapato, WA & Elmore, AL.

- Header, Bypass, Riser and Lateral Distribution Syst.
- Fan Stacks, Fan Ring, Inlet Bells, FRP Basins.
- Fiberglass Pipe Saddles, Tanks, Access Hatches, Doors, Molded Stairs & Distribution Splash Boxes.



*Your dynamic partner
in cooling tower components...*



Dynamic Fabricators

Toll-Free 877.604.6525

www.dynafab.net • Email us at: sales@dynafab.net

The different values of the ratio Ψ are shown in the table above. It can be seen that only the Blades A and B have a ratio above 0.5. The time history responses for Blade A and Blade C are shown in Fig. 4.3.

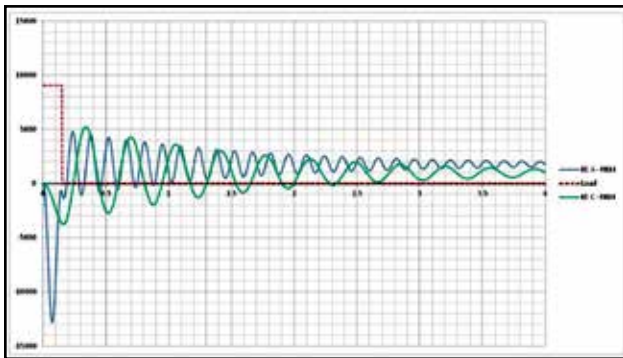


Fig. 4.3: Blades A & C response (RBM – N*m) for AoC = 90°

Cyclic Loads

Once the response to a single pulse is understood, the behavior of the system in case of cyclic (periodic) loads can be investigated. In fact, being the BOF higher than the pulses' frequency, the load can be considered as a sequence of single pulses. Therefore, for a fixed fan speed, pulses that, when applied singularly, cause the higher response, when applied cyclically cause the higher response as well. For this purpose, the same RPM is considered and the same 3 flow perturbations are considered with AoC of 10°, 30° and 90°.

With the same procedure used in chapter 4, numerical integrations were carried out. The results are shown in the following fig. 5.1 for the 3 blades.

It can be seen that Blade C has always a lower response compared to the stiffer ones. For all the AoCs investigated, Blade C's responses is much lower than Blade A's and in the range of 60% of Blade B's (see Fig. 5.1b).

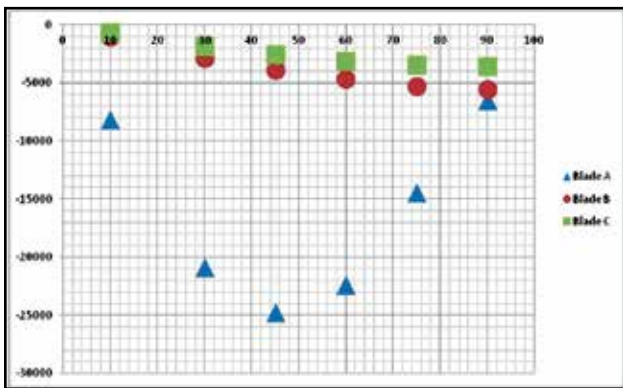


Fig. 5.1a: Blades max response (RBM fluctuation – N*m)

It is also confirmed that the Blade A has the highest response for an AoC close to 45° while the blades B and C have their highest for AoC = 90° as for the single pulse case.

A singularity can be noted at AoC = 90° for Blade A: despite a high maximum response to the single pulse according to the Fig. 4.2, its response to the cyclic load is low, similar to Blade B's. This is due to what is called “Residual Response” that gets to zero for $\Psi = \tau / T_n = 1$ (see Ref. a for further details.)

Load Transmission

In agreement with the action-reaction principle, the Root Bending Moment

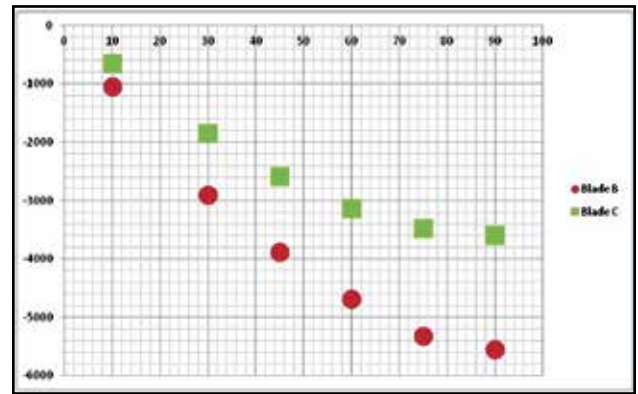


Fig. 5.1b: Detail of Fig. 5.1a - Comparison between Blade B and Blade C (RBM fluctuation – N*m)

$$RBM = -K * (\theta - \theta_0),$$

that the spring of the simplified model exerts on the blade, gets transmitted to the hub and, consequently, to the drive chain and supporting structure.

From the above consideration, it is obvious that the higher the RBM, the higher the load acting on the structure. In the same manner, the higher the RBM variation, the higher the load variation acting on the structure. As a result, higher vibration.

Going back to the actual blades, a similar situation can be seen: a structure subject to highly variable loads tends to respond with high displacement, meaning high vibrations.

While in the simplified model the spring at the hinge transfers the RBM to the hub, in the actual blade, clamped at the root, the stress close to the clamp gives a measure of the transferred RBM. A highly variable stress results in a highly variable RBM.

The below figure 6.1 sketches how the alternate stress measured at blade root, symptomatic of an alternate RBM, gets transferred to the hub and, consequently, to the drive chain and supporting structure. Rapid variations of the RBM results in “rocking” effect of the fan supporting structure, especially in its weakest direction. In an ACC, the “rocking” vibration in the horizontal direction perpendicular to the bridge is a common phenomenon.

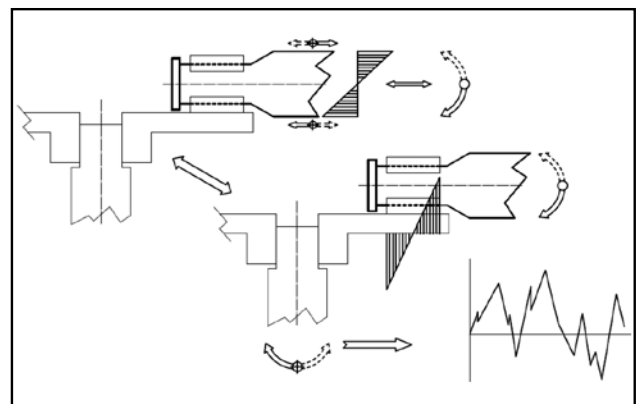


Fig. 6.1: RBM transmission to the drive chain and supporting structure

Damping

A significant help in reducing the vibration amplitude comes from damping, as well known from the technical literature, see Fig. 7.1.

Two kinds of damping have to be considered when dealing with fan blades: aerodynamic damping (AD) and mechanical damping (MD). AD is proportional to the fan speed, while the MD is more related to the mode's frequency. At high speed, the AD dominates, but at low speed the MD becomes important (i.e. with VFD driven fans).

Therefore, a device able to increase the damping would be of great help.

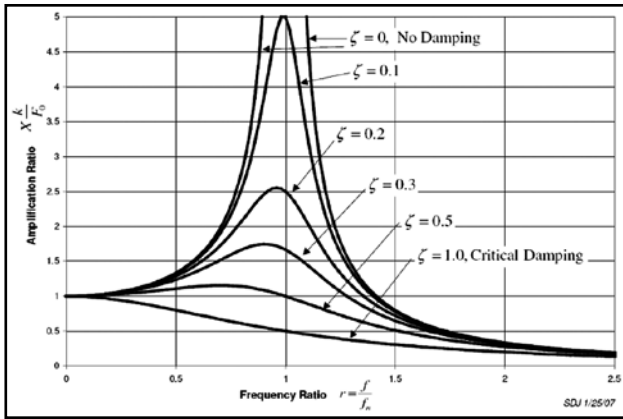


Fig. 7.1: SDOF response for various damping values (harmonic load)

This was the goal that led Cofimco to develop the innovative 35F blade equipped with low-stiffness FRP shaft and embedded friction-based damper: a combined action of low stiffness and high dissipation capability that brings the blade to cope well even in particularly tough working condition as, for example, temporary or transient resonance.

On-Site Measurements

Several test room and on site measurements have been carried out to verify the ability of 35F's mechanical features to reduce vibration amplitude. Thanks to its mechanical characteristics, matching with the concepts discussed in the previous chapters, significant vibration amplitude reduction was achieved compared with the usual values recorded on sites equipped with standard blades, see below table 8.1 and ref. (b) for further details:

Fan type	Direction			
	X	Y	Z	
	mm/s	mm/s	mm/s	
30 ft - 8 Conventional B-type blades	2.5	2.3	5.7	C. T.
30 ft - 8 FRP + C Shaft C-type blades (*)	2	1.8	2.1	
32 ft - 6 Conventional B-type blades	3.1	4.2	7.8	A. C. C.
32 ft - 6 FRP + C Shaft C-type blades (*)	2	2.1	2.7	



(*) FRP + C : Fiber Reinforced Plastic & Carbon fibers

Table 8.1: Comparison between on-site measured vibration.

Note:
C. T. measurement - conventional B-type fan replaced by FRP + C Shaft C-type fan
A. C. C. measurement - see below fig. 8.1
The achieved reduction in the vertical direction is higher than 63% (RMS Values).

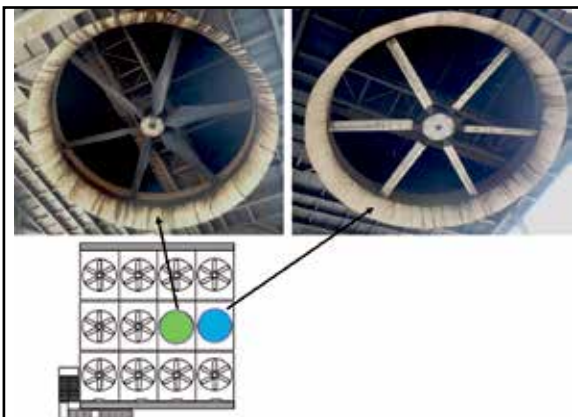


Fig. 8.1: A.C.C. test

Note:
X: horizontal, parallel to the bridge (ACC) or driving shaft (CT)
Y: horizontal, perpendicular to X
Z: vertical

The below figure 8.2 shows the stress recorded on two different 34 ft ACC fans:

Blade	FRP + C Shaft (C-type)	Conventional A-type
Blade count	12	6
Speed at measurement, RPM	80 (*)	87
Design Static Pressure, Pa	133	120
Design Flow Rate, m ³ /s	664	692
Design RBM, N*m	2604	4700
Measured Alternate Stress, MPa	27	45
Equivalent Flexural Modulus, mm ³	44432	103786
Alternate RBM, N*m	1199	4670
Ratio (Alternate RBM / Design RBM)	0.46	0.99

Table 8.1: Fans features

(*) Measurement on VFD at resonance speed

The strain gage, on both blades, was stuck on the blade at around 50 mm ($\approx 2''$) from the clamping to the hub. A preliminary calibration with known load allowed the evaluation, from the measured stress, of the bending moment variation at blade root.

The ability of the C-type blade to contain the alternate RBM is evident, Tab. 8.1: while the ratio (A-type to C-type) of the Design RBM is 1.8, the ratio of the Alternate RBM is 3.89, more than double.

Despite the different duty points of the 2 installations, the measurements confirm what stated in the previous chapters: a stiff blade transfers all the RBM variations to the hub, while a softer blade "uses" the centrifugal force to reduce the amount of RBM variations transmitted to it.

Furthermore, the larger displacement of the C-type blade allows a higher aerodynamic and structural dissipation of the oscillation kinetic energy. This holds the oscillation energy below critical levels.

Notes:

- In both measurements shown in figure 8.3, the strain gage was applied on blades already installed. Therefore, the stress due to the blade weight is not included. Being constant, this stress component is not relevant for the purpose of this paper.
- Both measurements were taken in calm environmental conditions, with negligible wind.

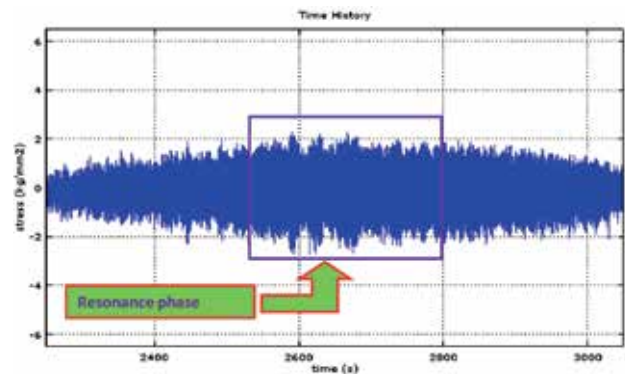


Fig. 8.2a: Stress recorded on Blade C (speed ramp)

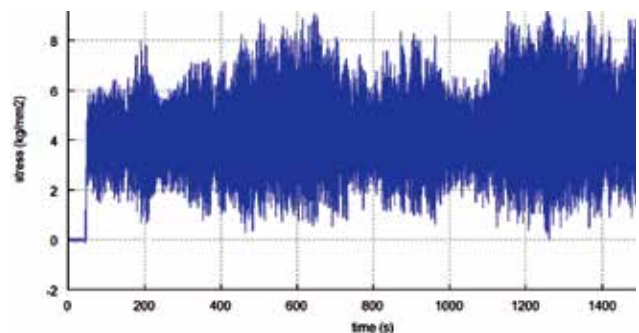


Fig. 8.2b: Stress recorded on Blade A (fixed speed)

Conclusions

The theoretical analysis, as well as on site measurements, show significant benefits using axial fans equipped with FRP or FRP + Carbon low-stiffness-shafts blades.

The following goals are achieved using the innovative blade configuration (low stiffness shaft and dampening device):

Vibration amplitude and loads induced by large fan blades in the supporting structure are greatly reduced thanks to the low-stiffness blades;

Fan blades are able to withstand severe working conditions and manage the high abrupt loads frequently caused by broad obstructions or flow asymmetries on large fans;

The high energy dissipation due to the combined action of aerodynamic damping and the embedded friction-based damper allow

the fans' blades to cope with cyclic load keeping the blade alternate (fatiguing) stress within low limits.

As a consequence, the drive system's life, as well as the fan's, is extended and the supporting structure preserved from high amplitude vibration which leads to stress on the components and structural noise.

On the other hand, the larger displacement of a flexible shaft blade requires a taller fan stack with more room for the blade to oscillate without interfering with fixed structural elements.

It must also be considered that, when using a flexible shaft blade, the connection of the shaft to the airfoil and of the shaft to the hub must be able to withstand the larger displacement and strain that occur over the life of the part.

FRP SPECIALIST

FOR YOUR COOLING TOWER

FANSTACK
PULTRUSION PROFILE
LADDERS & STAIRWAYS
INLET FLANGES
PIPES AND HEADERS
FLUMES
TANKS
DECKING SYSTEM
GRATINGS
SPOOL PIPE















MEMBER

PT. INTI COMPOSITE FIGLASINDO UTAMA

FRP, Composite Products Designer and Fabricator

Address:
 Jl. Tekno 5, Blok E No. 1 C - D, Kawasan Industri Jababeka III
 Cikarang - Bekasi 17530 ; Jawa Barat - Indonesia
 Phone : +62 21 2908 2999 ; Fax : +62 21 2908 2998
 e-mail : info@icfn.net ; website : www.icfn.net



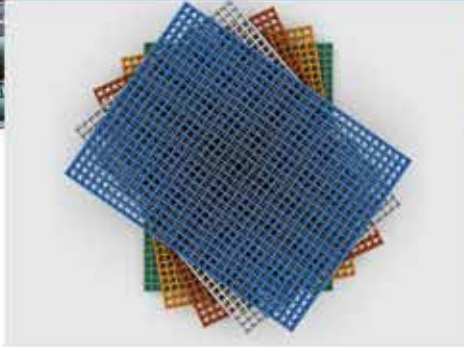
REGISTERED COMPANY

ISO 9001:2015

One stop shop
for all fiberglass/
FRP cooling tower
materials



Gratings



Pultruded Profiles



Deck Panels



Fanstacks/ Fanrings



All Arvind FRP products
meet CTI and EN
standards and are
being shipped globally

Time and Temperature Dependent Deformation Behavior of PP Fills

Nina Woicke, Daniel Dierenfeld
Enxio Water Technologies GmbH

Abstract

Mechanical behavior of plastic components are not only dependent on the pure load or load case (e.g. bending vs. pure compression), but also on the loading time and temperature. In this paper a simplified viscoelastic deformation model, based on the Findley creep model, has been derived to take these factors into account.

The model can be applied to a various range of polymer materials and types, however it has been fitted and validated to a specific fill type made from polypropylene.

Introduction

Besides the thermal performance, the mechanical behavior is the second most important property of the fill in a cooling tower. Additionally, to the final failure of the blocks [see also (Woicke & Dierenfeld, Mechanical Behavior of Polymer Fills, 2015)], the specific deformation under load is important information for the design of the whole cooling tower.

Nowadays, a lot of different block type fills are used in cooling towers. They vary in the following parameters:

- Material (PP, PVC and sometimes PE)
- Design
- Fill weight/Foil thickness
- Type of bonding

When an engineer cares about the mechanical behavior of a cooling tower fill, he has several concerns:

- Behavior at different temperatures
- Deformation for short term loads (e.g. during installation or maintenance)
- Creep deformation under static loads

Predicting the mechanical behavior of all fills would then need a lot of testing, because all factors are linked and important for the selection of fill and sizing of support structure.

The aim of this paper is to introduce and validate a deformation model for cooling tower fills, to help to reduce the testing effort without losing the validity of the results.

The model is mainly based on a commonly used material model, which will be modified to the specific characteristics of cooling tower fills.

Viscoelastic material modelling of polymers

The model, which will be presented in this paper, will focus on the strain behavior within a cooling tower fill in its operation conditions. It is not valid to extrapolate it to higher strains (approx. 1.2%), where additional failure modes (like break of bondage or secondary creep) may occur.

Linear models

To model the mechanical behavior of polymers, normally a connection of simple elements is used (Ferry, 1980). The most common



Nina Woicke

element is the spring element, where the strain ϵ and the stress σ are linked proportional by an elastic modulus:

$$\text{Equation 1: } \sigma = E \cdot \epsilon$$

The second most common element is a linear damping element, where the strain rate is linear to the stress. This behavior of a so called Newtonian fluid is as follows:

$$\text{Equation 2: } \sigma = \eta \cdot \dot{\epsilon}$$

There are two general possibilities to connect these elements: Parallel or in series.

In case you connect a spring element and a damping element parallel, you get a so called “Kelvin-Voigt” element:

$$\text{Equation 3: } \sigma = E \cdot \epsilon + \eta \cdot \dot{\epsilon}$$

If you divide the damping factor η by the modulus E , you get the so called characteristic relaxation time t_R . Then this equation looks like that:

$$\text{Equation 4: } t_R = \frac{\eta}{E}$$

$$\text{Equation 5: } \sigma = E \cdot \epsilon + E \cdot t_R \cdot \dot{\epsilon}$$

In case of a connection in series of a spring and a damping element, the resulting element is called “Maxwell” element:

$$\text{Equation 6: } \frac{\sigma}{t_R} + \dot{\sigma} = E \cdot \dot{\epsilon}$$

In case of a creep test (constant stress σ_0), the resulting strain of a Maxwell element looks like the following equation:

$$\text{Equation 7: } \epsilon = \frac{\sigma_0}{E} + \frac{\sigma_0}{E t_R} \cdot t$$

A graphical representation of all elements and connections can be seen in Figure 1.

Non-linear models

As shown by other publications [e.g. (Findley, Lai, & Onaran, 1989)], polymers often can't be modeled by this simple linear theory. One has to use either a much more complex linear equation with a high number of parameters (Woicke, 2006) or use a non-linear equation. In the first case, a lot of parameters mean a lot of independent testing, so this is rather unpractical for industrial use.

Since creep (deformation under constant load) is the major load case for cooling tower fill, the so called Findley model as a non-linear model can be used (Findley, Lai, & Onaran, 1989):

$$\text{Equation 8: } \epsilon = \epsilon_0 + \epsilon_+ \cdot t^n$$

By comparison of Equation 8 with Equation 7 there are some similarities. Since ϵ_0 and ϵ_+ are fittable material parameters, following definitions are chosen to accommodate for these similarities:

$$\text{Equation 9: } \epsilon_0 = \frac{\sigma_0}{E}$$

$$\text{Equation 10: } \epsilon_+ = \frac{\sigma_0}{E t_R^n}$$

A Complete Power Transmission Package to Keep You Cool.



Addax Composite Couplings

Repair and Asset Management Services

Solutions for the Cooling Tower Industry

Cooling towers are one of the harshest environments for power transmission equipment. Moisture, chemicals, and minerals attack the equipment driving cooling tower fans, making durability, corrosion resistance and superior customer service a priority.

That's why customers choose **Addax® Composite Couplings** and **Falk® Renew® Prager®** repair and asset management services.

- Lower total cost of ownership — properly maintained, the cost-effective Addax Composite Coupling can last the life of the cooling tower, while its lower weight results in less wear on other system components
- Professional on-site inspection, evaluation, service and repair or replacement of gear drives, couplings and bearings
- Same-day, emergency delivery of gear drives and couplings for many applications are available to maximize your uptime

t_R is chosen with the exponent n to resemble the idea that this parameter is a relaxation time.

This results in the following equation with the three parameters E , t_R and n :

$$\text{Equation 11: } \varepsilon = \frac{\sigma_0}{E} + \frac{\sigma_0}{E t_R^n} \cdot t^n$$

Findley et al. have shown, that for various polymers (including PE and PVC), n is independent of the stress and temperature and that its value is normally below 0.2 (Findley, Lai, & Onaran, 1989).

Influence of the temperature

The materials normally used for cooling tower fills (mainly PP and PVC) are used in other industrial products as piping or plastic tanks as well. Therefore, data is published on these materials, also applicable for cooling tower fill. One of the standards often used in Germany is the DVS 2205-1 (DVS, 2015).

This standard has first been published in 1974 and has been reviewed constantly since then. The newest version of the DVS 2205-1 is from 2015. The benefit of this standard is that it has tabulated values of the temperature dependent E-modulus. In Figure 2 you can see the data from that table (DVS, 2015) for PP together with an exponential fit, in analogy to the Arrhenius equation (Clark, 2002):

$$\text{Equation 12: } E(T_2) = E(T_1) \cdot e^{\alpha(T_2-T_1)}$$

Out of convenience, T_1 has been fixed to 23°C (296.15K or 73.4°F). Then, you can define a temperature scaling factor S (see also Figure 3):

$$\text{Equation 13: } S = e^{\alpha(T_2-23^\circ\text{C})}$$

$$\text{Equation 14: } E(T) = S \cdot E_{23^\circ\text{C}}$$

In analogy to the E-modulus, here the assumption is made, that the relaxation time is scaled by the same factor:

$$\text{Equation 15: } t_R(T) = S(T) \cdot t_{R,23^\circ\text{C}}$$

That transforms Equation 11:

$$\text{Equation 16: } \varepsilon = \frac{\sigma_0}{S \cdot E_{23^\circ\text{C}}} + \frac{\sigma_0}{S^{1+n} \cdot E_{23^\circ\text{C}} \cdot t_{R,23^\circ\text{C}}^n} t^n$$

Influence of the fill specifics

So far, all considerations in the model were purely made for the material itself. Even though, the material is an important factor in the overall behavior, additionally, the influence of different fill designs and weights have to be considered in the model.

Equation 17:

$$E_{\text{Fill}} = S \cdot E_{\text{Material},23^\circ\text{C}} \cdot f(\text{design, bonding}) \cdot f(\text{weight})$$

Equation 18:

$$t_{R,\text{Fill}} = S \cdot t_{R,\text{Material},23^\circ\text{C}} \cdot f(\text{design, bonding}) \cdot f(\text{weight})$$

The functions for design, bonding and weight will substantially reduce the fill modulus compared to the overall material modulus. In this paper the function concerning design, bonding etc. will not be covered. This is then the work of further investigations.

Test set-ups

All tests used for this investigation are pure pressure tests (between two flat plates) for cube size fill installations.

There are two test modes, which were chosen:

1. The fill is loaded in steps and each load step is maintained for 5 minutes before the next step, the load of each step is identical. This test set-up simulates short term loads as they are applied during installation or maintenance. The actual load value is adapted to the individual weight of the fill.

2. The fill is loaded once and then the creep is measured over time. This test set-up simulates the loading of a fill during operation. Please note: All data is acquired from new fill. So some long time effects (as aging of the material) are not included

Since this investigation is for the linear regime of the fill, this investigation focusses the first steps of this load tests, but single test have been done to test as well the limit of the model (see 5.3).

All tests have been conducted for the same fill design (KFP 627) and all fills have been thermally welded. The reference block had a void ratio v of 0,971. The void ratio is calculated by:

$$\text{Equation 19: } v = 1 - \frac{\text{specific fill weight}}{\text{material density}}$$

In Table 1 is an overview about the different test sets conducted. All results used in this paper are third party data.

In Figure 4 pictures of test set-up 2 (left) and 3 (right) can be seen.

Results and discussion

Fit of the model and influence of the temperature

To fit the data, Equation 11 was used as a base, where E was according to Equation 17 and t_R is according to Equation 18.

For the fit of the model parameters (n , t_R and E_{fill}) the first set of tests has been used. In this case, the same load steps were chosen for all three temperatures. In Figure 6 the results and the fit for 23°C (73.4°F) can be seen.

In this fit, n is 0.12, which is in the same order of magnitude as the data from Findley (Findley, Lai, & Onaran, 1989) and ranks between PVC and PE.

One effect, which can be observed, is that in the beginning of every test there is initial creep due to the fact that the blocks have waved edges and small offsets (see Figure 5). These offsets are in the magnitude of 0.1-0.2% of the block size and are not critical for the overall deformation. This is a one-time effect and will not be considered in the deformation model, but corrected case by case in the step loads as can be seen in Figure 6.

With the same model parameters, only with a changed S (see Equation 14 and Equation 17), the two other temperatures were fitted to the test data. Figure 7 shows these fits for 45°C (113°F) and 65°C (149°F).

For higher temperatures the fit starts to deviate stronger, especially the third step. This is comparable to the deviations seen in 5.3 and shows the limit of the presented model.

Influence of fill sizes

To rule out the question of influence of fill sizes in test set #2, the same stress is applied to test set-up 64 times larger, consisting of 4 single blocks, instead of one small block. The temperature, test mode, stress level and time steps are kept constant.

The overlay of the results can be seen in Figure 8. The bigger block size has slightly higher strains. This could be an effect of the additional edges within the set-up, but is negligible in the overall precision of the tests.

Limits of the model

To define limits of the presented model, a test until failure of the block has been conducted within test set #2. The comparison of this test with the model of the test before is shown in Figure 9. One can see that the model fits well for the first half of the curve. Then for each step the correlation gets worse. So the model is only applicable for stresses up to 50% of the failure stress.

POWERFUL CONNECTIONS

Unparalleled Versatility in
Maintaining Your Water Treatment Options



W600 Series

Up to 6 Complex Functions
featuring a large touchscreen
display for easy setup.



W900 Series

The Most Powerful Control
with Flexible Input and
Output configuration
plus Online Access.



W100 Series

3 Powerful Control Outputs
for use in more places than
other entry level models.

W A L C H E M

IWAKI America Inc.

Get more power over your water treatment processes
by connecting with your Walchem Representative today.

www.walchem.com
508.429.1110

Influence of the fill weight

To check the influence of different weights, four different classes with adapted stress levels have been tested. To fit this extra parameter, Equation 16 has been adapted:

Equation 20:

$$\varepsilon = \frac{\sigma_0}{S_v \cdot S_T \cdot E_{23^\circ C}} + \frac{\sigma_0}{(S_v \cdot S_T)^{1+n} \cdot E_{23^\circ C} \cdot t_{R,23^\circ C}^n} \cdot t^n$$

There is one additional parameter S_v to be fitted to the measured data (see Figure 10). All other data has been kept constant.

In the tested regime, there is a linear behavior between the measured data and the void ratio v (see Figure 11).

Extrapolation of this data is critical, because the deformation behavior changes with very thin foils as well as with very thick foils.

Obviously, in reality, the scaling factor should be 0, when the void ratio is 100%. Since this is not the case for the linear approach, it is to be expected, that at a high void ratio (very thin foils) will lead to an accelerated reduction of the E-modulus.

On the other hand, for a void ratio of 0 the E-modulus of the theoretical fill should be the same as for PP. If you use the extrapolation of the data presented in Figure 11, again you don't end up with this number but a 5 times lower value. So at a certain point, the behavior will change.

Therefore this linearity can only be used for interpolation and not for extrapolation.

Influence of the test mode

To check, if this model fits as well to a pure creep test, in the following test set #3 the fill has been tested for pure creep over a longer time (1 000h= 3 600 000s). The results have been compared to the model fitted before to this fill. Figure 12 shows these results. The model predicts about 0.1% higher strain, which is in the same magnitude as the “starting effect” presented in 5.1. Besides that, the overall time dependent behavior could be predicted very well.

Summary and outlook

In this paper a deformation model based on the Findley creep model was presented and modified to fit the characteristics of cooling tower fill.

Then model has been validated by test done with PP fills, showing the following aspects:

- The temperature dependent parameter could be derived from a widely used standard
- The time exponent is in the same magnitude as other polymers reported by Findley
- The behavior of load step and creep tests could be predicted with the same model
- The limits of the deformation model is at about 50% of the maximum stress level
- In the typical void ratio regime for cooling, a linear behavior of different fill weights could be derived from interpolation

Based on these results, the necessary testing can be reduced to two sets of measurements (one at low weight, one at high weight) at room temperature per design (including bonding method) and material.

Probably, even further reduction in measurements is possible, but for that further investigations have to be made:

- Comparison to PVC
- Influence of the different designs
- Influence of the bonding method
- Influence of bending vs. pure pressure

By these measures one can get a complete view on the mechanical behavior of cooling tower fills.

Figures

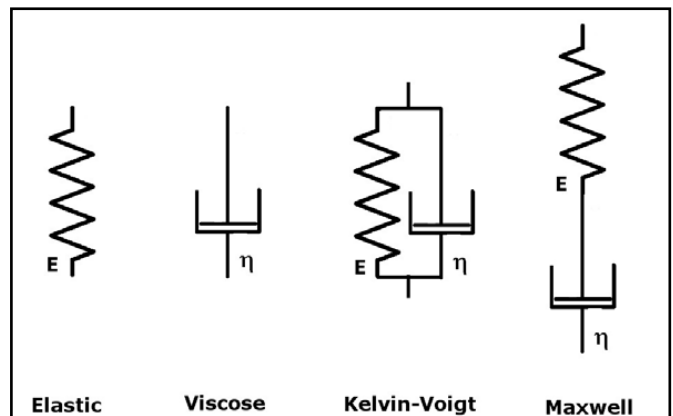


Figure 1: Linear viscoelastic model representations

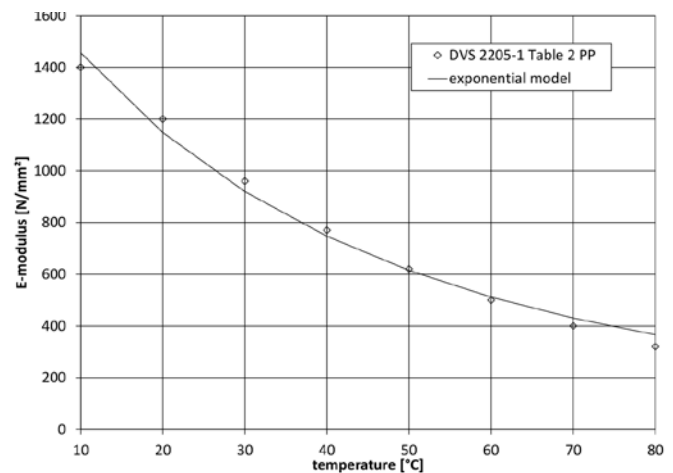


Figure 2: E-modulus of PP based on DVS 2205-1

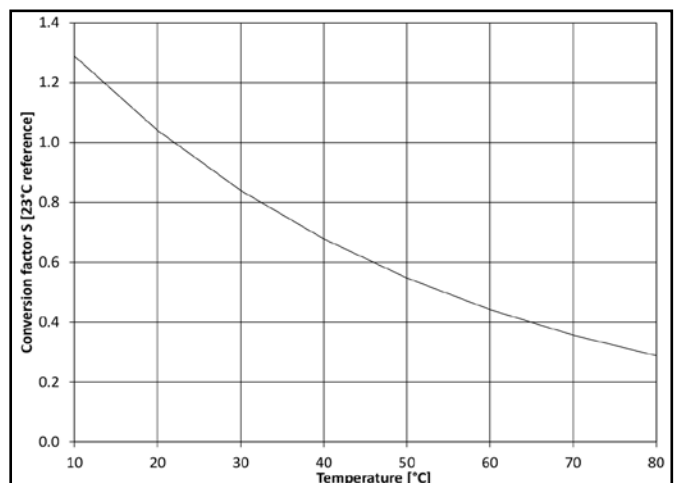


Figure 3: Temperature scaling factor S for PP based on DVS 2205-1



Figure 4: Test set-up #2 (left) and #3 (right)



Figure 5: Small offsets at the fill edges

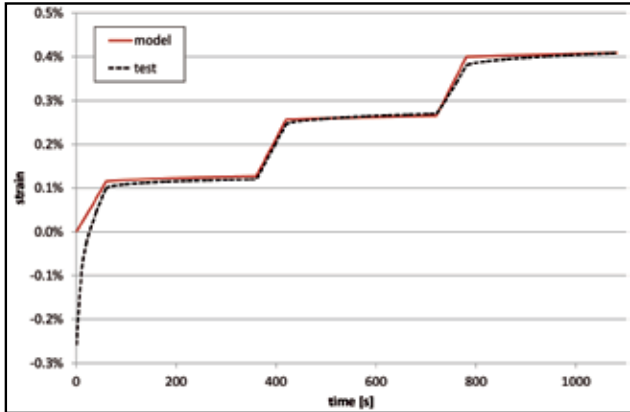


Figure 6: Step fit at room temperature

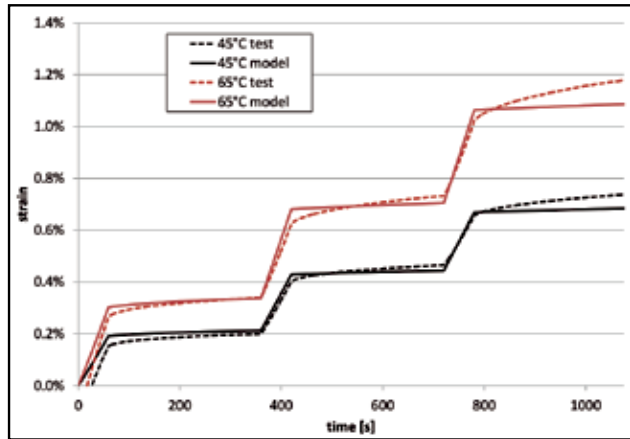


Figure 7: Step fit for elevated temperatures

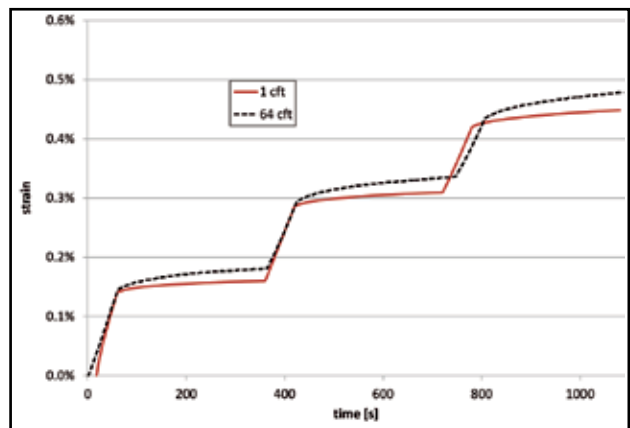


Figure 8: Comparison of tests for two different block sizes

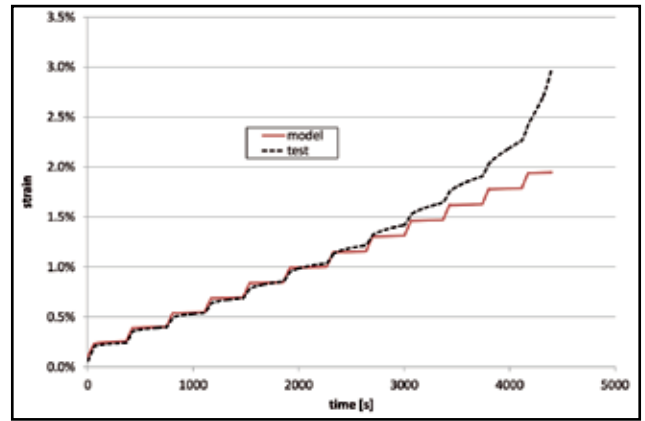


Figure 9: Comparison of the model with a test until failure

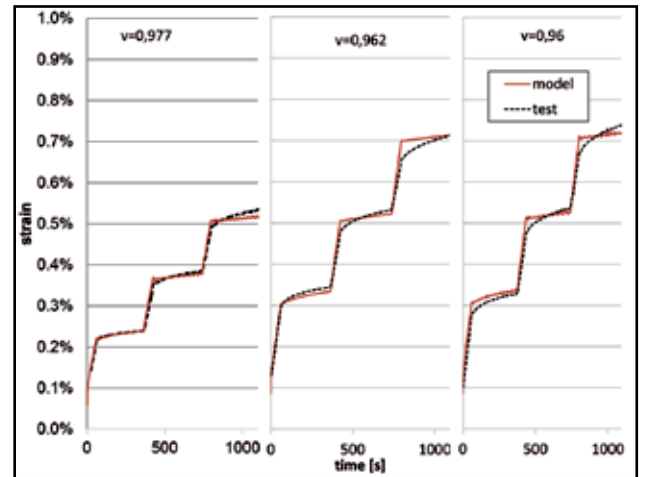


Figure 10: The fitted S_e (model and test data for different void ratios)

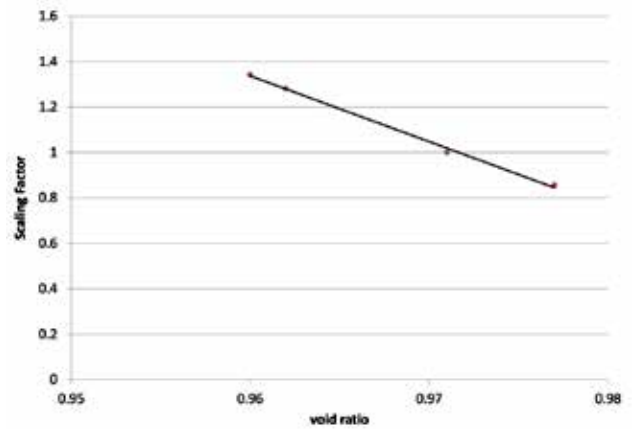


Figure 11: The fitted S_e for the corresponding void ratios (reference void ratio 0,971)

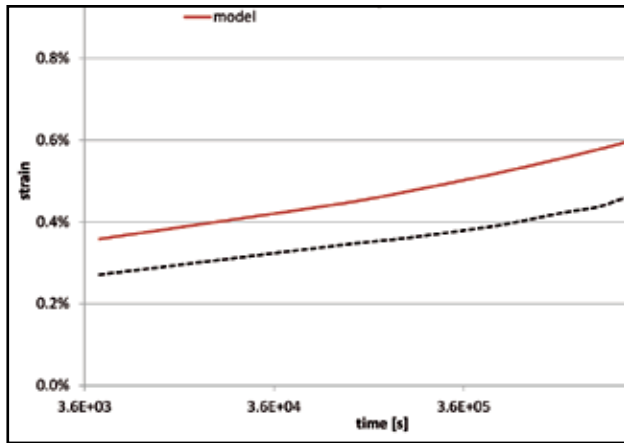


Figure 12: Comparison of the model to a test under pure creep

Bibliography

- Clark, J. (2002). Rate Constants and the Arrhenius Equation. Retrieved August 3, 2016, from <http://www.chemguide.co.uk/physical/basicrates/arrhenius.html>
- DVS. (2015). 2205-1. Düsseldorf: DVS Media GmbH.
- Ferry, J. D. (1980). Viscoelastic properties of polymers. New York: John Wiley & Sons.
- Findley, W. N., Lai, J. S., & Onaran, K. (1989). Creep and relaxation of non-linear viscoelastic materials. New York: Dover Publications Inc.
- Woicke, N. (2006). Viscoelastizität von Propylen im Glasübergang. Stuttgart: Universität Stuttgart.
- Woicke, N., & Dierenfeld, D. (2015). Mechanical Behavior of Polymer Fills. CTI.

Tables

Test set #	Specimen size	Test mode	Other boundary conditions
1	0.028m³ (1cft)	1	Different temperatures (23°C, 45°C, 65°C)
2	1.812m³ (64cft)	1	Different fill thicknesses at 23°C
3	0.227m³ (8cft)	2	1000h at 23°C

Table 1: Overview over the different test set-ups

hewitech
INNOVATION IN PLASTIC

Design Diversity
Sustainable Efficiency
Custom-made Solution

Our SOLUTION

Your PERFORMANCE

- ✓ Cross- & Counter-flow **FILL media** made of PVC & PP
- ✓ Blade and Element **Drift Eliminators**
- ✓ **Sprayers, Air Inlet Elements** and **Hanging Systems**
- ✓ **High efficiency media to low fouling designs**



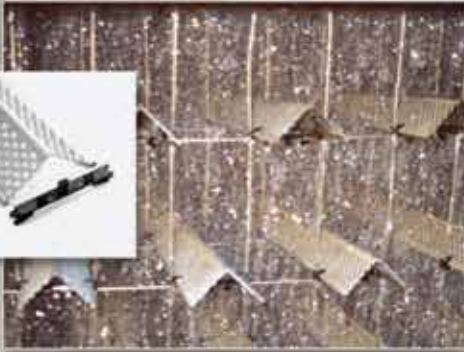
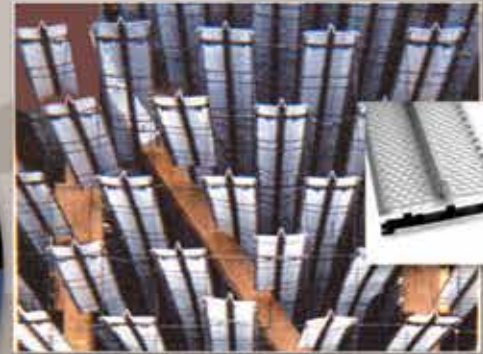
Our SERVICE

Your SATISFACTION

- ✓ **INHOUSE Tool production** – Custom-made Designs
- ✓ **Thermal Welding** and **Mechanical Assembly** equipment
- ✓ **World-wide** delivery and assembly service
- ✓ **References** around the globe



It's what's inside that really matters.



C. E. Shepherd Company, L. P.
www.ceshepherd.com



Better components make better towers.

**Since 1957, our primary business has been innovation!
We encourage inquiries for custom product solutions!**

Shepherd Standard High Quality products for cooling towers include:

- PVC Coated Hanger Grids
- Stainless Steel Hanger Grids
- Gull Wing Splash Fill Slats
- V-Bar Splash Fill Slats
- Film Pack
- Drift Reduction Units
- Nozzles & Accessories

C. E. Shepherd Company, L.P.
2221 Canada Dry Street
Houston, TX 77023
Telephone: 713.924.4300
Fax: 713.928.2324
www.ceshepherd.com
sales@ceshepherd.com

Whether your project requires new construction or retrofit, standard products or custom solutions, Shepherd Tower Components are a perfect fit.

Simplifying Corrosion Control With A Safer Choice Inhibitor

Eric C. Ward, Emily M. Crane, Gregory J. Koniges
Rivertop Renewables

Abstract

It is well known that phosphorous-based corrosion inhibitors cause fouling with calcium if they are not adequately treated with a stabilizing product to prevent foulant precipitation. This shortcoming makes this stabilizing product an essential component of any phosphorous-based inhibitor program. In this paper, a new corrosion inhibitor will be presented that provides a single-component replacement for the aforementioned dual-component system. This new inhibitor can not only replace phosphorous-based inhibitors used for mild steel corrosion control; laboratory testing has shown the product has corrosion inhibition properties for zinc and galvanized metal and can also reduce white rust formation in high pH, high alkalinity water chemistry. This new inhibitor performs well across a wide range of hardness conditions and pH values, it allows for the reduction of the product used to stabilize phosphorous-based inhibitors, and is an environmentally friendly alternative for corrosion control. It has also shown excellent compatibility with other commonly used corrosion inhibitive chemistries. To demonstrate this new corrosion inhibitors performance benefits, both laboratory and pilot testing performance data will be presented.

Introduction

Since the ban on chromates over thirty years ago, the cooling water industry has predominantly relied on phosphorous-based corrosion inhibitors. Initially, these treatment programs were stabilized phosphate programs that used sulfuric acid to control pH and limit calcium phosphate saturation. Over time, these programs transitioned into alkaline phosphate and all organic phosphonate programs; largely in response to industry trends to reduce the use of sulfuric acid and operate at higher cycles of concentration. Both of these trends drove the pH and hardness values for a typical cooling water systems to a higher range, which in turn increased the drive for calcium phosphate or calcium phosphonate precipitation. This precipitation, if not controlled, can result in system fouling, loss of corrosion inhibitor and thus loss of corrosion protection. To combat these problems, the water treatment professional must increase the dosage of calcium phosphate inhibitor to control system fouling. 1-2 As more stringent water conservation efforts continue to loom, the challenge posed with using phosphate-based inhibitors in high hardness, high pH water will likely become more and more challenging.

Further exacerbating treatment challenges, phosphorous-based chemistries are increasingly facing both local and federal regulations to control the contamination of surface water. Since the 1972 Clean Water Act, controls to limit phosphorus discharge from point sources have grown exponentially. Figure 1 depicts the total active discharge permits containing restrictions on phosphorus levels. In 2005 only 3,705 permits had any phosphorus limits while 10 years later in 2015, 12,643 such permits were active representing over a 300% increase in restrictions.3-4

Active phosphorus effluent limit permits by year, 1973-2015 [Source of Data: U.S. Environmental Protection Agency Permit Compliance System data-base retrieval, 2016].

This paper presents a new corrosion inhibitor chemistry that provides a replacement for phosphorous-based inhibitors and all the problems and looming regulations with which they are associated. This new inhibitor forms a protective film on both steel and galvanized surfaces and does not pose a fouling concern with calcium. Furthermore, the new inhibitor chemistry is made from sugar via a unique oxidation process that converts



Eric C. Ward

glucose to sodium glucarate. This paper will present this glucarate based corrosion inhibitor (GBCI) as a viable alternative to the phosphorous-based inhibitors used today.

Laboratory Evaluations

Corrosion testing of the GBCI product was predominantly based on the use of electrochemical test methods. This methodology allows for quick assessment of inhibitor performance, including general corrosion rate and inhibitor mechanism. All electrochemical tests were performed using a Gamry Series G 300 Potentiostat in both 1L jacketed Gamry corrosion cells and 200mL jacketed Gamry EuroCells. Two commonly used methods were utilized for these evaluations: Linear Polarization Resistance (LPR) and Tafel polarizations.

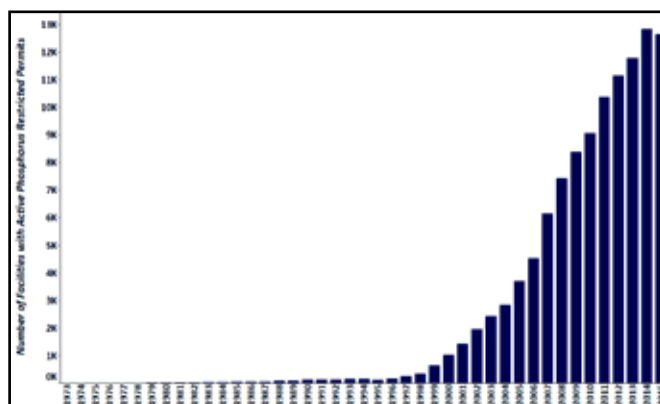


Figure No. 1

LPR

LPR experiments provide quick estimations of general corrosion rates and allow for unlimited monitoring of corrosion rates within a system over time. An LPR experiment is conducted by applying a potential range to a working metal electrode that extends $\pm 20\text{mV}$ from the measured potential of the electrode at rest, or open circuit potential (OCP), or corrosion potential (E_{corr}). These graphs are generally linear and the slope of the line can be used to calculate the corrosion current density in amps/cm^2 , which can then be converted to a corrosion rate. The small polarization range is non-destructive to the metal surface, allowing these tests to be run repeatedly on one specimen.

Tafel Polarizations

Tafel plots provide more detailed information on the inhibitor mechanism of corrosion inhibition. A Tafel plot is generated by applying a potential range to a working metal electrode that extends $\pm 250\text{mV}$ from E_{corr} . For each applied potential, a current is measured that can be plotted on a logarithmic scale of measured current versus each applied potential. The lower portion of the curve that lies between -250mV from E_{corr} is known as the cathodic curve. The upper portion of the curve between $+250\text{mV}$ from E_{corr} is known as the anodic curve. E_{corr} is indicated by the inflection point where the measured current drops to very low amperage between the two curves. The introduction of an inhibitor to an electrolyte solution can suppress one or both of these curves. The degree of suppression and shape of these curves can then predict the possible mechanisms of corrosion inhibition.



KIMCO, The Altimate in environmental-friendly Cooling Tower!

KIMCO serves all kinds of cooling towers with numerous new options. Enjoy the benefits!



- PLUME ABATEMENT DESIGN
- SUPER LOW NOISE DESIGN
- ANTI-BACTERIA, LEGIO-FREE TOWER
- HIGH EFFICIENCY, ENERGY SAVING DESIGN
- NON-CORROSION FRP STRUCTURE CONSTRUCTION
- CTI CERTIFIED MODELS ARE AVAILABLE :
DYNA-COOL / CKL / ENDURA-COOL



MODULAR TYPE, FRP TOWER



COUNTER FLOW
FRP TOWER



FIELD ERECTED, COUNTER
FLOW, PLUME ABATEMENT,
CONCRETE TOWER



FIELD ERECTED, COUNTER
FLOW, STEEL TOWER

COOLING TOWER
KIMCO
www.kimcoct.com

FOR MORE INFORMATION, CONTACT
E-mail : kimco@kimcoct.com



ISO 9001
ISO 14001



MEMBER



93-18-01
05-18-02
09-18-03

Carbon Steel Corrosion Inhibition

Simulated Cooling Water Test Methodology

One-liter corrosion cells were modified to allow for a simulated cooling water feed, blow-down and an Oxidation-Reduction Potential (ORP) system to control the oxidizing biocide feed into the system. Each system was aerated and equipped with a C1018 carbon steel working electrode. These modifications allowed for the evaluations of corrosion inhibitor programs in more “realistic” cooling water conditions, including the continuous feed of water treatment formulations with make-up water or more concentrated (high cycle) water to raise the cycles of concentration in the cell and a separate biocide feed controlled to a specific free halogen concentration. Each cell was equipped with an inlet water feed and an outlet water feed that equaled approximately 0.70L/min. This chosen feed rate allowed for a turnover volume within the cell of approximately 1.0-liter per day, which provided a turnover rate of around three days. Tests could then be started at a predetermined cycle of concentration, with a more concentrated, higher cycle water being fed into the system. This design allowed for a test to be started at a low cycle of concentration and fed to a higher cycle of concentration within a 3-day period. It also allowed for the continuous feed of treatment formulations, which were added to the incoming feed water to maintain their desired dosages. A diagram of the modified corrosion cell can be seen in Figure 2.

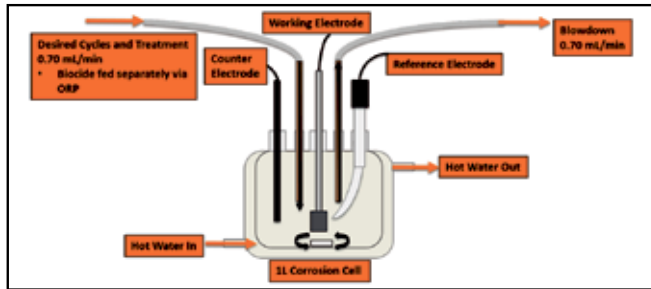


Figure No. 2 Modified corrosion cell with simulated cooling water feeds.

The purposes of these tests were to evaluate the GBCI as a viable alternative to the traditional “all organic” programs used in the Heating, Ventilation and Air-Conditioning (HVAC) segment of water treatment today. The make-up water chemistry and general parameters chosen for these tests can be found in Table 1. The table provides conditions for both the make-up water and the water at five cycles of concentration, which is considered a “typical” operating condition.

Component	HEDP		HPA		GBCI	
	Low LSI	High LSI	Low LSI	High LSI	Low LSI	High LSI
HEDP	10	10				
HPA			20	20		
AA:AMPS Copolymer	10	10	10	10		
GBCI					25	25
PAA	10	5.0	5.0	5.0	10	5.0
PMA		5.0		5.0		5.0
PBTC			2.5	2.5		
TTA	3.0	3.0	3.0	3.0	3.0	3.0

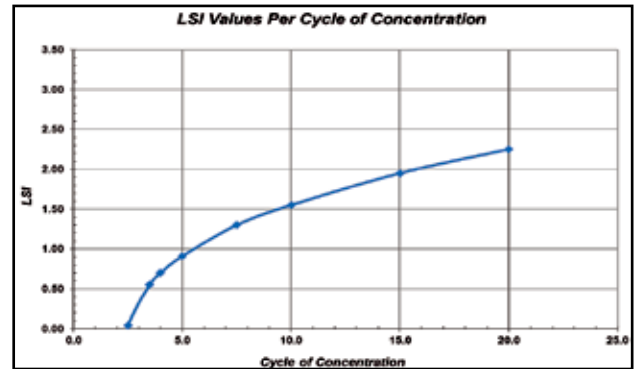
Table 1: Simulated HVAC Cooling Water for Simulation Testing

The LSI values of the simulated HVAC cooling water as the cycles of concentration are increased are shown in Figure 3

As representatives of common “all organic” formulations used in the industry, two formulations containing either 1-Hydroxy Ethylidene-1,1-Diphosphonic Acid (HEDP) or 2-Hydroxyphosphonoacetic Acid (HPA) were prepared. These formulations were then used for comparative testing to comparable formulations containing the GBCI product. A “low LSI”

and “high LSI” version of each formulation was prepared, with the “high LSI” version being used for testing when the cycles of concentration were carried to concentrations greater than ten. Additional common components used in these formulations included a copolymer of Acrylic Acid and 2-Acrylamido-2-MethylPropane Sulfonic Acid (AA:AMPS), a polyacrylic acid homopolymer (PAA), a polymaleic acid homopolymer (PMA), 2-Phosphonobutane 1,2,4-tricarboxylic acid (PBTC) and tolyltriazole (TTA).

Figure No. 3 LSI values per cycle of concentration of the simulated HVAC water.



In addition to the common industry formulations, another set of formulations were prepared using the GBCI product. Both the HEDP and HPA components were removed from these formulations. With there being no phosphorous-based components to require stabilization, the AA:AMPS copolymer was also removed. Each of these formulations can be seen in Table 2.

Table 2: Simulated HVAC Cooling Water “all organic” Formulations

Ion	Concentration (mg/L)	
	Make-Up	5.0 Cycles
Ca ⁺⁺ (as CaCO ₃)	40.3	201
Mg ⁺⁺	4.76	23.8
Na ⁺	9.60	48.0
Cl	42.4	212
HCO ₃ (as CaCO ₃)	20.0	100
SO ₄ ²⁻	5.0	25.0
Additional Parameters		
TDS (mg/L)	102	511
Conductivity (µS/cm)	159	797
Temperature (°C)	32.0	32.0
pH	7.80-7.90	8.40-8.60
Langelier Saturation Index (LSI)	-1.09 ± 0.05	0.91 ± 0.10

The optimization of treatment methods with the GBCI product revealed that the product’s performance is improved with an initial passivating dosage of a higher concentration that can then be reduced to a maintenance dosage of a lower concentration; the latter of which can then be fed into the system via formulation.

For all tests presented in this section, an initial passivating dose of 25.0mg/L GBCI was added to the test water already containing 25.0mg/L dose obtained from its formulations given in Table 2. The combination of these two dosages provided a 50.0mg/L total active dose of the GBCI, which was then allowed to deplete to the 25.0 mg/L dose obtained from the formulation.

Oxidizing Biocide Compatibility

LOW RANGE HYPOCHLORITE BIOCIDE TESTS: The simulated HVAC cooling water and parameters shown in Table 1 were chosen for these evaluations. The water was started at 1.0 cycles of concentration and then fed to 5.0 cycles of concentration to observe inhibitor performances at lower calcite saturations that can be more corrosive. The “low LSI” formulations were chosen for these evaluation and were fed with the 5.0 cycle water feed. A separate hypochlorite/make-up water solution was fed via ORP to maintain a low level of free chlorine within the range of 0.15-0.25mg/L. This GBCI “low LSI” formulation, plus passivating dosage, was then compared to the two commonly used “low LSI” industry formulations, all of which are shown in Table 2.

STD-202: Standard for Publication of Custom Cooling Tower Thermal Performance Test Results

The Performance & Technology technical committee has developed Standard STD-202 to encourage cooling tower capacity of 100% or better.

- Composite Cooling Solutions, L.P.
- EvapTech, Inc.
- SPX Cooling Technologies, Inc.

Custom cooling towers built by the Participating Manufacturers (PM) are field-tested for thermal performance by CTI-Licensed Thermal Performance Testing Agencies and the results are published in accordance with this Standard.

CTI STRONGLY RECOMMENDS THAT YOU SPECIFY STD-202 FOR YOUR COOLING TOWER NEEDS:

This program provides big benefits to owners/operators of custom field-erected cooling towers:

- Performance tests demonstrate the actual thermal performance,
- Power generation is increased due to proper thermal performance,
- Heat exchanger efficiency is increased due to lower water temperature and lower energy consumption in the entire system.

1. The cooling tower vendor shall be a Participating Manufacturer in the Cooling Technology Institute (CTI) STD-202 program for Publication of Custom Tower Thermal Performance Test Results, as validated by listing as such on www.cti.org.
2. The cooling tower shall be subject to acceptance testing conducted by a CTI-Licensed Thermal Performance Testing Agency, according to the latest edition of CTI ATC-105. Testing shall occur within one year of commercial operation of the cooling tower.

This is a voluntary program. For the period of publication of these results, the PM are:



Participating Manufacturer	Composite Cooling Solutions, L.P.	EvapTech, Inc.	SPX Cooling Technologies	All Multi-Agency Acceptance Tests for the previous year*
Testing during the Period:	8/21/2013 to 08/16/2016	10/26/2013 to 10/18/2016	05/20/2015 to 08/30/2016	2015
Percentage of tests at or above 100% Capability	N.A.	100	60	62
Percentage of tests at or above 95% Capability	N.A.	100	100	82
Average Capability of tests below 95% Capability	N.A.	None	None	89.4
Average Water Flow Rate	N.A.	74,059	108,282	58,583

N.A. = At the time of this publication the minimum number of CTI licensed tests required to publish results by STD-202 have not been performed.



The test results reveal that the GBCI formulation, with slug dose, performed better than both industry standard formulations. These findings are significant, as the HEDP-based formulations degraded in the presence of hypochlorite to produce significant concentrations of ortho-PO₄ that were in the range of 3.2 to 5.1mg/L PO₄. The HPA-based formulation degraded in the presence of hypochlorite to produce significantly higher concentrations of ortho-PO₄ that were in the range of 1.2 to 7.9mg/L PO₄. These numbers would seem to indicate the vast majority of the HPA was degraded in the presence of hypochlorite. This finding was not necessarily a surprise, given HPA's well known incompatibility to oxidizing biocides. The GBCI-based formulation performed better, with no phosphorous present in the water. These test results can be found in Figure 4. The provided PO₄ range in the legend of Figure 4 indicates the low to high ends of PO₄ concentrations measured in solution throughout testing. The increase in ortho-PO₄ is directly related to the degradation of phosphonate in the presence of hypochlorite. It is important to note that both the HEDP and HPA formulations are frequently used as "indirect" methods of adding ortho-PO₄ to the system via their degradation when used with oxidizing biocides. Yet, even though the generated ortho-PO₄ was adequately stabilized, these formulations were unable to perform better than the GBCI formulation.

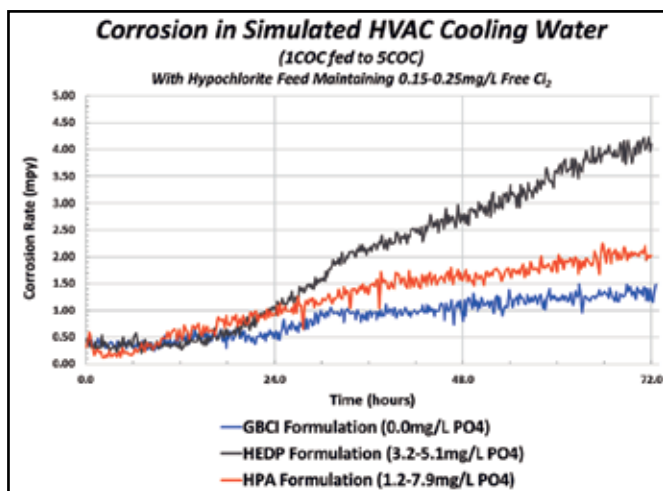


Figure No. 4 Corrosion test results of "low LSI" formulations in Simulated HVAC Water.

HIGH RANGE HYPOCHLORITE BIOCIDES TESTS: The simulated HVAC cooling water and parameters shown in Table 1 were again chosen for these evaluations. The water was started at 1.0 cycles of concentration and then fed to 5.0 cycles of concentration. The "low LSI" formulations were chosen for these evaluation and were fed with the 5.0 cycle water feed. A separate hypochlorite/make-up water solution was fed via ORP to maintain a higher level of free chlorine within the range of 0.40-0.60mg/L. This GBCI "low LSI" formulation, plus passivating dosage, was then compared to the commonly used "low LSI" HPA industry formulation, both shown in Table 2.

The test results reveal that the GBCI formulation, with slug dose, performed better than the HPA-based formulation. It should also be noted that the GBCI treated system experienced a significant overfeed of hypochlorite throughout the first 96 hours of testing, where free chlorine readings were frequently above 1.0mg/L. Despite this overfeed of hypochlorite, the GBCI formulation maintained lower corrosion rates than that of the HPA formulation, which was not subjected to the high free chlorine concentrations. Figure 5 depicts both the corrosion rates and free chlorine measurements for these tests, with the corrosion rate plotted on the primary y-axis and mg/L free chlorine plotted on the secondary y-axis. Note that the intended range for free chlorine is highlighted in green to emphasize the free chlorine overfeed for the GBCI treated system.

STABILIZED BROMINE BIOCIDES TESTS: The simulated HVAC cooling water and parameters shown in Table 1 were again chosen for these evaluations. The water was started at 4.0 cycles of concentration and then maintained at 4.0 cycles of concentration throughout the test. The "low LSI" formulations were chosen for these evaluation and were fed with the 5.0 cycle water feed. The stabilized bromine was slug-fed into the system

to achieve 10.0mg/L total bromine with each dose. A new slug dose was then added each time the measured free bromine fell below 1.0mg/L. The GBCI "low LSI" formulation, plus passivating dosage, was then compared to the commonly used "low LSI" HPA industry formulation, both shown in Table 2.

The test results reveal that the GBCI formulation, with slug dose, again performed better than the HPA-based formulation. Figure 6 shows that the initial corrosion rates for the GBCI treated system were significantly better than the HPA treated system, but as the test progressed both treatments provided very similar performances, with the GBCI formulation being slightly better.

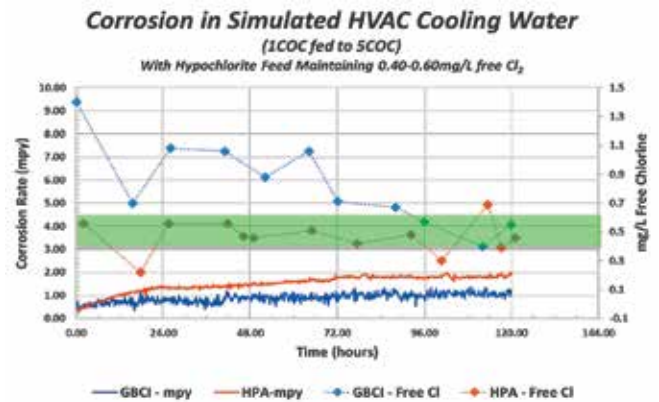


Figure No. 5 Corrosion test results of "low LSI" formulations in Simulated HVAC Water.

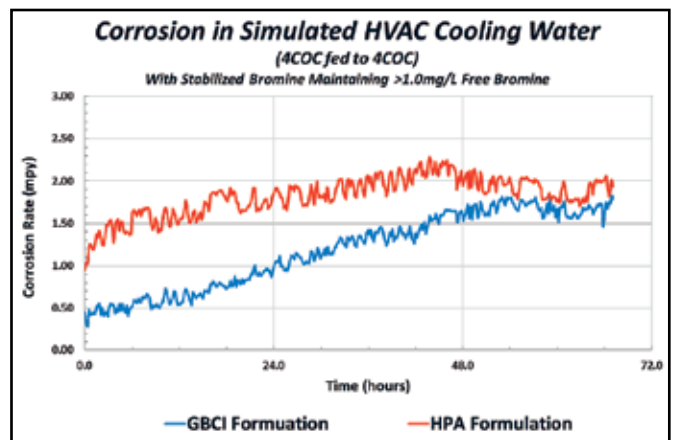


Figure No. 6 Corrosion test results of "low LSI" formulations in Simulated HVAC Water.

Performance in High Hardness Water

The simulated HVAC cooling water and parameters shown in Table 1 were chosen for these evaluations. The water was started at 5.0 cycles of concentration and then fed to 10.0 cycles of concentration to observe inhibitor performances at higher calcite saturations that can cause fouling concerns with phosphate-based chemistries. The "high LSI" formulations were chosen for these evaluation and were fed with the 10.0 cycle water feed. A separate hypochlorite/make-up water solution was fed via ORP to maintain a low level of free chlorine within the range of 0.15-0.25mg/L. The GBCI "high LSI" formulation, plus passivating dosage, was then compared to the commonly used "high LSI" HEDP industry formulations, both shown in Table 2.

The test results reveal that the GBCI formulation, with slug dose, performed significantly better than the HEDP-based formulation. Figure 7 depicts both the corrosion rates and ortho-PO₄ measurements for these tests, with the corrosion rate plotted on the primary y-axis and mg/L ortho-PO₄ plotted on the secondary y-axis. Note that the GBCI treated system maintained very good corrosion rates throughout testing, while the HEDP treated system failed at around 18 hours. This time period would coincide with calcium concentrations reaching around 300mg/L Ca as CaCO₃. The



Tower Performance, Inc.

Exclusive Bayonet Nozzle Adapter (Convert from Twist-Lock to Threaded Adapter)

If you have one of these
And this happens to you



Poor Water Distribution

You need one of these



dek-Spray® Nozzle

To adapt with one of the state-of-the-art
low clogging nozzles—S.P. or L.P.



S.P. Nozzle



L.P. Nozzle

Contact:
Jalene Fritz
800-314-1695
jfritz@towerperformance.com

incompatibility of the high calcium concentrations and HEDP are further emphasized by the separation of the soluble (filtered) versus total (unfiltered) ortho-PO₄ concentrations measured during testing. This separation can be attributed to the loss of phosphate corrosion inhibitor in the presence of high calcium concentrations, which is also reflected by the increasing corrosion rates that occur at around 18 hours.

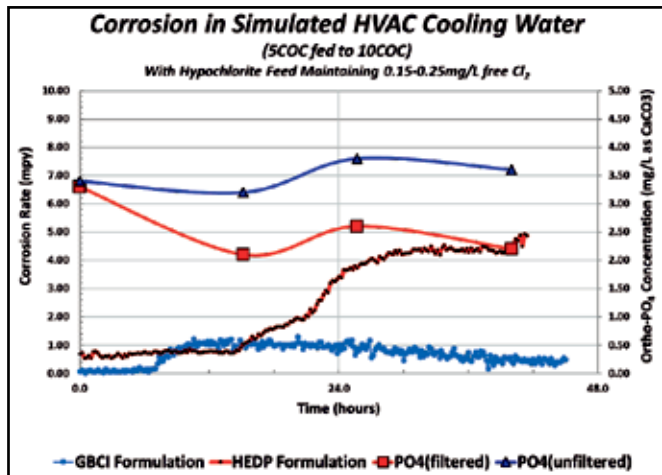


Figure No. 7 Corrosion test results of "high LSI" formulations in Simulated HVAC Water.

Mechanism of Inhibition

Tafel polarization experiments were performed using the same water chemistry given previously in Table 1. These test were performed on an untreated electrode and one treated with the GBCI to observe how its Tafel polarization graph compared to that of the untreated electrode. These results can be seen in Figure 5. Note there appears to be significant suppression of both the cathodic and anodic branches of the Tafel curves. These observations seem to indicate that the GBCI may provide both anodic and cathodic protection.

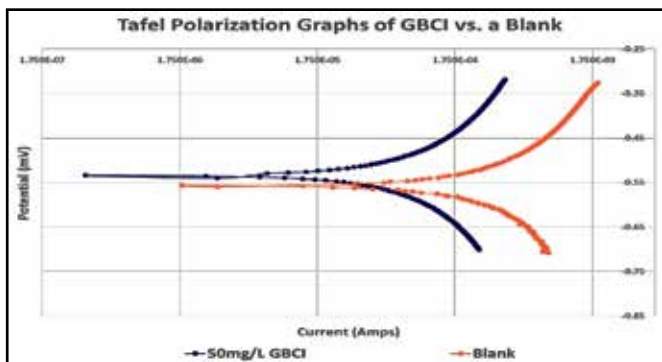


Figure No. 5 Tafel polarization plots of a GBCI treated electrode compared to an untreated electrode.

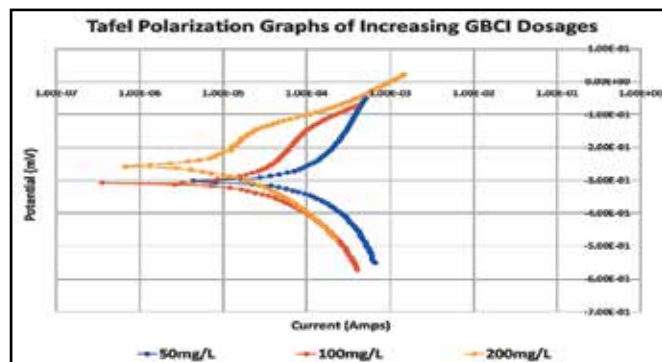


Figure No. 6 Tafel polarization plots of increasing concentrations of GBCI treated electrodes.

Further Tafel polarizations were performed to evaluate the shifts in both branches of the Tafel curve as the concentrations of the GBCI were increased. These results can be seen in Figure 6. Note that the 100mg/L dose continues to show further suppression of both the cathodic and anodic curves; but that the 200mg/L dose only showed suppression of the anodic branch. The combined analysis of both Tafel experiments seems to indicate the GBCI has an effect on both the cathodic and anodic corrosion reactions, either directly or by a general film-forming mechanism. However, the continued shift in the anodic curve with increasing concentration, coupled with an anodic shift in the corrosion potential, both seem to indicate the influences on the anodic reaction may be greater.

Calcium Tolerance

As discussed in the introduction, many of the commonly used phosphonates for scale and/or corrosion inhibition also have a tendency to precipitate with calcium. In most cases, these undesired characteristics are well known in the industry. The purpose of these experiments was to compare the calcium tolerance of GBCI to that of many of the commonly used phosphonates chosen as part of the "all organic" corrosion inhibitor programs common in the industry today. The calcium tolerance of GBCI was compared to that of various water treatment products. These products are shown in Table 3.

Product	ACRONYM	% Active	%P
1-Hydroxy Ethylidene-1,1-Diphosphonic Acid	HEDP	60.0	30.07%
2-Phosphonobutane 1,2,4-tricarboxylic acid	PBTC	50.0	11.47%
2-Hydroxyphosphonoacetic Acid	HPA	50.0	19.85%
Polyacrylic Acid	PAA	50.0	0.0

Table 3: Products tested for calcium tolerance comparisons to GBCI

Tests were conducted by adding a known volume of stock calcium chloride solution to 30mL glass vials containing 20.0mL of an 800mg/L NaCl salt solution. These conditions obtained a final concentration of calcium ions of 200.0mg/L as Ca with total dissolved solids of approximately 1000mg/L. To each of these calcium salt solutions were added varying volumes of product stock solutions to obtain increasing concentrations of active product that ranged from 0.00 to 320mg/L active product. The pH of each solution was adjusted to a range of 8.90 to 9.10. Each vial was then capped and placed in an oven set to 50°C for four hours. Each vial was then removed and percent transmittance was measured using a HACH DR 900 colorimeter.

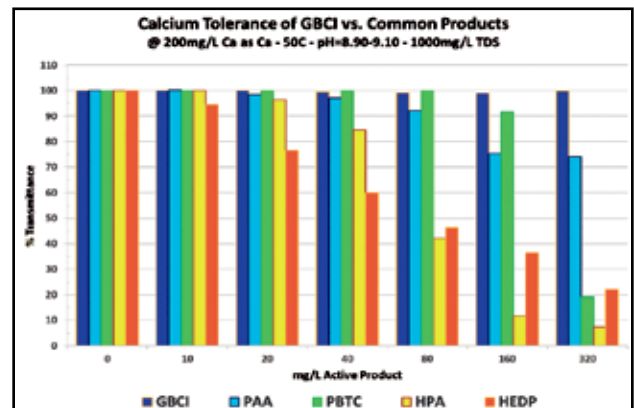


Figure No. 7 Calcium Tolerance of GBCI compared to that of other commonly used products

These results can be seen in Figure 7. Note that HEDP and HPA exhibit the poorest calcium tolerance, with indications of precipitation at active product concentrations of 20mg/L or less. HEDP and HPA are both common choices for "all organic" programs used by the water treatment professional today. These results would indicate these types of programs would likely struggle in high hardness water. PBTC was the best performing phosphonate, which was an expected result given its well-known calcium tolerance. PAA performed similarly, with both needing well over 80mg/L active product before any measurable precipitation occurred. In strong contrast, the GBCI performed remarkably well, showing no signs of precipitation at the highest concentrations tested. These results would

indicate that the GBCI could be an excellent choice for high hardness water or in systems operating at high cycles of concentration.

Galvanized Metal Corrosion Inhibition

Passivating Conditions

Using zinc electrodes, LPR test were conducted in a simulated cooling water chemistry representative of the conditions typically recommended for passivating a galvanized system. The GBCI product was compared to a typical dosage of ortho-PO₄ that would be used for protecting carbon steel at these water conditions. An untreated system was also evaluated as a control. For all systems, 5.0mg/L PAA and 20.0mg/L AA:AMPS copolymer were added for calcium carbonate and calcium phosphate control. The specific water conditions are shown in Table 4.

Ion	Concentration (mg/L)
Ca ²⁺ (as CaCO ₃)	300
Mg ²⁺	38.4
Na ⁺	97.8
Cl ⁻	395
HCO ₃ ⁻ (as CaCO ₃)	<82
SO ₄ ²⁻	208
Additional Parameters	
TDS (mg/L)	959.2
Conductivity (µS/cm)	1499
Temperature (°C)	40
pH	7.00-8.00

Table 4: Simulated Passivating Cooling Water for Galvanized Towers

Test results can be seen in Figure 8. Note the resulting corrosion rates for GBCI indicate comparable corrosion rates to that of the untreated system. In contrast, ortho-PO₄ maintained higher corrosion rates throughout the test.

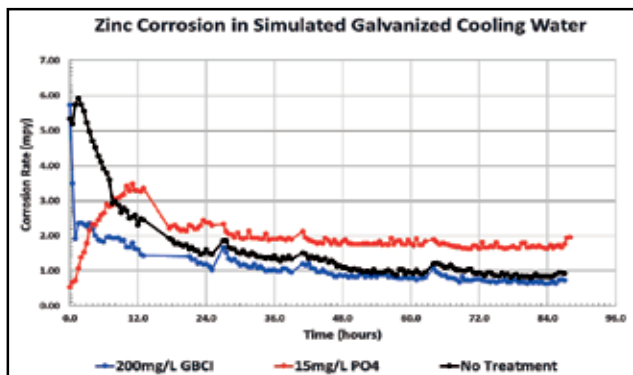


Figure No. 8 Corrosion rates for zinc in passivating water conditions.

Further evidence of the compatibility of GBCI with zinc is shown in the pictures in Figure 9. The formation of white rust is visibly evident on the electrode treated with ortho-PO₄ while the Waterline treated system showed no sign of white rust.

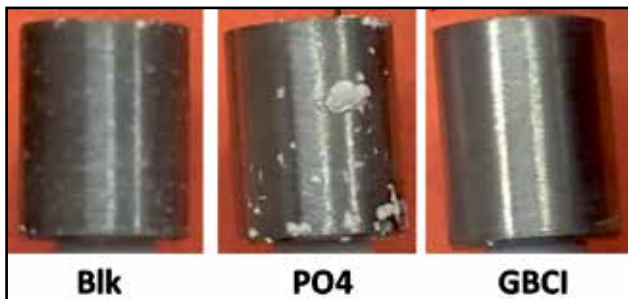


Figure No. 9 Zinc electrodes of various treatments in passivating water conditions.

White Rust Inducing Conditions

Using zinc electrodes, LPR test were conducted in a simulated cooling water chemistry representative of the conditions that would promote white rust formation on newly exposed galvanized metal. The GBCI product was again compared to a typical dosage of ortho-PO₄ that would be used for protecting carbon steel at these water conditions. An untreated system was again evaluated as a control. For all systems, 3.0mg/L PBTC, 5.0mg/L PMA, 2.5mg/L PAA and 20.0mg/L AA:AMPS copolymer were added to control calcium carbonate and calcium phosphate in these more stressed conditions. The specific water conditions are shown in Table 5.

Ca ²⁺ (as CaCO ₃)	300
Mg ²⁺	38.4
Na ⁺	161
Cl ⁻	395
HCO ₃ ⁻ (as CaCO ₃)	303
SO ₄ ²⁻	288
Additional Parameters	
TDS (mg/L)	511
Conductivity (µS/cm)	798
Temperature (°C)	40
pH	8.60-8.80

Table 5: Simulated Aggressive Cooling Water for Galvanized Towers

Test results can be seen in Figure 10. The GBCI maintained corrosion rates below that of an untreated system for a significant portion of testing. Meanwhile, ortho-phosphate again indicated higher corrosion rate than that of the untreated system.

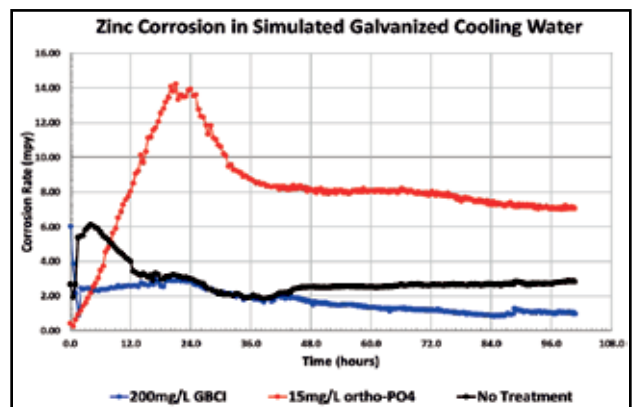


Figure No. 10 Corrosion rates for zinc in aggressive water conditions.

The photographs in Figure 11 reinforce the LPR test data by showing significant white corrosion deposits on both the phosphate and untreated electrode. In stark contrast, the GBCI treated electrode had significantly fewer areas containing these localized white deposits.

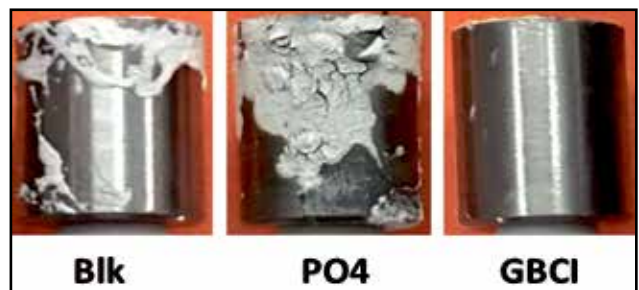


Figure No. 11 Zinc electrodes of various treatments in aggressive water conditions.

As a follow-up to the previous test in aggressive galvanized system water, a dosage curve of GBCI was generated to see its full effectiveness of GBCI as a zinc corrosion inhibitor. For these evaluations, individual dosages of 0.00, 100, 200, 400 and 800mg/L active GBCI were added to individual corrosion cells containing the aggressive water. LPR test were then conducted to monitor the corrosion rates of each cell. These results can be found in Figure 12.

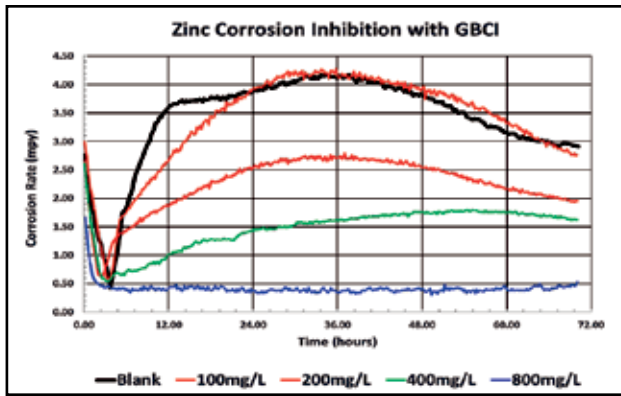


Figure No. 12 GBCI Dosage Curve for zinc metal in aggressive water conditions.

Test results indicated a clear trend in the reduction in zinc corrosion rates and applied dosage of the GBCI product. 100mg/L active GBCI performed comparably to the blank, while 800mg/L active GBCI reduced zinc corrosion rates to below 0.50mpy. These results suggest the GBCI product may be able to provide a significant degree of corrosion protection of galvanized surface in high pH, high alkalinity water conditions.

Additional testing was then conducted using electroplated galvanized metal coupons instead of zinc electrodes. These test were performed in two modified 14L aquariums equipped with aeration and circulation. The temperature was maintained at around 95°F. To each aquarium, a very aggressive water chemistry was applied that was very conducive to white rust formation. The specific water conditions are shown in Table 6.

Ion	Concentration (mg/L)
Ca ²⁺ (as CaCO ₃)	400
Mg ²⁺	38.4
Na ⁺	437
Cl ⁻	395
HCO ₃ ⁻ (as CaCO ₃)	410
SO ₄ ²⁻	288
Additional Parameters	
TDS (mg/L)	1818
Conductivity (µS/cm)	2841
Temperature (°C)	35
pH	8.90-9.10

Table 6: Simulated Aggressive Cooling Water for Galvanized Towers

Each aquarium was treated with 10.0mg/L active maleic acid homopolymer to control calcium carbonate precipitation. 3.0mg/L tolyltriazole was also added. One aquarium was treated with 200mg/L active GBCI while the other was not treated with any additional inhibitor. Four galvanized coupons were then degreased in acetone, rinsed and hung in each aquarium to then be removed weekly for visual observations and coupon analysis. Figure 13 depicts the front side of the coupon removed after one week. Figure 14 depicts the back of each coupon.

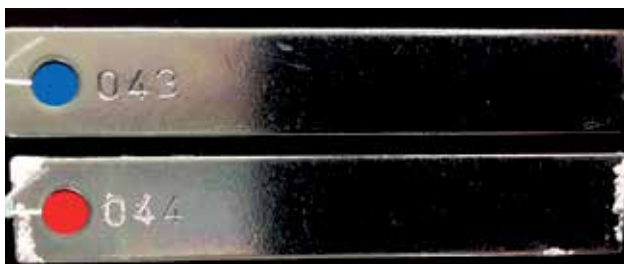


Figure No. 13 Front of galvanized coupons after one-week submersion in water Blue dot: 200mg/L GBCI | Red dot: no inhibitor

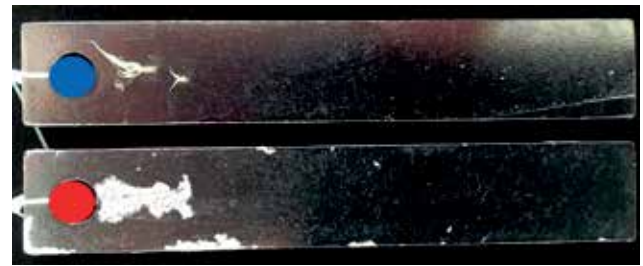


Figure No. 14 Back of galvanized coupons after one-week submersion in water. Blue dot: 200mg/L GBCI | Red dot: no inhibitor

Conclusions

While ongoing field trials will confirm the results, the laboratory performance data for both carbon steel and galvanized metal are very encouraging for the GBCI product's future in the industry. The product has several key benefits that can provide the water treatment professional a simplified approach to water treatment.

- For carbon steel, the GBCI has demonstrated the ability to outperform the existing phosphorous-based corrosion inhibitors at various conditions. With its excellent compatibility in high hardness water, there is no concern over corrosion inhibitor loss to calcium precipitation. This characteristic makes it a good alternative to the current alkaline phosphate and "all organic" corrosion programs used in the industry today. With no concern of fouling with calcium, phosphate stabilizing copolymers can also likely be eliminated or significantly reduced.
- For galvanized metal, the product offers a possible alternative to the recommended passivation procedures for when starting up new galvanized towers. Meanwhile, it would also be protecting carbon steel surfaces.

In addition, the GBCI product has demonstrated remarkable stability to oxidizing biocides as well as excellent formulation compatibility with other water treatment additives. When one considers the ongoing phosphorous regulations occurring on a global level, the GBCI appears to be a very good option as the alternative inhibitor for the industry.

References

1. Boffardi, B.P. "Chapter 4 Cooling Water" AWT Technical Reference and Training Manual, p. 4-76
2. Rey, S.P. "Carbon Steel Corrosion Control in the Past Twenty Years and in the New Millennium," The Analyst: Summer 2001
3. "Permit Compliance System (PCS) and Integrated Compliance Information System (ICIS) Databases." Envirofacts. U.S. Environmental Protection Agency. Web. 25 Apr. 2016. <<https://www3.epa.gov/enviro/>>.
4. United States. U.S. GEOLOGICAL SURVEY. NATIONAL WATER-QUALITY ASSESSMENT PROGRAM. Review of Phosphorus Control Measures in the United States and Their Effects on Water Quality. By David W. Litke. 99-4007 ed. Denver: U.S. GEOLOGICAL SURVEY, 1999. 1-43. Print. Water-Resources Investigations Report.

ENGINEERING PROBLEMS... INTO SOLUTIONS

**FOR 30 YEARS, KIPCON HAS BEEN
DESIGNING AND INSPECTING
COOLING TOWERS OF ALL TYPES.**

YOU NEED IT... WE DESIGN IT

Kipcon Inc. provides structural designs for new cooling towers and retrofits of existing towers, whether it be cross-flow, counter-flow, wood, concrete, fiberglass, wet and/or dry system. This includes basin design and basin load tables.

YOU HAVE IT... WE INSPECT IT

Kipcon Inc. provides complete cooling tower inspection services and can develop remedial plans of action for retrofitted towers. Kipcon Inc. now provides high quality and exceedingly efficient **drone inspections** for cooling towers. These inspections are easier, safer, and more accurate than ever before.

YOU WANT IT... WE WILL DRAW IT

Kipcon Inc. prepares drawing packages, including erection plans, connection and fabrication details using Autocad.

KIPCON ALSO OFFERS...

Structural evaluations of air cooled condensers for windscreen additions.



CALL US TODAY TO DISCUSS YOUR COOLING TOWER NEEDS.

kipcon.com ♦ info@kipcon.com ♦ (800) 828-4118



Wet-Dry Technology to Abate the Visible Plume From An Existing Cooling Tower

Mark Scholl, Alliant Energy
Jean-Pierre Libert, Evapco Inc.
Darin Baugher, Evaptech, Inc.

Project Background

In 2015, Alliant Energy (owner) undertook a test project to reduce the visible plume and its associated negative consequences in one cell, cell #4, of a 10 cell cooling tower at a combined cycle power plant located in Wisconsin. Not only was the plume severely reducing visibility at an adjacent Operations Center, causing yard operations to be suspended at times for safety, but icing also occurred on the parking lot and walkways, causing safety concerns. Additionally, plume would reduce visibility on a well-traveled country road north of the facility, and on heavy fog days, the plume would drift over the neighborhood located to the north-east of the plant, causing ice to form on resident's driveways and walkways.



Jean-Pierre Libert



Mark Scholl

In wet-dry mode of operation, a portion of the recirculating water flows inside the coil tubes while they stay dry outside. The remaining part of the recirculating water is sprayed over the wet fill. A schematic of the wet-dry mode of operation is shown in Figure 3.

In wet-dry mode of operation, the ambient air flowing over the coils heats up and mixes in the plenum with the saturated air from the wet fill. This lowers the relative humidity of the air leaving the tower and reduces the plume visibility. At the same time, the amount of water consumed by the tower is less because water evaporation only occurs in the wet fill.



Figure 1: Plume from Cooling Tower Blowing East over Utility Operations Yard

Several different options were investigated to reduce the plume, and the owner chose the EvapDri wet/wet-dry technology for a demonstration test.

The innovation of this technology is that the water to be cooled can be sprayed over the finned coils as an evaporative fill media (which retains summer-time efficiency) or flow inside the tubes as a dry heat exchanger.

What is EvapDri?

EvapTech (OEM) has developed a new wet/wet-dry plume abatement cooling tower. It combines wet fill and metallic heat exchangers in a counterflow cooling tower in a parallel-path wet-dry arrangement. The heat exchangers consist of elliptical finned-tube coils. This technology offers two main advantages: water conservation and plume abatement. Two key features include a low profile and the ability to retrofit existing equipment without significant modifications. The aesthetics of the existing tower remain unchanged and the footprint is not altered. No additional permitting is required and the system pumping head is not increased.

In wet mode of operation, a portion of the recirculating water is sprayed over the coils using them as fill media. As the coils operate as wet fill, the entire tower works as a wet (evaporative) cooling tower. A schematic of the wet mode of operation is shown in Figure 2.

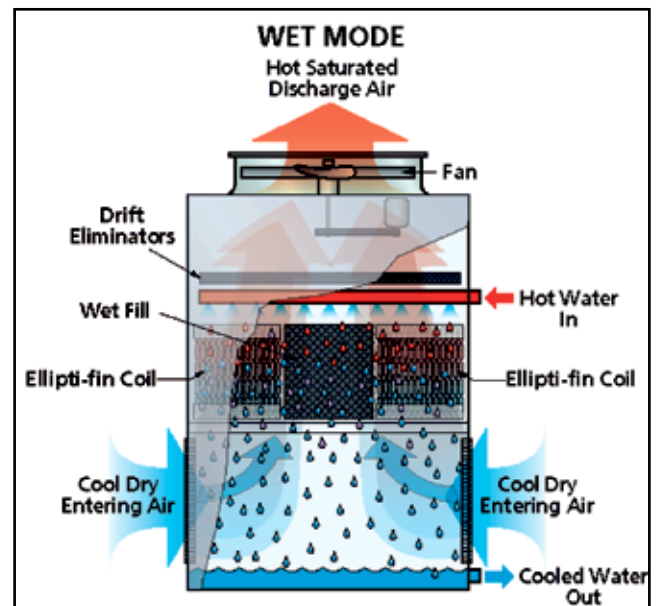


Figure 2: Wet Mode of Operation

The application of this technology in a cooling tower offers plume abatement and water conservation at the same time. Because the heat exchanger coils are located at the same level as the wet fill, this technology can be applied to new cooling towers as well as to the retrofit of existing cooling towers without dramatically changing their existing geometry. The height of the air inlet, fill air travel and plenum height are essentially the same as a conventional counterflow wet cooling tower so the overall height of this wet-dry cooling tower is the same as a typical cooling tower.

Technological Challenges

The use of heat exchanger coils does not convert this technology to a closed water loop. The recirculating water sprayed over the fill is still exposed to the atmosphere. In wet-dry mode, the recirculating water flows inside the tubes so the material used for the tubes must be corrosion-resistant inside. Typical tube material in closed water loops is carbon steel but for this application a corrosion resistant stainless steel must be selected.

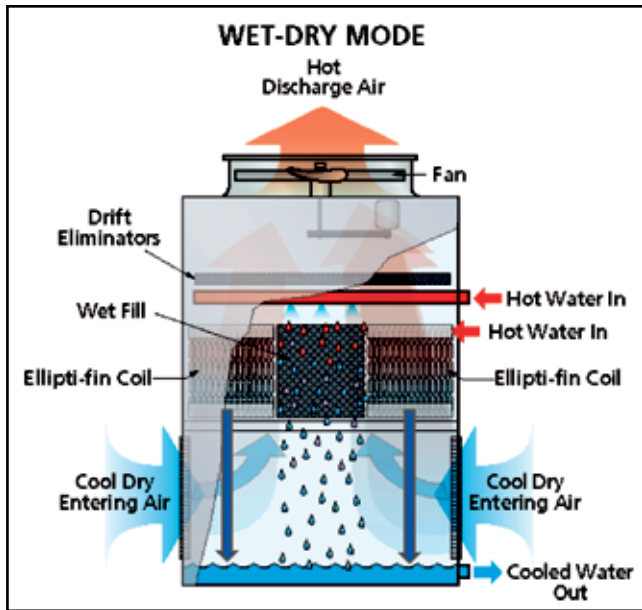


Figure 3: Wet-Dry Mode of Operation

Typical carbon steel coils are hot dip galvanized for corrosion protection. The stainless steel wet-dry coil tubes resist corrosion, but they are still galvanized. Why? Steel fins are tension-wound on patented elliptical tubes by a proprietary process. Even though there is a strong contact between fin base and tube surface, tests have demonstrated a significant difference in thermal performance between bare stainless steel coils and the same coils hot-dip galvanized. Elliptical finned-tube coils need to be galvanized to maximize heat transfer by enhancing the bond between fin base and tube wall. Austenitic stainless steels, such as 304 and 316, are subject to liquid metal embrittlement (LME) by molten zinc when welded to galvanized steel (Reference 1). LME can lead to cracking and potential leaks in the system. On the other hand ferritic stainless steels like 409, 439 and 444, are immune to attack by molten zinc so they are not subject to LME. They have corrosion resistance comparable to 304 and 316, which have a successful track record in cooling tower environments. In this application, the tubes are made of stainless 439 and headers and plates are made of stainless 409Ni. The fins can be either carbon steel or stainless 439.

Serpentine tubes assembled in a coil like the one shown in Figure 4 have multiple passes. The water-side pressure drop must be measured and known as a function of water velocity inside the tubes.

When operated in wet-dry mode, another challenge of this technology is to balance the water pressure drop inside the coils against the pressure drop of the water cascading through the wet fill. In a typical application the dry area and the wet area are evenly distributed. To increase plume abatement or water conservation, the dry area can be expanded and the wet area reduced accordingly.



Figure 4: Elliptical Finned-Tube Coil

Cooling tower spray nozzles typically operate at a relatively low pressure of 0.07 to 0.14 bar (1 to 2 psi) but the water-side pressure drop through a coil is of 0.28 to 0.55 bar (4 to 8 psi). Fortunately, the coils are installed at

the same level as the wet fill which is typically 3.05 to 6.10 m (10 to 20 feet) above the water level in the basin. By connecting the bottom header of the coil with vertical pipes that

drop down below the water level in the cold water basin, a siphon leg is created. In general "A practical siphon, operating at typical atmospheric pressures and tube heights, works because gravity pulling down on the taller column of liquid leaves reduced pressure at the top of the siphon (formally, hydrostatic pressure when the liquid is not moving)." The application of Bernoulli's equation to a siphon to calculate the flow rate can be found here: (https://en.wikipedia.org/wiki/Siphon#Explanation_using_Bernoulli.27s_equation)

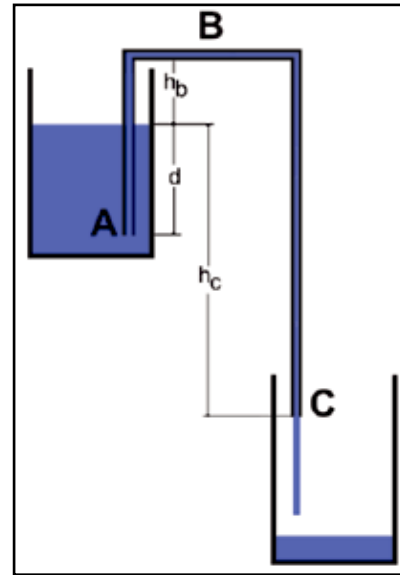


Figure 5: Siphon Principle

The height of the siphon is equal to the distance between the coil and the water level in the basin, and that distance is practically equal to, or even greater than, the pressure drop through the coil. So in wet-dry mode of operation the siphon assists in balancing the water pressure loss through the wet fill and the heat exchanger coils as it naturally pulls down the expected water flow through the coils without requiring the use of a booster pump. We validated this concept by physically testing it in a laboratory setting and measuring the flow through the coil in a typical geometry of installation, as shown in Figure 6.



Figure 6: Validation of Siphon in the Laboratory

Field Validation - Challenges

Installing this new technology into an existing operating cooling tower was the ideal way to prove the wet/wet-dry concept would adequately reduce plume, as it would provide a direct side-by-side comparison of performance. However, since the original cooling tower design never contemplated the addition of plume abatement equipment, the engineering team was presented with a variety of design and construction challenges. Once the decision to proceed was made, the owner wanted to install the wet/wet-dry "proof of concept" as soon as possible. This meant working in the

Introducing the Latest in Rental

Aggreko's new GT Series Cooling Towers combine the modularity of the AG cooling tower with the portability of an intermodule freight container.

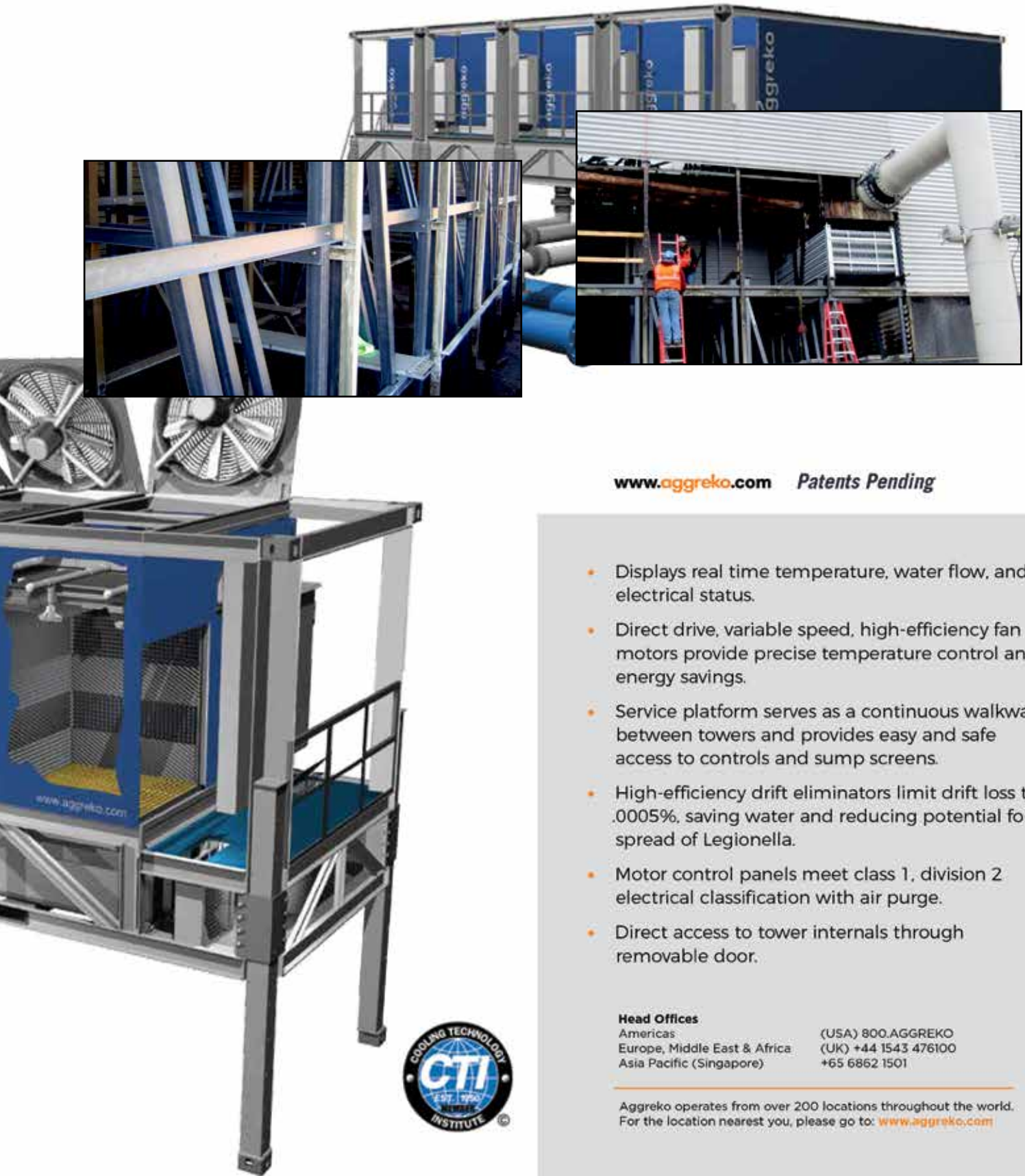
GT-20 400-1600 GPM



GT-40 900-4000 GPM



- Freight cost reduced by 40% with 20 ft. and 40 ft. ISO container frame.
- Modular design and interconnectability allows infinite expandability.
- Telescoping substructure provides safe and easy extension during installation.
- Integrated basin and air inlet system reduces tower height, saving space and improving energy efficiency by reducing pump head.
- External sump provides easy access to two sets of dual sump screens and the make-up water float valve.
- Internals constructed from stainless steel, FRP and PVC allow for operation in harsh conditions, including sea water applications.
- Proprietary water distribution system with no moving parts maintains constant thermal performance at ALL flow rates without the need to change nozzles or nozzle orifices.
- Equipped with remote monitoring capabilities, increasing efficiency and decreasing downtime.



www.aggreko.com Patents Pending

- Displays real time temperature, water flow, and electrical status.
- Direct drive, variable speed, high-efficiency fan motors provide precise temperature control and energy savings.
- Service platform serves as a continuous walkway between towers and provides easy and safe access to controls and sump screens.
- High-efficiency drift eliminators limit drift loss to .0005%, saving water and reducing potential for spread of Legionella.
- Motor control panels meet class 1, division 2 electrical classification with air purge.
- Direct access to tower internals through removable door.

Head Offices

Americas
Europe, Middle East & Africa
Asia Pacific (Singapore)

(USA) 800.AGGREKO
(UK) +44 1543 476100
+65 6862 1501



Aggreko operates from over 200 locations throughout the world.
For the location nearest you, please go to: www.aggreko.com

cold winter weather of December and January. The construction crew mobilized in December 2015 to begin with the retrofit of one cooling tower cell at the site.

Existing Tower – Structural Upgrades

The existing fiberglass cooling tower structure was not deemed to be sufficient to support the new coils. Rather than use some of the existing framework to support the new coils, the decision was made to design and install a 100% independent fiberglass framing system to avoid overtaxing the nearly 15 year old tower framework. Each of the 16 coils weighed approximately 8500 pounds, so a new system of columns and diagonals was needed in the air-inlet region of the tower (Figure 7). The new framing was anchored to the cold water basin as well.

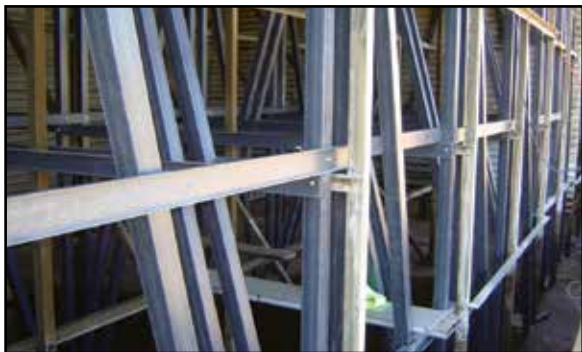


Figure 7: New Fiberglass Coil Supports alongside Existing Supports

Construction Challenges

The existing cooling tower distribution header pipe is located at the end bay of each cell. Rather than supply a new system of headers and laterals, we were able to reduce costs by field-modifying the existing 30" diameter FRP header pipe. The dimensions of the each cell is 52.48' L x 52.48' W x 32.88' H. Each cell consists of 8 bays on 6.56' centers in both directions. Approximately half of the laterals (each of the outer 2 bays) were removed and capped off, and each of these areas received a new 16" diameter wet section sub-header and a new dry section sub-header pipe. The inside half of the tower used the existing system of laterals and nozzles unaltered. All of the existing fill was removed. The inside half received new high efficiency film fill, with the outer portions containing the coil bundles. Installing the 8500 pound coil bundles in the pre-existing cell presented a special challenge, since they had to be "shoehorned" through the side of the tower, not unlike sliding a kitchen drawer in a cabinet. Special industrial rollers and lifting rigs were employed to carefully move the coils into place. Near the hot water riser, a section of column had to be cut away to maneuver the coils into place (Figure 8).



Figure 8: First Coil in Place

Weather Challenges

Working on an operating cooling tower in winter presents inherent challenges. These include fogging and leaks from adjacent cells that resulted in ice formation. Because the crews were working over water, the cold water basin was planked over with plywood to prevent debris from entering

the circulating water system. Cold weather also slowed and complicated the field pipe work: gluing PVC piping and making fiberglass field joints required additional time to set and portable heating devices to create a suitable environment.

Safety Challenges

Due to the exposed work area where the coils were installed, temporary supports were needed for worker access and safety. Coils weigh approximately 8500 pounds each, so since the new coils were lifted by crane any "swing" had to be eliminated. Workers had to be conscious of pinch points during coil installation. Also, with up to 40 workers spread out across the ten cell tower, exceptional communication was a must to prevent delays in schedule and to maintain a safe environment.

Startup activities

In February 2016, water was turned on over cell #4 with the valves set up to operate in wet-dry mode and the fan was turned on. The air inlet is 12.33 feet tall without louvers. The tower is set on a common concrete basin with a centrally located flume leading to the cold water pumps. Water is piped in from the plant via two underground headers which combine to feed each of the ten 30" risers, each having a single thermo-well installed at the base with dual taps placed further up to facilitate flow measurement with a Pitot tube.

The modified cooling media includes 16 elliptical finned-tube coils paired with new high efficiency film fill to balance the wet performance of the coils during wet mode operation. There are two banks of coils, each placed adjacent to the air inlet on either side of the tower. The tower is also fitted with new drift eliminators to further reduce the discharge air mass by reducing the drift discharge to an estimated 0.0005% drift rate.

Measurement of the effluent air and plume characteristics

As part of the effort to determine the effectiveness of the plume reduction, after a few weeks of operation in wet-dry mode, we attempted to perform a plume abatement test in accordance with Cooling Technology Institute (CTI) Standard ATC-150, with mixed results. A number of operation parameters and safety requirements prevented us from conducting a complete plume abatement test.



Figure 9: Clear Boundary between Dry and Wet Areas in the Tower Plenum

Plume abatement test Standard ATC-150 was used as the basis of conducting plume reduction testing (Reference 2). The standard dictates both environmental and equipment operating conditions which must be present during testing along with the acceptable locations and methods to take the required measurements.

Temperatures were collected using 4-wire precision platinum resistance temperature detectors (RTDs). Temperature data was collected every 30 seconds with a data acquisition system having a resolution up to 0.01°F. RTDs were used for entering wet-bulb, entering dry-bulb, hot water, exhaust wet-bulb, and exhaust dry-bulb temperatures. Cold water temperature from the retrofit cell could not be isolated from the adjacent cells.

The exhaust and inlet air temperatures were averaged over several hours of measurement. Exhaust air velocity, air wet-bulb and dry-bulb temperatures were measured over the fan for 5 minutes at each of the 20 positions speci-

fied by ATC-150. The final exhaust temperatures were determined by finding the most stable 3 minutes out of the 5 minutes recorded. Some points where temperatures drastically changed showed a slope as readings approached steady-state. This slope was seen in the transition from no plume to visible plume, as the measurements approached the center of the fan.

The pitot measurement found a water flow rate of 90.4% of design flow. The measurement showed a relatively well developed flow.

The cold water temperature from cell #4 could not be measured because the tower sits on a common basin and it was not possible to isolate it from the other cells. The lack of accurate hot and cold water temperatures alone (the temperature range) eliminate drawing firm conclusions because this data point forms the foundation of plume abatement performance curves used for analysis as part of the CTI Standard.

The wind velocity and directions were measured with a weather vane located upwind from the tower. During stack measurements, the wind velocity was higher than specified by the standard, well above the limits of 6.5 MPH average and 10 MPH gusts. Because of the high gusting winds, anemometer readings above the fan were erratic, which added scatter to the averages. A significant number of readings fluctuated more than 200 FPM between minimum and maximum instantaneous readings while others pushed over 500 FPM fluctuations. This caused us to question several of the recorded data points.

The test conditions detailed by ATC-150 define both the methods and operating characteristics required to achieve an acceptable test per the code. The purpose of the defined methods and operating limits is to provide reliable plume abatement test results with a low level of uncertainty. Unfortunately, compromises were made on site to address operational availability and safety in the taking of measurements. During testing, most data sets were collected in accordance with the defined testing methodology using calibrated instrumentation, but several data sets were collected from uncalibrated plant instruments.

The main goal of the testing efforts was to derive a quantified result of the leaving air relative humidity and temperature to compare it to the theoretical predictions, using the Tower Plume Indicator defined by ATC-150. Some test conditions and compromises due to plant operation and safety concerns added a substantial amount of uncertainty in the test results. The uncertainty is high enough to not be able to calculate an accurate Tower Plume Indicator. Furthermore the sensitivity analysis, discussed below, shows the effect of key parameters on the results. Because of these challenges and uncertainties, it is not possible to draw a definitive quantitative conclusion on the plume reduction outcome using CTI Standard ATC-150 guidelines with a reasonable level of accuracy. When we calculate the effluent air relative humidity using common sense assumptions the anticipated result between measured effluent air relative humidity and predicted effluent air relative humidity lies within a +/- 5% tolerance on the measurements.



Figure 10: The 4th Cell from the Left Is Operating In Wet-Dry Mode

Visual observations of the tower retrofit clearly demonstrate the plume abatement achieved is significant when compared to the adjacent cells (Figure 10). The owner installed a time-lapse camera on the roof of the plant building with web access to visualize the plume in real time day and night. Images leave little doubt that the retrofit effectively provides a significant reduction in plume versus the pre-retrofit operation.

Additional measurements and testing following the comprehensive retrofit of the remaining cells will yield quantifiable results. During future testing we intend to add testing measurements within the tower plenum above the dry and wet sections to further validate our predictions and provide the owner with additional insight.

Measurement Sensitivity Analysis

In an effort to gain a better understanding of the test data gathered for our own internal purposes and a better understanding on the effect of the measurements that were out of code, our test engineers conducted an extensive sensitivity study which included several variables.

Exhaust Velocity Angle: The measured velocity exiting the fan stack is not vertical. There is a horizontal vector added due to the characteristics of rotating axial fan blades (yaw). The yaw correction is used to compute the vertical component of the velocity to calculate the mass flow of air. If this correction is removed, in other words if we ignore the angle measurement, the effect on the calculated exhaust relative humidity would only be 0.1%, which is statistically irrelevant.

Exhaust Air Traverses: Like the exhaust velocity angle, the velocity measurements themselves showed little statistical significance on the result. No matter how we skewed the velocity measurements, the calculated exhaust relative humidity did not significantly change.

The largest impact on the performance uncertainty was found in the leaving air conditions of the four measured quadrants of the fan. The first two quadrants traversed showed a much lower exhaust relative humidity than the last two that were measured.

Fan Quadrants	Exhaust RH
All Quads	75.7%
Just Q1	56.8%
Just Q2	66.7%
Just Q3	91.9%
Just Q4	87.3%
Q1+Q2+Q4	69.9%

In the table above which compares exhaust relative humidity averaged by quadrant, each of the quadrants should be symmetrical. Removing one quarter of the fan should have no statistical bearing on the result. However, looking at the average of Q1, Q2 and Q4 (removing Q3), the exhaust RH drops by nearly 6%, which is significant.

This can further be seen in Figure 11 below. The four fan traverses can be seen distinctly. The first two have a much greater margin between the exhaust wet-bulb and dry-bulb (indicating lower relative humidity), while the last two traverses do not.

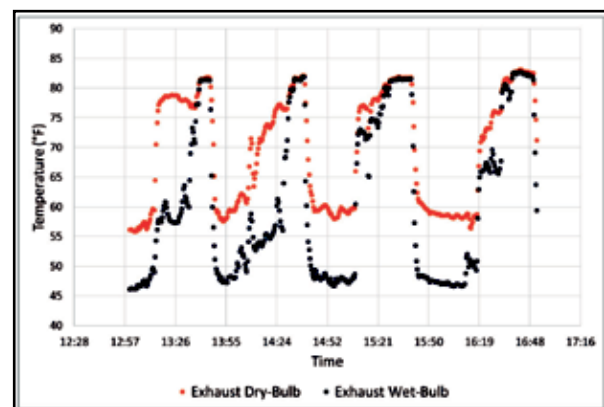


Figure 11: Time vs exhaust temperatures. The peaks represent the four distinct quadrant measurements. The trends show the difference in measurement between the early and later quadrants.

Wind: The large differences between the exhaust air wet-bulb and dry-bulb are likely due to the wind. The test took place over a time of nearly 5 hours. There was wind present the duration of the test. Figure 12 below shows the wind velocity and direction during the length of the test.

It's subtle, but the wind does shift directions midway through the test. And when this is overlaid over the exhaust temperatures measured during the four traverses, it is probable that the wind shift account for the differences seen in the average exhaust humidity of each quadrant.

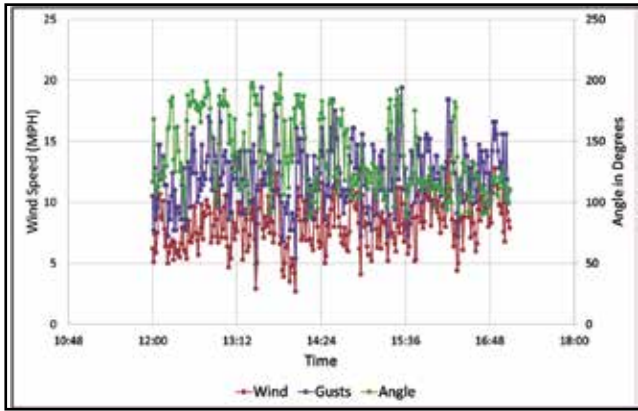


Figure 12: Time vs Wind Speed and Wind Direction. This 3-axis chart shows the wind speed average and gusts as well as the direction of wind measured by the wind station. The chart shows the highly inconsistent winds with respect to velocity and direction. A direction change can be denoted midway through of the test.

Ambient Temperature: There appeared to be recirculation with the tower, which was measured by wet-bulb instruments located in the air inlet. The minimum inlet relative humidity was measured to be 39.4% during the length of the test, while the maximum was measured to be 54.6%.

While this may seem sizeable, the effect on the predicted outlet relative humidity is only 5%, which is only +/- 2.5% from the relative humidity calculated from the average.

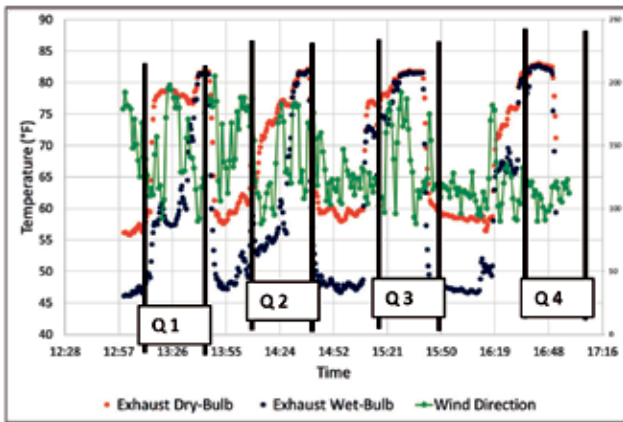


Figure 13: Exhaust measurements. 4 peaks show the 4 radii measured with some visual steps for the measurement starting from the outside of the fan stack. The first axis references the temperatures while the second axis is reference to the wind direction measured.

The sensitivity study showed that high winds and hot air recirculation had the largest effects on the exhaust temperature measurements, which resulted in a higher than normal uncertainty of the test results.

Benefits

The wet/wet-dry technology provides for both plume abatement and water conservation, and these are the fundamental advantages of the product. In addition, the unique positioning of coils in the fill region of a counterflow tower provides some inherent advantages over traditional plenum mounted heat exchanger designs. These advantages include:

1. Proven Coil Technology – Although reconfigured in an innovative way, finned stainless steel coil technology has been used for over 40 years in plume abated cooling towers. The coils are pressure-tested at the factory and shipped pressurized to ensure they are leak-free. Coils are durable and are not susceptible to embrittlement, folding or bonding concerns like non-metallic heat exchangers.
2. Low Profile compared to traditional parallel path wet-dry – With the coils in the fill area, this means the tower plenum remains a standard height, thus reducing the overall height of a new tower from 15' to 30', which also makes fan deck access easier and safer.

3. When installing the coil bundles as a retrofit, tower operational characteristics, footprint and aesthetics remain intact, thus no permit changes are needed.
4. Simple Operation – This wet/wet-dry concept eliminates the need for a complicated system of dampers, actuators and controls, and instead uses simple butterfly valves (Figure 14) to switch from summer to winter operation. Dampers are subject to freezing and mechanical failures that do not affect flow control valves.
5. Hydraulically speaking, it is self-starting and does not need the assistance of vacuum pumps to prime it or to hold vacuum, like tall vertical dry coils do.



Figure 14: Valve Actuators on Fan Deck

Surprise Advantages

By doing a full scale test cell in the field, the new technology exhibited several unexpected benefits to the owner. These include:

1. Same Pumping Head – When originally conceived, the wet-dry coils were expected to require the addition of booster pumps to properly drive water flow. However, lab testing showed, and field results confirmed, that the existing circulating water pumps can drive the system with enough head to establish a siphon loop without the need for booster pumps.
2. Reduced Ice Formation – During winter operation, water flows over the interior sections of the cooling tower only (Figure 15 below), which is far away from the coldest air at the tower air inlet. This greatly reduces ice formation on the tower framing and lowers the risk of structural damage.
3. Reduced Sound Levels – With no plenum mounted dampers to allow sound from the mechanical equipment to escape, the new design will project less sound than other systems when in wet/dry mode. Further, air inlet sound levels were measured 3 dB lower when the tower was in wet/dry mode due to falling water being well inboard of the tower perimeter (Figure 15).



Figure 15: Falling Water in Wet-Dry operation



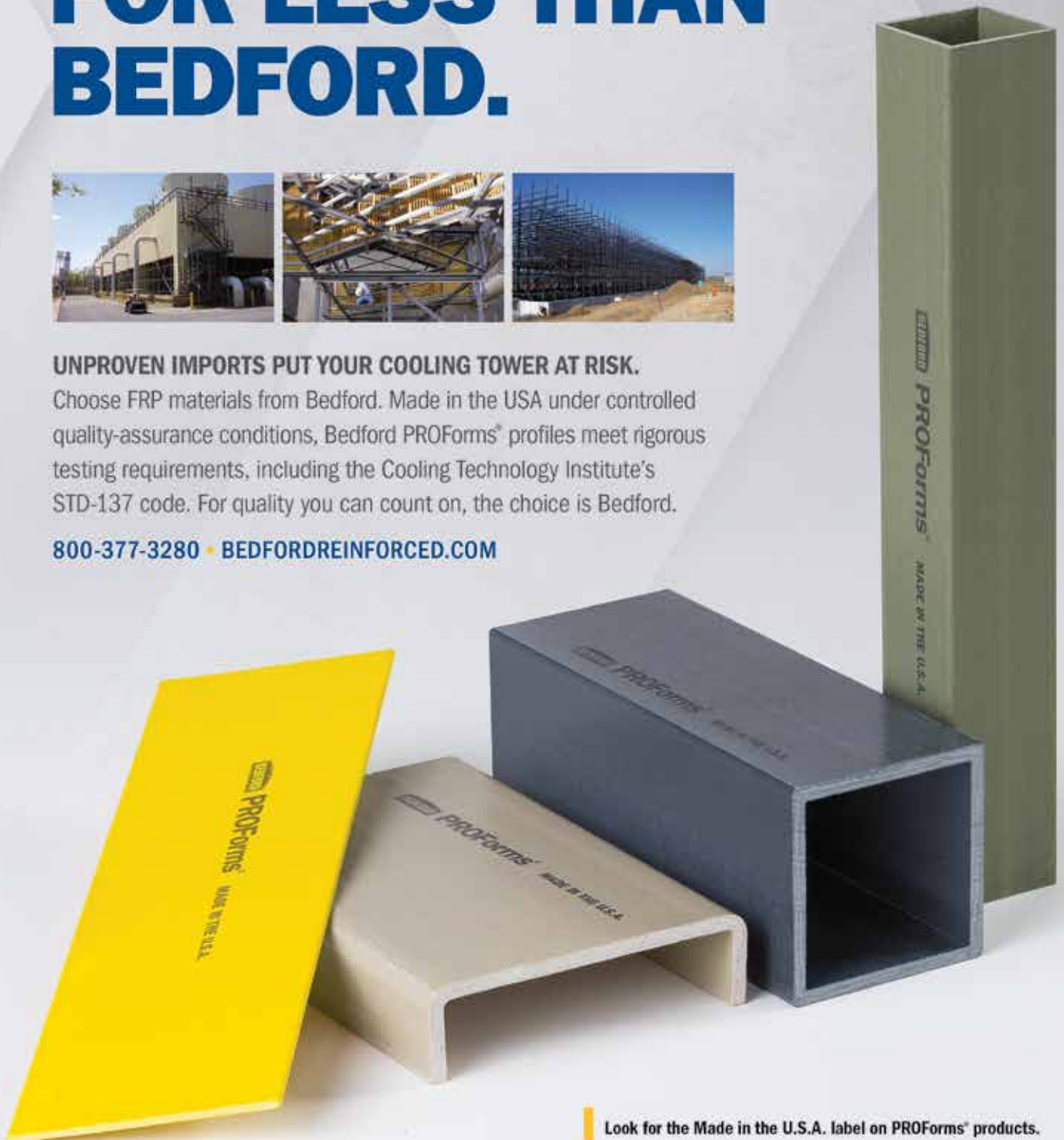
DON'T SETTLE FOR LESS THAN BEDFORD.



UNPROVEN IMPORTS PUT YOUR COOLING TOWER AT RISK.

Choose FRP materials from Bedford. Made in the USA under controlled quality-assurance conditions, Bedford PROForms® profiles meet rigorous testing requirements, including the Cooling Technology Institute's STD-137 code. For quality you can count on, the choice is Bedford.

800-377-3280 • BEDFORDREINFORCED.COM



Look for the Made in the U.S.A. label on PROForms® products.

Water chemistry control, passivation control

Passivation is a process that results in the formation of a protective film on galvanized surfaces. Passivation protects against the creation of white rust, which can reduce coil longevity and also prevents zinc from leaching into the plant discharge water. Passivation of the galvanized coils was accomplished in place by reducing the tower pH from 8.3 to 7.8 and adjusting tower cycles as necessary to minimize effects on cooling water systems. Zinc concentrations were monitored in the water droplets from the coils as well as the basin. Zinc loss was minimal during the passivation process.



Figure 16: Triangle of Clarity over Cell #4



Figure 17: Heavy Plume Conditions during Night-time Operation in Winter

Finishing the Job – Completion of the Remaining 9 cells

With the success of the test cell, the owner and the OEM are currently working together to outfit the remaining 9 cells. The lessons learned from the test cell installations are proving valuable as the team completes the full scale installation. The tower is expected to be fully operational by January 2017.

Conclusions

Although this wet/wet-dry technology has been utilized for several years in unitary packaged towers for both plume abatement and water conservation applications, this is the first large scale installation designed specifically to reduce troubling plume in a large scale field-erected counterflow cooling tower.

Using one cell of the existing tower as a plume abated pilot over several winter months, the owner was able to demonstrate the benefits of the technology to all stake-holders, including local authorities, neighbors and corporate leadership.

Acceptance of this wet-dry technology opens up new opportunities for the retrofit of existing cooling towers, as well as easier siting and faster permitting of new plants in densely populated areas where plume abatement and water conservations are key issues.

Bibliography

1. Liquid Metal Embrittlement of Austenitic Stainless Steel When Welded to Galvanized Steel, R. M. Bruscatto, Welding Research Supplement, December 1992
2. Cooling Technology Institute (CTI) Standard ATC-150 Acceptance Test Procedure for Wet-Dry Plume Abatement Cooling Towers, July 2011

evaptech RESEARCH POWERED SOLUTIONS

Series **ES** & Series **ESP**

**SINGLE & MULTI-CELL FIELD ERECTED,
FIRE-RETARDANT COUNTERFLOW
COOLING TOWERS**

evaptech

EVAPTECH, INC.
A WHOLLY OWNED
SUBSIDIARY OF EVAPCO, INC.
8331 NIEMAN ROAD
LENEXA, KS 66214
913.322.5165
MARKETING@EVAPTECH.COM
WWW.EVAPTECH.COM

evaptech

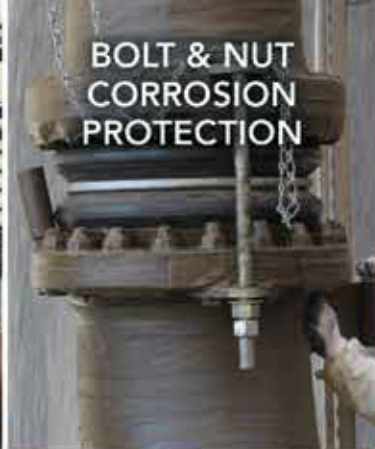
EVAPTECH ASIA PACIFIC, SDN. BHD.
B-6-1, IOI BOULEVARD
JALAN KENARI 5,
BANDAR PUCHONG JAYA
47170 PUCHONG
SELANGOR DARUL EHSAN
MALAYSIA
PHONE: (60-3) 8070-7255
FAX: (60-3) 8070-5731
MARKETING-AP@EVAPTECH.COM
WWW.EVAPTECH.COM

- Reliability of Operations
- Hardened to Survive - SafeWall™ casing technology resists damage from airborne debris.
- Cost Effective – Cost comparable to fire protection systems.
- Customizable Fill Components – High performance low-fouling fills.
- Low Drift Rates – as low as 0.0005%.
- Air Inlet Treatments – Optional cellular PVC or wide-spaced louvers available.
- Product Quality is a Given – Quality audits of all combustible components by FM Approvals.
- Avoid Thermal Redundancy – Extra or over-sized cells not required.

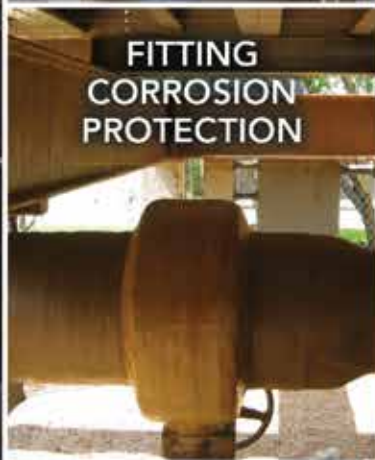
**TECHNOLOGY FOR THE FUTURE,
AVAILABLE TODAY!**



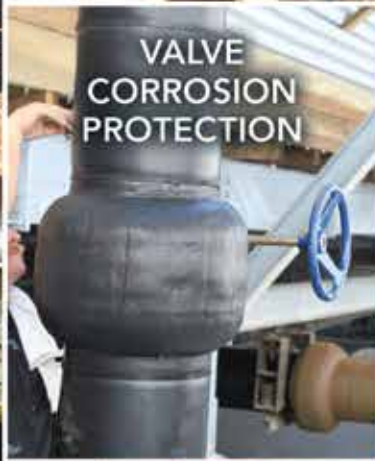
Denso[®]



**BOLT & NUT
CORROSION
PROTECTION**



**FITTING
CORROSION
PROTECTION**



**VALVE
CORROSION
PROTECTION**



PIPING CORROSION PROTECTION



STRUCTURAL STEEL CORROSION PROTECTION

LEADERS IN CORROSION PREVENTION

Denso provides easy to apply corrosion prevention through our petrolatum tape system that is non-toxic (No VOCs), requires no special training to install and only minimal surface preparation with no abrasive blasting needed.

www.densona.com

Call: +1 281-821-3355 E-mail: info@densona.com

Since 1886
135
Years of Science & Industry



Denso[®]

Modeling Scale Inhibitor Upper Limits: In Search of Synergy

Robert J. Ferguson, French Creek Software, Inc.

Existing models for calculating the minimum effective inhibitor dosage for scale control have been applied to industrial and oil field scale control treatment optimization since the 1970s. Standard correlations are routinely used in developing the models.^{1,2,3,4,5,6,7} The models typically apply to a single inhibitor. There is a driving force limit for each inhibitor, above which scale control cannot be achieved regardless of the inhibitor dosage. Knowing the upper limit is critical for selecting the optimum treatment program and in specifying control limits for a system such as an open recirculating cooling tower or membrane system. Limits for individual inhibitors have been well documented. Studies have been conducted to determine the impact of blending inhibitors on the upper driving force limit. Upper driving force limits, as expressed by calcite saturation ratio, were measured for calcium carbonate inhibition by individual inhibitors and combinations. Results were evaluated and blends found to:



Robert J. Ferguson

- increase the upper limit above that of either inhibitor when applied alone (synergism),
- decrease the upper limit (antagonism or competitive inhibition), or
- provide an upper limit in between that of the individual inhibitors (equivalent efficacy).

Test methods, data, and correlations are presented and discussed with respect to mechanisms.

How Inhibitors Work

When reactants are mixed, a solution is heated, cooled, undergoes a pressure change or is otherwise perturbed, the impact of the environmental changes is not immediate. A finite time passes before the perturbation affects any susceptible reaction. In the case of scale formation, induction time can be defined as the time before a measurable phase change (precipitation or growth) occurs after perturbation.^{4,7} In a pure system, with only the reactants present such as calcium and carbonate, or barium and sulfate, scale formation might proceed as follows:

1. Aqueous calcium carbonate molecules congregate, and form larger and larger clusters.
2. The clusters grow to a critical size and overcome the "activation energy" needed for the change from the "aqueous" to "solid" phase to occur.
3. The phase change is then observed. In the case of CaCO_3 , pH drops as the salt changes phase, and the induction time can be defined.
4. Crystals will then grow.

Scale inhibitors do not prevent scale. They delay the inevitable. The minimum, effective dose for a given water will prevent scale formation, or growth, until the water has passed through the system. The time until scale formation or growth is initiated is termed induction time. Scale inhibitors are induction time extenders. Untreated, there is a baseline induction time before scale growth occurs ($T_{\text{induction } 0}$). This baseline induction time decreases as the driving force for scale formation increases. So induction time decreases as scale driving force like saturation ratio increases.

$$\text{Equation 1) } T_{\text{induction } 0} = \frac{1}{k [x \text{ Saturation}]^M}$$

Inhibitors extend this time by interfering with one of the steps in scale formation or growth (T_{extended})

$$\text{Equation 2) } T_{\text{extended}} = \frac{[\text{inhibitor}]^N}{[x \text{ Saturation}]^M}$$

where

$T_{\text{induction } 0}$ is the induction time untreated

T_{extended} is the induction time when treated

inhibitor is the scale inhibitor molar concentration

M is a coefficient related to the number of molecules in a critical cluster

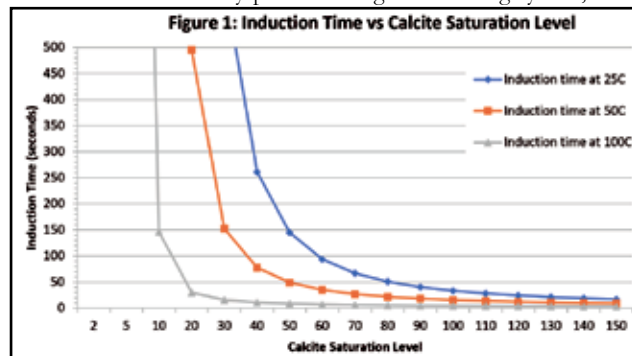
N is a coefficient

k is a temperature dependent rate constant

Saturation is the saturation ratio^{8,9,10,11,12} as defined in Table 1.

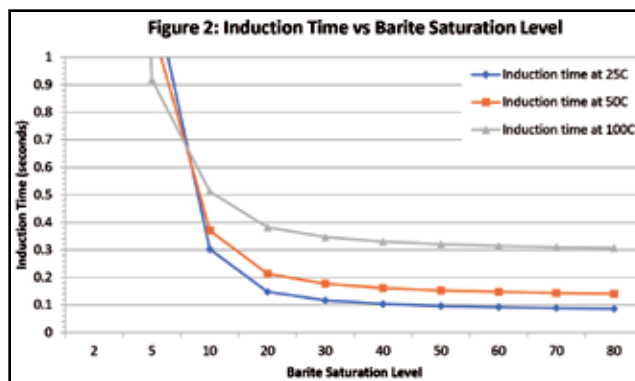
Induction time has been studied extensively for industrial processes. Original crystallization studies were conducted for sucrose crystallization to maximize production. In the case of sucrose crystallization, the objective is to minimize induction time and maximize crystallization.

In the case of scale control, the objective is to extend the induction time until a water has safely passed through the cooling system, or other



process adversely affected by scale. The induction time, in the absence of a scale inhibitor, has been modeled for common scales, including barite (BaSO_4) and calcite (CaCO_3) for oil field brines. Figures 1 and 2 are derived from this study, and compared to related works.⁴ The same laboratory procedures used to model induction time in oil field brines have been found to apply equally as well to cooling water and other scale forming systems.

Figure 1 profiles the untreated induction time for calcite in the practical operational range for calcite of 0 to 150x saturation. This range was chosen because it is the effective range for most scale inhibitors. The 150x saturation level limit is a commonly accepted upper limit for operation with common inhibitors such as phosphonates and polymers. Figure 2 profiles the saturation level range for barite, 0 to 80x saturation.



It should be noted that the induction times for both calcite and barite are several orders of magnitude below the typical residence time in an open recirculating cooling water system, oil field production process, or membrane

Quality & Workmanship Backed By
Amarillo Gear 1 Year Warranty.

RENEWING YOUR AMARILLO® GEAR AS EASY AS 1-2-3.



Great
Value!



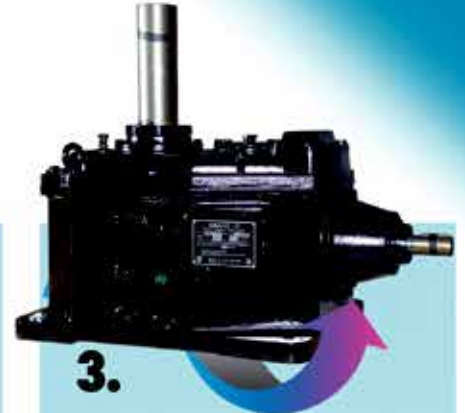
1.

When you contact **Amarillo Gear Service™** about RENEWING your drive, we will send you a Not To Exceed quote to give you an idea of the potential total cost of RENEWAL.



2.

After receiving your drive, an **Amarillo® Gear Technician** will inspect for wear and damage. Many times there are parts that can be cleaned and reused providing you, the customer, with considerable cost savings. You will then receive an As Found Condition Report, photographs and an updated quote.



3.

Finally, after your approval, your drive will be **RENEWED**, inside and out, tested, painted and returned to you with an As New one year warranty.

(806) 622-1273 • info@amarillogear.com • AmarilloGearService.com

Amarillo Gear Service™ is focused on keeping existing gear boxes, ...existing. A gear drive that you may have thought was ready to be replaced, may now have the opportunity for a new life with quality, Amarillo parts and service. Ask us about our ACC and Industrial gear box renewal programs.

Contact us and let's see if we can take the **stress** out of your old gear drive.



**Amarillo
Gear Service™**



Amarillo
Gear
Company LLC

A division of Amarillo Gear Company, LLC



A Marmon Water/Berkshire Hathaway Company

system. As a result, the use of the thermodynamic saturation ratios for predicting scale is accurate and an acceptable practice in typical operating ranges for these systems.

Actual induction times in practical operating systems will typically be lower than those of a pure system. Existing "seed" crystals and deposits provide a substrate for crystal growth without the necessity for achieving the "activation energy" for the initial phase change. In other words, it is easier to keep a clean system clean than to keep a dirty system from getting dirtier. Other factors can also decrease induction time. Ideally, studies will incorporate both "seeded" and "unseeded" conditions.

It is imperative that the upper driving force limits for inhibitors be known so that dosages curves and inhibitors are not applied to waters above the point where no dosage of the inhibitor will be effective.

Growth on Existing Substrates

At low saturation ratios, below the critical saturation ratio where seed crystal formation occurs, precipitation occurs by growth at active sites on an existing substrate. For precipitation from a pure solution, the substrate would be the scale of interest. In an operating practical environment such as oil field production, an industrial cooling system or a reverse osmosis unit, the substrate could be any surface where growth might occur.

TABLE 1 - SATURATION LEVEL FORMULAS	
Calcium carbonate	$S.L. = \frac{(Ca)(CO_3)}{K_{sp} CaCO_3}$
Barium carbonate	$S.L. = \frac{(Ba)(CO_3)}{K_{sp} BaCO_3}$
Strontium carbonate	$S.L. = \frac{(Sr)(CO_3)}{K_{sp} SrCO_3}$
Calcium sulfate	$S.L. = \frac{(Ca)(SO_4)}{K_{sp} CaSO_4}$
Barium sulfate	$S.L. = \frac{(Ba)(SO_4)}{K_{sp} BaSO_4}$
Strontium sulfate	$S.L. = \frac{(Sr)(SO_4)}{K_{sp} SrSO_4}$
Tricalcium phosphate	$S.L. = \frac{(Ca)^3(PO_4)^2}{K_{sp} Ca_3(PO_4)_2}$
Amorphous silica	$S.L. = \frac{H_4SiO_4}{(H_2O)^2 * K_{sp} SiO_2}$
Calcium fluoride	$S.L. = \frac{(Ca)(F)^2}{K_{sp} CaF_2}$
Magnesium hydroxide	$S.L. = \frac{(Mg)(OH)^2}{K_{sp} Mg(OH)_2}$

Seed Crystal Formation and Growth

Above the critical saturation ratio, spontaneous nucleation can occur, followed by growth on the seed crystals. As the degree of supersaturation increases, the rate of seed crystal formation increases.

The Behavior of Inhibitor Blends – Saturation Ratio Limit

Inhibitors have an upper driving force that they can handle. Once this upper limit is reached, even increasing inhibitor dosage drastically will not provide scale control. Inhibitors included in this study are outlined in Table 2. Typical upper limits for single inhibitors are outlined in Table 3.

Table 2: Inhibitors and Blends Included in the Saturation Limit Evaluation	
Inhibitor	
ATMP	amino tris (methylene phosphonic acid)
HEDP	1-hydroxy ethylidene-1,1-diphosphonic acid
PBTC	2-phosphonobutane-1,2,4-tricarboxylic acid
Enh PMA	polymaleic anhydride, enhanced
ATMP:HEDP blends	
HEDP:PMA blends	
PBTC:PMA blends	

It has been known that blending inhibitors can increase the upper limit. The combination of a phosphonate and PMA, for example, has been observed to raise the upper limit well above that of the phosphonate alone. Not all combinations or ratios show this positive effect. Possibilities for the impact of inhibitor blends on the upper limit include:

- The limit for the blend would be the lower of the limits for the inhibitors in the blend
- The limit would be a weighted average of the limit for each inhibitor when applied alone.
- The limit would be the higher of the limits for the individual inhibitors in the blend.
- The new limit would be higher than the limit for any of the inhibitors in the blend.

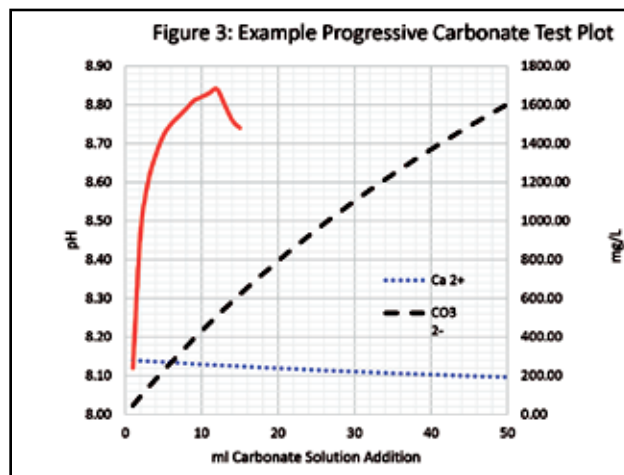
Table 3: Typical Treated Limits Comparison				
SCALE FORMING SPECIE	FORMULA	MINERAL NAME	TYPICAL TREATED SATURATION RATIO LIMIT	STRESSED TREATMENT LIMIT
Calcium carbonate	CaCO ₃	Calcite	125 - 150	200 - 225
Calcium sulfate	CaSO ₄ *2H ₂ O	Gypsum	2.5 - 4.0	4.0 +
Barium sulfate	BaSO ₄	Barite	80	80+
Strontium sulfate	SrSO ₄	Celestite	12	12
Silica	SiO ₂	Amorphous silica	1.2	2.5
Tricalcium phosphate	Ca ₃ (PO ₄) ₂		1500 - 2500	125,000

A laboratory study reproduced the impact of polymaleates observed in field applications when blended with PBTC, and for the phosphonate blend of HEDP and ATMP. The study measured the upper saturation ratio limit for calcium carbonate for the individual inhibitors, and when blended in various ratios. Two solutions were prepared:

- An anion solution of bicarbonate and carbonate.
- A cation solution of calcium.

The scale inhibitor, or blend being tested is included in the anion solution. No inhibitor is added for the blank, untreated, tests.

The test is initiated by mixing the cation and anion solutions. pH is monitored as anion solution is added to the mixture. The additional anion solution increases carbonate, pH, and the calcium carbonate saturation ratio.





Attention Owner/Operators of Heat Transfer Systems*!

*(*Water Cooling Towers, Air Cooled Condensers, Evaporative Condensers and Fluid Air/Evaporative Coolers)*

Benefits of CTI Membership:

- Networking with industry peers/experts in all aspects of heat rejection equipment, including water treatment, mechanical equipment, structural design and testing/certification procedures.
- Exclusive access to the Owner/Operator Council which provides a forum to meet with other Owner/Operator's to discuss problems and issues related to your specific operation.
- The knowledge gained can help set priorities for solving specific problems. Industry standards and guidelines optimize the operation, maintenance of the equipment; maximizing value for the Owner/Operator.
- Two CTI meetings a year, an Annual Conference and Summer Committee Workshop. The Annual Conference includes the presentation of Technical Papers, Owner/Operator Seminar, Education Seminar, Committee Meetings and a Technical Exchange Exhibition.
- CTI Annual Conference provides a platform to publish and present technical papers.
- CTI offers an opportunity to all members to participate in developing standards and guidelines for their industry.

Become a Member of the Cooling Technology Institute (CTI)
Visit www.CTI.org to Sign UP



***At the Owner/Operator Council meeting an attendee told us:
"it helped solve a recurring problem which saved the company over \$100,000."***

The upper limit for the inhibitor is indicated by loss of control, and a drop in pH as calcium carbonate precipitates. The solution is also observed for turbidity. Figure 3 profiles a typical plot of pH as the solution is “titrated” to the upper saturation limit for the inhibitor.

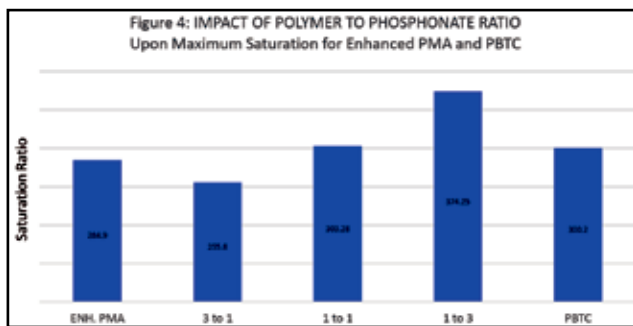
Care must be taken in the experimental design so that the solubility of inhibitor salts does not interfere, such as through the formation of Ca-HEDP. The time for the test must also be less than the treated induction time to prevent precipitation other than that from exceeding the upper limit.

In Search Of Upper Limit Synergy: Laboratory Results

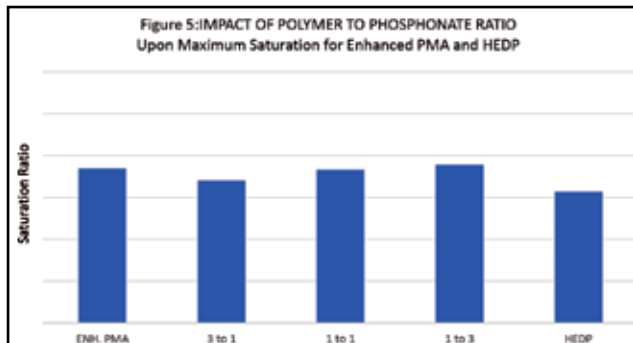
PBTC:PMA Combination: The combination of PBTC and PMA demonstrated the most dramatic impact of blending upon the upper saturation limit, as depicted in Figure 4. As the blend ratio in the test goes from polymer only to phosphonate only, there appears to be a drop in the upper limit at high polymer to PBTC ratios, possibly indicating an antagonistic effect when the polymer is the primary inhibitor. The upper limit failure point increases to a maximum at a ratio of 3 to 1 PBTC to polymer, with the upper limit of the higher ratios indicating a synergy between the PBTC and lower levels of PMA. This trend has been observed in field applications.

Antagonism might occur as a result of polymer adsorbing near newly formed active sites and blocking the PBTC from nearby active sites, or by changing the surface charge to decrease attraction. In this case, the upper limit for the blend would be expected to have a lower limit than either inhibitor alone.

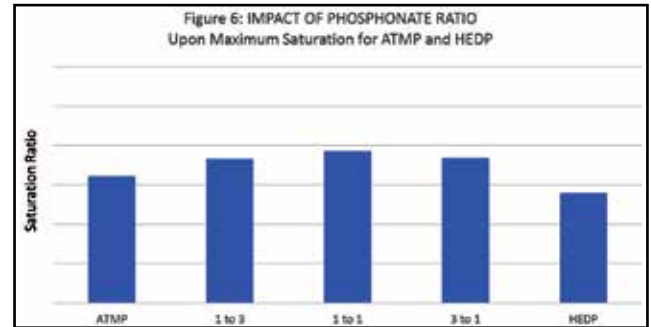
Synergy might occur as a result of polymer attaching near newly formed active sites and by changing the surface charge to increase the attraction of PBTC to nearby active sites. In this case, the upper limit for the blend would be expected to have a higher limit than either inhibitor alone.



HEDP:PMA Combination: The combination of HEDP and PMA demonstrated a similar impact trend to the PBTC:PMA blend on the upper saturation limit, as depicted in Figure 5. As the blend ratio in the test goes from polymer only to phosphonate only, there appears to be a drop in the upper limit at high polymer to HEDP ratios, possibly indicating an antagonistic effect when the polymer is the primary inhibitor. The upper limit failure point increases to a maximum at a ratio of 3 to 1 HEDP to polymer, with the upper limit of the higher ratios indicating a synergy between the HEDP and lower levels of PMA. The overall impact of blending the phosphonate HEDP with PMA upon the upper saturation limit appears to be less than the PBTC:PMA blend.



HEDP:ATMP Combination: The combination of ATMP and HEDP demonstrated a positive impact upon the upper saturation limit, as depicted in Figure 6. As the blend ratio in the test goes from HEDP only to ATMP only, the upper limit failure point increases to a maximum at a ratio of approximately 1 to 1 HEDP to ATMP, with the upper limit indicating a synergy between the HEDP and ATMP at all ratios.



A similar trend in inhibitor effectiveness was observed in similar studies that demonstrated an increase in percent inhibition for phosphonate blends.⁸

The Behavior of Inhibitor Blends – Inhibitor Solubility

As mentioned as a caveat for test protocols, inhibitor upper limit tests should be conducted in a range where the solubility of the inhibitor will not decrease the limit measured. The formation of salts such as a Calcium–Inhibitor or Iron–Inhibitor have been known to limit the maximum dosage in a water. Incorporation of copolymer and higher polymers into a blended inhibitor formulation allows the product to function at higher dosages, and has been observed to prevent deposition or inhibitor activation of inhibitor salt solubility limited treatments. A reduction in dosage is not necessarily observed. The added protective polymer allows the original scale inhibitors(s) to function at a higher dosage, a dosage above their normal solubility. Some might term this Synergy. Others may call it Smart Formulating. In either, or both, cases, the end result is the addition of another molecule into the formula allows the inhibitors to function at a higher dosage under the same conditions.

Inhibitor salts can be modelled like any scale. Their solubility, and the inhibitor dosage required to prevent their precipitation or deactivation, can be modelled using the same methods used for mineral scale inhibitors. The degree of supersaturation for the Metal–Inhibitor reactant is calculated. Studies can be run to determine the impact of copolymer dosage on Metal–Inhibitor induction time and degree of saturation.

Conclusions

Blending inhibitors can raise the maximum driving force limit where the inhibitor is effective, and demonstrate synergy. Blends can also decrease the upper driving force limit when individual inhibitors compete for active sites or modify seed crystals to interfere with the second inhibitor in a blend. When present, the degree of synergy or antagonism between inhibitors is a function of the ratio of inhibitors. A given blend might be antagonistic at lower ratios, and synergistic at higher ratios.

Recommendations

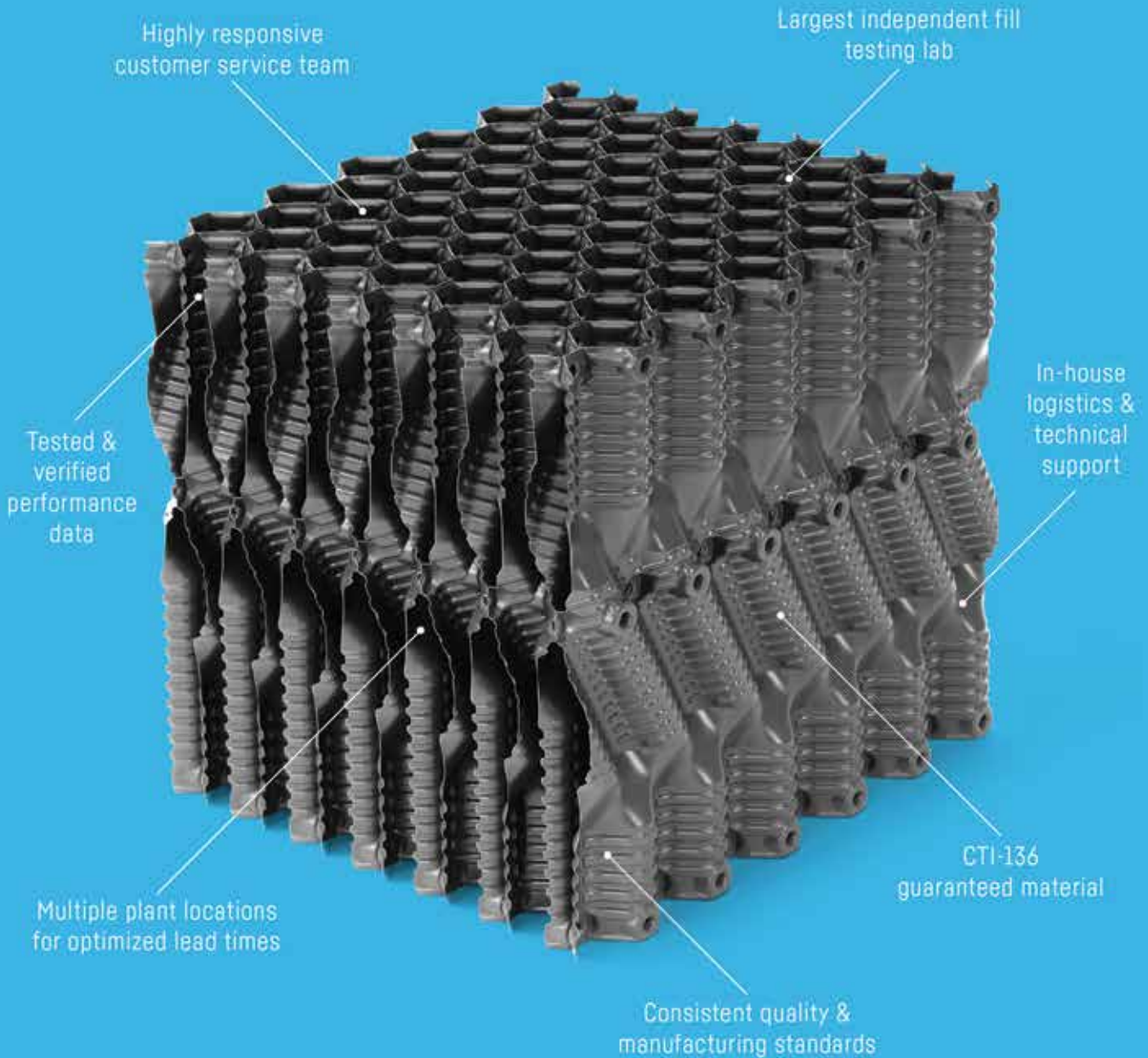
Inhibitor blends should be evaluated to determine their impact upon the upper limit of effectiveness for the particular inhibitors, and ratio. Limits for individual inhibitors should not be assumed to apply to blends.

Further Work

Additional inhibitors and blends will be studied using the procedure outlined for measuring the upper saturation ratio limit.

The impact of inhibitor blends upon induction time extension will be studied for inhibitors with existing models (Table 4) and blends until the standard arsenal of phosphonates and proprietary inhibitors has been studied.

VALUE.



Value means a product you can rely on, a team of experts available when you need them, and a partnership beyond the sale.

Invest in a supplier who invests in you.



Table 4: Typical Scale Inhibitor Models Available

Inhibitor	Chemical Name	Scales Modeled
ATMP	amino tris (methylene phosphonic acid)	CaCO ₃ , CaSO ₄ , BaSO ₄
HEDP	1-hydroxy ethylene-1,1-diphosphonic acid	CaCO ₃ , BaSO ₄
PBTC	2-phosphonobutane-1,2,4-tricarboxylic acid	CaCO ₃ , BaSO ₄
HDTMP	hexamethylenediamine tetra(methylene phosphonic acid)	CaCO ₃ , CaSO ₄ , BaSO ₄
DTPMPA	diethylene triamine penta (methylene phosphonic acid)	CaCO ₃ , CaSO ₄ , BaSO ₄
PAA	polyacrylic acid	CaCO ₃ , CaSO ₄ , BaSO ₄
PMA	polymaleic acid	CaCO ₃ , CaSO ₄
AA-AMPS	acrylic acid-2-acrylamido-2-methylpropane sulfonic acid	Ca ₃ (PO ₄) ₂ , CaCO ₃
Proprietary copolymers, terpolymers	Various	Ca ₃ (PO ₄) ₂
Proprietary polymers	Unknown	SiO ₂ , MgSiO ₃ , Mg ₂ SiO ₄

Studies for both upper limit and induction time extension will be run in both a "clean" system and when "seeded" with the solid phase of the scale under study.

Scales studied will be expanded to include CaCO₃, CaSO₄*2H₂O, BaSO₄, and where appropriate, Ca₃PO₄.

As data is available, the laboratory results and trends will be validated to operating industrial systems.

References

1. Ferguson, R.J., "Developing Scale Inhibitor Models", WATER-TECH, Houston, TX, 1992.
2. Ferguson, R.J., D.A. Weintritt, "Developing Scale Inhibitor Models For Oil Field", NACE, CORROSION 1994, Baltimore, MD.
3. Ferguson, R.J., B. R. Ferguson, and R. F. Stancavage, "Modeling Scale Formation and Optimizing Scale Inhibitor Dosages in Membrane Systems", AWWA Membrane Technology Conference March 30, 2011 Long Beach, CA, USA
4. Tomson, M.B., Fu, G., Watson, M.A. and A.T. Kan, "Mechanisms of Mineral Scale Inhibition, Society of Petroleum Engineers, Oil-field Scale Symposium, Aberdeen, UK, 2002.
5. B.W. Ferguson, R.J. Ferguson, "Sidestream Evaluation of Fouling Factors in a Utility Surface Condenser," Journal of the Cooling Tower Institute,2, (1981):p. 31-39.
6. Ferguson, R.J., Codina, O., Rule, W., Babel, R., Real Time Control Of Scale Inhibitor Feed Rate, International Water Conference, 49th Annual Meeting, Pittsburgh, PA, IWC-88-57.
7. Ferguson, R.J., "30 Years of Ultra Low Dosage Scale Control", NACE, CORROSION 2003, San Diego, California
8. Ferguson, R.J., "The Kinetics Of Cooling Water Scale Formation And Control," Association of Water Technologies Annual Meeting, Association of Water Technologies Annual Meeting, September 14 - 17, 2011 Atlanta, GA, USA
9. Ferguson, R.J., Computerized Ion Association Model Profiles Complete Range of Cooling System parameters, International Water Conference, 52nd Annual Meeting, Pittsburgh, PA, IWC-91-47.
10. Ferguson, R.J., A.J. Freedman, G. Fowler, A.J. Kulik, J. Robson, D.J. Weintritt, "The Practical Application of Ion Association Model Saturation Level Indices To Commercial Water Treatment Problem Solving," (Washington, DC: American Chemical Society Annual Meeting, Division of Colloid and Surface Chemistry Symposia, Scale Formation and Inhibition, 1994).
11. Ferguson, R.J., A Kinetic Model for Calcium Carbonate Scale, CORROSION/84, Paper No. 46, (Houston, TX: NACE INTERNATIONAL 1984).
12. Ferguson, R.J., "The Impact of Inhibitor Speciation on Efficacy: pH, Ionic Strength and Temperature Impact," Presented at the 2015 Cooling Technology Institute Annual Conference, New Orleans, Louisiana February 9-12, 2015
13. Griffiths, D.W., Roberts, S.D., and Y.T. Liu, "Inhibition of Calcium Sulfate Dihydrate Crystal Growth by Phosphonic Acids – Influence of Inhibitor Structure and Solution pH," Society of Petroleum Engineers, International Symposium on Oil Field and Geothermal Chemistry (1979).

MIST COOLING SYSTEM

Superior Alternative To Induced Draft Cooling Tower & Spray Pond

MREPL is proud member of CTI & pioneer of Mist Cooling System a "Green Product". With over 300 installations running in India & abroad up-to Central America, it finds applications in wide range of industry viz. chemical, power, petroleum, pharmaceutical, oil extraction, sugar factories, etc. The latest louver type design reduces plot size & drift loss is limited to 0.02%.

SALIENT FEATURES OF MCS:

- Guaranteed Energy saving up to 30% as compared to IDCT
- Patented choke-less design of nozzle ensuring high efficiency cooling with Mist formation.
- Guaranteed drift loss of less than 0.02% with special louver type design.
- A payback period of around 1 to 2 years is guaranteed irrespective of higher plot size requirement up to 2 times the IDCT area.

Open Type MCS

Approach to
WBT of 1°C,
Not a dream
any more, a
reality!!

Louver Type MCS

Fill less,
Fin Less
& Fan less
design

Mist Resonance
Engineering Pvt. Ltd.

"Anand", 1304-1/7, Shukrwar peth, Bajirao road, Pune - 411 002. India.
Tel: (+91 20) 2447 2726/ 2447 1184. Fax: (+91 20) 2447 4972.
E-mail: mistcreation@gmail.com | mistcool@vsnf.com Web: www.mistcreation.com

Midwest COOLING TOWERS

FROM START TO FINISH!

QUALITY, SERVICE & VALUE

DESIGN • PARTS PRODUCTION • SUPPLY • CONSTRUCTION

- ▶ Over 45 years experience
- ▶ Counterflow & Crossflow
- ▶ Pre-engineered & custom designs
- ▶ Extensive manufacturing facilities
- ▶ Complete control of material & labor
- ▶ Full-time project management & cooling tower construction staff
- ▶ Outstanding safety performance
- ▶ 24 hour Emergency response & repair



 **Midwest**
COOLING TOWERS

405-224-4624

mwcooling.com



Distribution – Distribution – Distribution

James L. Willa, Willa, Inc.

Distribution is at least three times more important than any other factor in cooling tower performance. We test cooling towers to make sure they are within 1°F to 2°F of their design. Then in the next few years the performance quite often drops 10% to 20% because of water maldistribution.

No matter how much water and air you have going through your tower, it will not perform satisfactorily if they are not thoroughly and evenly mixed throughout the tower.

Construction

In choosing the original site location, try not to locate the cooling tower near a coal pile or a dirt road. Make the cold water basin deep enough to hold several inches of mud.

Crossflow Cooling Tower Construction

The distribution basin should include a stainless steel ½” mesh wire fence around the perimeter of the flow control boxes, in order to catch any particles or debris over ½” in size. This fence should be 8” to 10” tall and should be located one foot from the outside perimeter of the flow control box, on all four sides. Be certain that the support strips for this fence do not cover any of the distribution nozzles. ½” x ½” pultruded fiberglass angles can be used to fasten to the distribution deck for fence support. Place the stainless steel wire against the upright side of the angle. Place another angle on the outside of the wire fence to secure it. This fence is important to stop the majority of particles over a ½” in size from spreading out over the distribution deck and plugging nozzles. This debris can be collected periodically by kneeling down on the flow control box, and with a gloved hand pick this debris up and put into a bucket. A drawing of this fence is at the end of this paper.

This is extremely important in instances where power plant cooling towers are being replaced. During the down time to replace the tower, the pipes to and from the condenser to the tower, and the condenser itself and tube sheets, are all allowed to dry out. When reactivated, there are pieces of scale and rust that detach from the pipes to and from the tower and in the condenser and tube sheets, and flow directly to the cooling tower. This fence mechanism around the hot water flow control boxes will help control this type of nozzle pluggage.

Last year, in one instance where I had written this type of fence into the specification, a field trip revealed they were not being installed. It turned out that the plant manager had said he did not have personnel to clean the fences, therefore to not install them. A cost analysis was run on what this type of nozzle pluggage could cost the plant in megawatt production. Then, the annual cost to purchase replacement power was calculated. This calculation method is as follows. It is based on a 500 megawatt operating generation plant.

Data Used

Financial Calculations – Based on Current Full Load Heat Rate

- Plant Unit Size (Net Dependable)
- Assumed Average 2016/2017 Replacement Power Cost
- Assumed Average Plant Capacity Factor
- Hours/Year (52 x 7 x 24)
- Annual Generation (Based on 85% Cap Factor)
- Decrease in Annual MW Hours Due to Tower Degradation at 10% and 20% Tower Shortage



James L. Willa

- Annual Cost to Purchase Replacement Power:
- 10% - \$172,122; 20% - \$475,866

You will note that the loss of 10% cooling tower performance will cost more than the annual cost of another operator. This operator could spend his entire time maintaining a clean and balanced cooling tower distribution system.

The distribution basin should not be allowed to go behind the vertical short wall between the fan deck and the distribution deck. This fiberglass vertical wall should extend from the underside of the fan deck to the top of the back wall of the distribution basin. Any nozzles placed in the area behind the short wall will

quickly plug. This is important as any basin with or without nozzles that goes under the short wall and behind it into the plenum area is normally not accessible. If accessible removable panels are included in the short wall on both sides of each cell, this area can be reached. However, in order to clean anything in this area you must have full water flow and airflow, to make it physically possible to withstand the heat in this area. With current safety rules, working in this area with a tower in full operation is normally prohibited. Therefore, this basin should not be allowed to go behind the short wall.

A 6” PVC standpipe should be mounted on the far end of the main header on top the tower, and extended to the level of the fan deck handrail. This will protect the hot water distribution main from being damaged by surges in pressure from starting too many pumps at a time. If water comes out the top of this standpipe, then the valves on the flow control boxes are closed too tight and need to be opened more. Power plants quite often over pump water to the cooling towers.

In order to prevent algae growth in the hot water distribution basin, a consideration should be given to covering the distribution basin with an extension of the fan deck all the way to the louver columns. One disadvantage to this is that work in the distribution area must be done by flashlight and it might be considered a confined area by the safety department. In this case, from the distribution cover there should be a fiberglass wall vertically from the outside edge of this fan deck cover, down to the top of the outboard distribution basin wall. This cover will prevent algae from plugging up the nozzles, and will also appreciably reduce the amount of chlorine necessary in the cooling tower.

Crossflow nozzles should be placed one foot on center. The head on crossflow nozzles is only 6” to 8”. Therefore, due to this low pressure, the crossflow nozzles must be utilized closer together. The inside diameter should not be smaller than ½”. They should have a bottom splash plate molded into the nozzle. Large nozzles have been available, at times, to be used three foot on center. However, these nozzles generally do not have a pattern in the center one foot circle, therefore, they are not satisfactory.

Counterflow Cooling Tower Construction

There should be a 2” PVC pipe attached to the bottom side of the main distribution header in each cell, at the far end from the riser. This PVC pipe should then run down through the fill, in-



Carbon Fiber Composite Drive Shafts & Gear Boxes For Cooling Towers

NSCTPL serves all sizes with numerous new options... Contact us today!



- Longer spans with smoother operation
- High strength to weight ratio
- High misalignment capability
- Superior fatigue life
- Easy installation
- UV stabilized
- Dynamically balanced
- Load tested at 3 times the operating torque

- Designed for rugged cooling tower conditions
- Heavy duty, right angled- single and double reduction
- Designed as per AGMA standards
- Timken and NTN bearings for 100,000 hours L₁₀ service life
- Both bi-directional and uni-directional gear-boxes are available
- Gear box dynamically load tested at twice the operating load



North Street Cooling Towers Pvt. Ltd.

C-14, Sector-22, Meerut Road Industrial Area, Ghaziabad-201003 (U.P.), India

Email: sales@nsctpl.in

Website: www.nsctpl.com

Phone No: +91-120-2788571, 2788572 Fax: +91-120-2788574



An ISO 9001:2008(QMS), 14001:2004(EMS) & OHSAS 18001:2007 Certified Company

side the casing, to the air inlet level, at a location that can be reached by the operators at grade. The lower end of this pipe should have a PVC valve. Most of the debris will collect in the far end of the main, and eventually fill up and begin to plug the individual lateral arms and nozzles, on that side of the tower. Therefore, the above described flushing pipe should be utilized once a month by the operator, going around and opening the valves on each cell and then after 5 or 10 minutes of flushing, go back through and shut the valves down. If this procedure is done regularly, it will help a great deal to avoid plugging of the laterals. A bucket with a screen bottom should be attached to the lower end of this line, to catch any debris and allow the flushing water to fall back into the basin. These buckets should be removed and emptied after the flushing.

The ends of the laterals should have removable PVC caps or PVC valves to open for cleaning. Install a 4" to 6" PVC standpipe on top of the end of the main header in each cell. This standpipe should come up to just below the bottom side of the fan deck, to prevent overflowing water spilling onto the fan deck. This will serve the same purpose as in a crossflow tower, to avoid pressure surges in the main from blowing out nozzles or laterals.

Counterflow nozzles usually have a two to three foot of head, therefore, larger nozzles can be used, normally three foot on center.

There have been some ceramic nozzles with ceramic turbulators inside, used in the past. However, their pattern is easily destroyed by such a minor item as a paper match across the center hole in the turbulator. Therefore, strict cleaning procedures must be used on these type nozzles.

Multiple smaller nozzles used on counterflow cooling towers, very closely spaced, are sometimes used. They have a small inside diameter and are easy to plug.

I have seen a counterflow tower used in a steel mill with the small nozzles. They were over 90% plugged with iron oxide residue off the rolling mill. These smaller nozzles are also not used in counterflow towers in power plants, due to pluggage.

Film pack fill is difficult to use in industrial size crossflow towers. Film pack fill, which is often used in counterflow towers, presents an additional problem for distribution systems. When film pack fill is used in counterflow towers, it is necessary to have clean water and adequate chlorine to prevent clogging nozzles and the fill. Remember that the "clog free" film pack fill used many times is extremely sensitive to proper distribution, as hot water must be distributed in every square inch, because the flutes are vertical. Without water being distributed in every square inch, performance will be lost. Incidentally, "clog free" film fill should be renamed "longer to clog" fill.

Crossflow and Counterflow Construction

There are some other construction features that can serve both crossflow and counterflow towers. The first and most important is placing a double screen in the sump area, where the basin flows into the sump. These screens should have stainless steel framing, 1/2" to 3/4" stainless steel mesh wire, and 6" wide x 6" deep "cups" at the bottom front, to catch any debris that rolls down the screens when they are being lifted for cleaning. These screens should be cleaned after the water head across them exceeds 2" to 3". There should be a steel framework over the screens, with a pulley arrangement to lift the screens for cleaning. They can be lifted with either a hand operated or an electrical operated hoist. The screens should then be washed clean on a concrete pad next to the cooling tower, not over the sump or against the louvers.

Another construction item that can be of help for both crossflow and counterflow cooling towers, is the installation of a side stream filter, being fed by a line taken off the cold water pump discharge. This water will go through a sand and gravel filter. After running through this filter, the water can be dumped back into the cold water basin. Blowdown water can be utilized to back flush this filter

when it becomes plugged with debris. This blowdown flush water can then be disposed of with regular blowdown.

The above two suggestions will prevent debris and mud from the basin getting into the tower. However, when the unit is put back on line, the scale and rust from the lines and condenser will turn loose and go to the hot water riser (in both types of cooling towers) to the distribution system. The basin screens or filters will not help as this type of debris is down stream of the cold water basin and/or side stream filter. They do not prevent the accumulation of scale and rust coming from the "out of service" unit, plugging the nozzles. Therefore, the fence around the flow control boxes is your only defense against this type of plugging in a crossflow tower. Your only defense in a counterflow tower are the flush lines at the ends of the distribution mains. This is the most prevalent cause of pluggage in cooling towers, from pipes and condensers on jobs involving unit turnaround.

Detecting Poor Water Distribution Crossflow Towers

Water accumulation on the lower louvers, in a crossflow cooling tower, indicates that water is pouring over the top of the outside wall of the distribution basin. The valves should be rebalanced and/or the nozzles cleaned.

If a crossflow distribution basin has a lower water level, which prevents water getting to the far nozzles on the sides and the outside edges, then the water flow needs to be increased to the cell.

Plugged nozzles in the distribution basin can be observed by a close inspection of the basin. The water depth in the distribution basin should be level across the area of the basin.

Another good approach to detecting bad distribution in a crossflow tower is to walk through the plenum walkway at the basin curb level, and notice the temperature of the air coming through the drift eliminators. It should be a rather constant temperature all the way across the face of the cell at this level. However, quite often you will find that it is hotter in the center of the cell. This implies the nozzles are either not getting water or are plugged around the perimeter of the distribution basin.

A better way to observe bad distribution is to walk through the cold water basin, with palms up, feeling the difference in temperature as you move. The hot areas in a crossflow tower will indicate bottom plates on the nozzles are missing or hot water is flowing over the back wall of the distribution basin.

In a crossflow tower when the flow nozzles are plugged on the sides of the distribution basin, this reduces static pressure on air through this area and consequently more air flow will go through this area with less air flow where there is more water. This will result in a degradation of thermal performance.

Counterflow Towers

The same walk through the cold water basin, with extended palms up, is also the very best way to distinguish poor distribution if there are hotter and colder areas in the basin. However, this type of inspection will have some problems with the safety department.

Light water flow hitting the cold water basin on the far side from the risers, on the counterflow tower, indicates plugging of the laterals. This can be avoided by the previously mentioned blowdown lines from the end of the mains.

Observations can be made of the water hitting the cold water basin surface on both counterflow and crossflow towers. The density of this water will show heavier and lighter areas. Lighter areas will, of course, represent plugged nozzles.

Of course, another surefire way of noticing bad distribution is a gradually rising cold water temperature to the plant. This is where the real damage is being done to the unit.

Examples Of Poor Distribution

A power plant in the mid-west area had 40 acres of air conditioning type counterflow cooling towers, with multiple nozzles with 1/2" inside diameter openings. 90% of these nozzles were plugged.

The towers were located approximately a quarter mile from the condenser in the plant. The condenser hot water ran through an open ditch to the vertical lift pumps at the end of the ditch. The vertical lift pumps sent the water to the cooling towers. The so called "screens" were 1/2" thick vertical steel bars placed 3" on center. This situation would, of course, keep 2" x 4" boards out of the pumps, but little else. This was the reason for 80% to 90% of all the nozzles being plugged. The plant was being limited on megawatt output, due to high condenser temperatures and resultant back pressure.

Cleaning Distribution Systems Crossflow Towers

Lower the water flow to the distribution basin by partially closing the distribution valves from the main header to the flow control boxes. With approximately an inch of water in the hot water basin, clean the screen around the flow control box. Then check each nozzle to be sure they are open. The best tool for this is shown in a drawing on the last page of this paper. It consists of a steel rod with a handle that has a large washer welded near the bottom, to keep from hitting the plate on the bottom of the nozzle. This tool is extremely important. The diameter of the lower 2" of the tool, below the welded washer, should be 1/8" less than the inside diameter of the nozzles. The big washer 2" above the bottom will prevent the tool from hitting the bottom plate. If a broom handle or rod is utilized to clear these nozzles, then the bottom distribution plate will be knocked off. In essence, you will have reduced the height of your crossflow tower by six feet (one cube). This is because with the bottom distribution plate missing it will take at least six vertical feet of fill to finish spreading the water out as it should have been from the distribution plate on bottom of the nozzle. Therefore, it is extremely important to use the above described tool. You can use gloved fingers to clean these nozzles without detaching the bottom plate. However, this method requires crawling on your knees rather than standing up. After all the nozzles have been cleaned, be sure that all the mud has been swept down through the nozzles. Then, open the flow control valve and add water back to the proper level.

Counterflow Towers

Be certain that before you start this cleaning procedure, the valves on the blowdown lines on the ends of the mains have all been open for several minutes each. If the safety department will allow, a man should go into the distribution area and remove the caps on the lateral ends, or open the valves on at least three or four laterals on each side of the main, beginning at the far side from the riser. After these laterals have been flushed for a while, repeat the procedure in the next several laterals until all the laterals have been flushed, then close the valves or replace the caps. Then go back and unplug any nozzles with a gloved hand or use a screwdriver to loosen anything still in the nozzles.

Be certain on both crossflow and counterflow towers that the screens at the sump are cleaned regularly. Also, be certain the cold water basin has been cleared of mud when it reaches 10" to 12" deep. After the mud depth reaches over this depth, it should be cleaned out with vacuum hoses, either in service or out of service. If out of service, wheelbarrows and shovels can be used.

If the cold water basin is cleaned in service, a suction hose from a tank truck, with a steel nozzle on the end should be used. The diver should start at the far corners from the sump and sweep the mud out ahead of himself. During this operation a 2" x 10" board should be placed on edge across the bottom of the sump entrance, to help the mud that is stirred up to resettle. After the vacuum-

ing has reached all the way to the sump, then of course the board should be removed.

Balancing Water Flow

For maximum performance it is very important that the water flow be balanced between cells and throughout each cell.

Crossflow Cooling Tower

Cut a 12" to 14" long piece of 6" diameter steel pipe. Use a welding torch to cut inverted slots in the bottom edge of this pipe. Place this pipe, vertical slots down, in the four corners of each distribution basin, but not over a nozzle. Measure the depth of the water in this "stilling well", and record this depth in all four corners of each distribution basin.

Open the flow control valves on the cells with the lowest water depth, to full open. On the cells with higher levels, start closing the flow control valves. Remember that it will take several turns to make much of a difference in water flow, with this type of valve. Continue in this process of opening the low level basins and closing the high level basins, until you get all of the distribution basins to within plus or minus 1" of the average water depth.

Record on waterproof paper the final set of water depth readings and the measurement of the exposed valve stems between the face of the valves and the handles. Then post these recordings in the top of the stairwell, so that the valves may be reset to the proper levels after cleaning or maintenance, without going through the balancing procedure again.

Counterflow Cooling Tower

Go through the access panel in the fan deck, and through the access panel in the drift eliminators. Take a rubber stopper big enough to fit tightly into a distribution nozzle. Drill a hole in the center of this rubber stopper, and insert a 4" long piece of copper tubing. Attach a clear Tygon tube onto this copper tube and run it up through the access panels to the top of the handrail on the fan deck. Attach the tube to this handrail. Plug the rubber stopper into the nozzle closest to the main header and closest to the access panel. Finish this setup on all of the counterflow cells.

Then measure and record the height of the water in the Tygon tubes, in inches above the fan deck floor. They should be within 2" of the average level. In some cooling towers with high plenum areas, the water level in the tube may be below the fan deck instead of above the fan deck. Of course, in this instance, the measurement will be inches below the fan deck. This procedure takes two people in radio contact. The man on the ground will proceed to close the valves on the risers to the heaviest loaded cells, and full open the valves to the lower level cells. It takes several turns on the handle, of this type valve, to change the water flow rate.

The man on top will continue to monitor the height of the water in the Tygon tubes. This procedure and cooperation should be continued between the two operators until the heights in the tubes on all of the cells are within 2 to 3 inches of the same height.

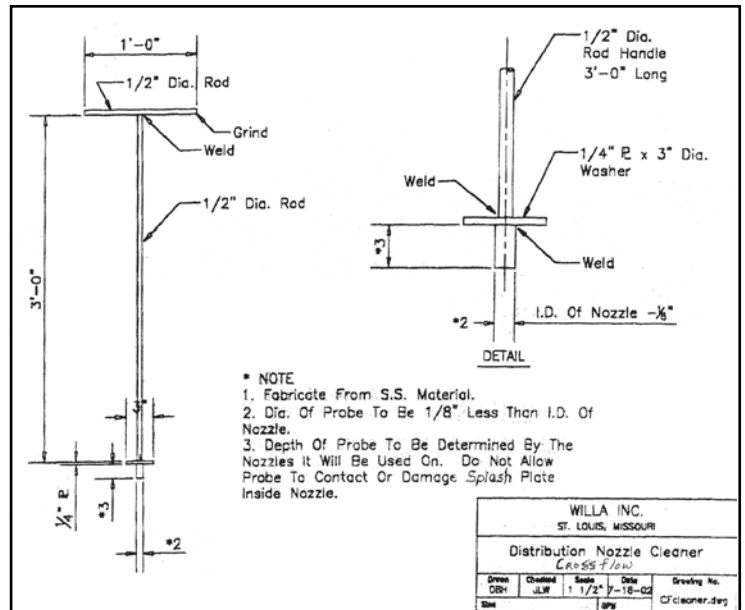
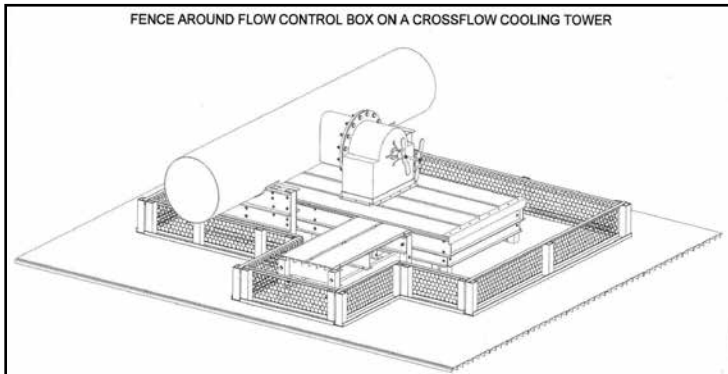
Record the length of the exposed stem and thread count between the face of the valve and the handle, similar to that used on a crossflow tower. Record on waterproof paper and place in the top of the stairwell, as on a crossflow. This will allow getting back to a balanced condition after turning off for cleaning or maintenance. Be certain to follow through this balancing procedure on either type of tower. This is most important in maintaining maximum thermal performance of the cooling tower.

Maintaining The System

Be certain to treat your water appropriately. Do not use a "hot lime" treatment on your water without proper low pH, as it will cause calcium carbonate precipitate, which will plug up nozzles. Maintain a pH so that no calcium carbonate debris will form.

Conclusion

Follow the above listed recommendations and you will maintain maximum performance throughout the life of your cooling tower. This will result in maximum output from the units being served in the plant, and will make money for your company.



The weight is over.

Introducing Oxi-King®
commercial water treatment system

Ironically, making water safe has long been a dangerous job, requiring lots of protective gear and a very strong back. Oxi-King just did for water treatment what Steve Jobs did for computers—made it way friendlier. No exposure to strong odors and accidental chemical spills. Everything is pre-filled and light weight. One 5 pound pac will treat up to 500,000 gallons with a 0.6 ppm residual and no load. Past winner of the Occupational and Health Safety Magazine

New Product of the Year Award in Hazmat Safety!

Think Safe • Think Simple • Oxi-King

Learn more at www.oxiking.com



The International Water Conference®

THE 79TH ANNUAL

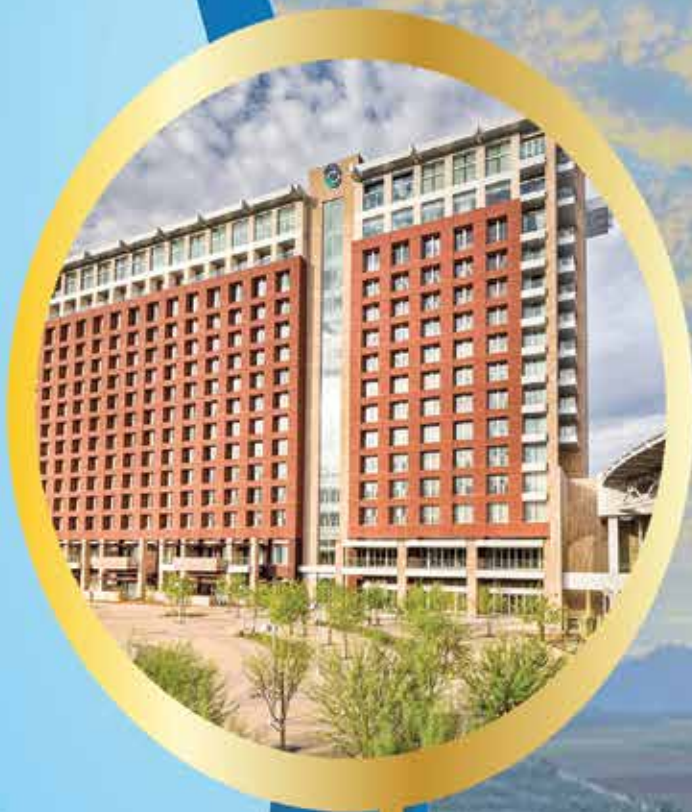
Call for Papers Now Open

Conference Dates:
November 4-8, 2018

Save the Date!

New Location!

Talking Stick Resort, Scottsdale, AZ, USA



A Fresh Perspective on Controlling Yellow Metal Corrosion

Jon Cohen, Jeff O'Brien, Ray Post
Chemtreat, Inc.

Current methodologies for using azoles to control yellow metal corrosion have existed for years with little advancement. Although these strategies have met corrosion rate requirements for a majority of industrial systems, there are still many failures as a result of yellow metal corrosion. This paper will highlight some mechanisms of yellow metal corrosion, new data on the effects of halogens on azoles, and a new control strategy.

Introduction

Cooling water treatment programs target three main areas of control: scale, corrosion, and microbiological activity. Within the water treatment community, this triad is classified as the water treatment triangle. A triangle was chosen to show the interconnectivity of each element. Corrosion control changed significantly, like the two other elements of the triad, after hexavalent chrome was no longer permitted for use in cooling water treatment. Subsequent corrosion inhibitors have been challenged to maintain the high standards set with chromate, leading to decreased asset life and an area for improvement within the water treatment community.

Since the era of acid, phosphate, and hexavalent chrome, many other combinations have been used. Countless papers have been written in the last 35 years on the use of phosphonates in cooling water systems. One of the earliest papers detailing post-chromate cooling water treatments describes three approaches for preventing scale (Strauss and Puckorius, 1984):

1. Remove the calcium hardness or scaling mineral from the water prior to use.
2. Keep the scale-forming constituents in solution.
3. Allow the impurity to precipitate as a removable sludge rather than as a hard deposit.

This article also described the foundation of many modern-day scale inhibition programs: the use of phosphonates. Phosphonates are not the only chemistry in play and are never used without other chemical additives (at least in modern-day treatment strategies); they are always a component of the formulation. Two common phosphonates, still employed today, are mentioned in the article, while many others are used for varying purposes.

Development in organophosphorous compounds has continued over time. Presentations at the Cooling Technology Institute (CTI) like Geiger who (Geiger, 2008) discussed the development of high-stress organophosphates, or Gill presenting (Gill, 2013) synergies of high-performance phosphonates with mechanical separation. Both studies show the continuing importance of organophosphates in cooling water chemistry.

Puckorius (Strauss and Puckorius, 1984) describes the relationship between organophosphorous compounds and increases in yellow metal corrosion rates. Although these compounds were known to have corrosive tendencies, alternatives were not developed until over 25 years later, when regulatory pressures to reduce or eliminate phosphorous contaminants from discharge waters provided a greater impetus. (Post, 2014) Although current alternatives like RPC showed promising results for reducing corrosion rates for copper, non-phosphorous cooling water chemistries for scale inhibition have not had enough market share to significantly reduce organic phosphate use. Rather, many have been promoted to replace inorganic phosphate products traditionally used for steel alloy corrosion inhibition.



Jon Cohen

Both Geiger and Gill also discuss challenges with phosphonate chemistries in the presence of halogens. Phosphonates are not the only chemistry in cooling water treatment to undergo unfavorable reactions with halogens. Geiger (Geiger, 2008) describes the need for halogen-resistant azoles in the presence of halogens. Halogen chemistry, bleach, and bromine compounds are common microbiocides used in cooling water programs. However, they combine unfavorably with most azoles used for yellow metal corrosion inhibitors. Previous efforts for controlling this effect have focused on alternate oxidizing biocides. (Baron, 2016)

Azoles are a class of organic corrosion inhibitors, generally containing three heteroatoms in or on a five-membered ring. A previous paper outlined azole chemistry for several commonly-used azoles in cooling water treatment. (Cohen, 2013) Reactions between

halogens and azoles increase biocide demand and decrease the effectiveness of the azole as a yellow metal corrosion inhibitor.

Other methods previously investigated include targeted azole feed. Cohen, et al. studied the rate of formation and thickness of several azoles. (Cohen, 2013) Varying azole dose and feed length had significant impacts on the film thickness. These studies did not include the effect of halogens on film formation or tenacity, but it looked at how targeted feed ahead of heat exchangers could be accomplished to prevent corrosion on critical system components.

Issues With Current Strategies

While azole use is the cornerstone of corrosion inhibition in modern cooling water treatment chemistries, high corrosion rates, especially for copper, are still fairly common. Several reasons for high corrosion rates exist, mainly:

- Insufficient azole feed
- Poor halogen control
- Poor pH control
- Other factors like phosphonates and ammonia

The literature suggests azole should be maintained at approximately 2.5 ppm; however, many water treatment programs suggest far higher azole concentrations. A review of recent bid proposals written by industry consultants shows azole concentrations to be maintained at 5 ppm or higher, with several recommending a concentration of at least 10 ppm. Besides cost being a considerable factor, monitoring azole concentrations on-site is difficult. This point will be addressed in the subsequent pages. Other industry experts found positive corrosion results with concentrations as low as 1.5 ppm, although there are no studies to support that residual concentration's effectiveness.

As described above, poor halogen control can contribute to poor corrosion inhibition with azole use. Nalco and GE Betz published studies in the 1990s regarding halogen control and its effects on copper corrosion. Modern halogen feed and control has had a positive impact on limiting biocide overfeed; however, excursions still occur. Probes fail, calibration is not maintained, pumps lose prime, or equipment fails.

Likewise, pH impacts the ability of azole films to form and their persistence. pH equipment has similar limitations to halogen control. pH probes are also highly sensitive to water quality. With increasing use of reclaimed water, especially effluent waters, pH probe poisoning has become a greater mode of failure and cause of pH excursions.

Azole control and monitoring also has its difficulties. Currently, the

only field test for azoles requires the use of an ultraviolet (UV) lamp digestion method. There is no documented literature on the chemistry of this test method. One manufacturer describes the test as a “proprietary catalytic ultraviolet photolysis procedure in the presence of a chemical catalyst to form a dimer or polymer of the triazole” (see Figure 1). This UV photolysis test method does not differentiate between isomers or different azoles. Performing this test method in a field application introduces a lot of error and is rarely confirmed with laboratory results.

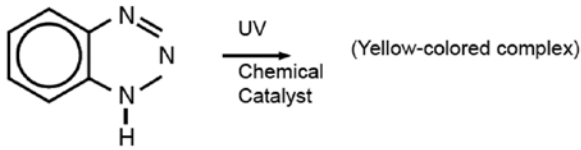
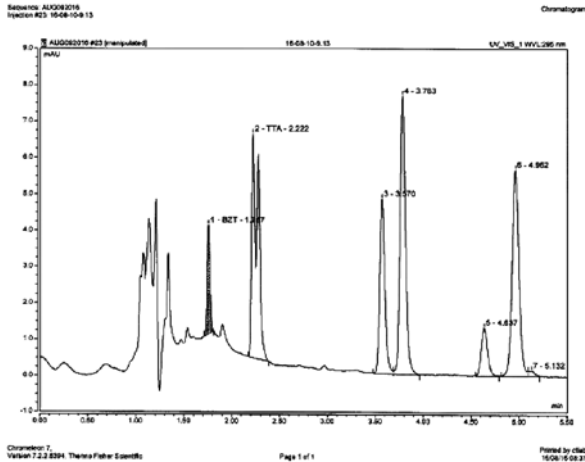


Figure 1. Chemistry of the UV photolysis reaction (provided by Hach Company).

Laboratories are able to differentiate between some azole species in water samples using various techniques, such as HPGC. However, some azole species are lumped together as total azole. Results from HPGC can be seen in Figure 2. While these results are more accurate and can differentiate between azoles, sending samples to a laboratory and receiving test results is a poor method of maintaining proper water chemistry. By the time results are provided, tower conditions are different from the sampling time and may not correct for current conditions.



The Solution

As previously stated, chlorinated azoles that are highly resistant to halogens are not new. Some have been in use since the mid-1990s, when GE Betz introduced the first commercially-available version. Over the past 20 years, continued research and development has led to greater halogen resistance. A new, halogen-stable triazole (HST) has been developed. HST shares its ability to resist degradation in the presence of halogens with previously released technologies.

Figure 3 shows how tolyltriazole (TTA) corrosion inhibition for copper reacts to higher-than-normal chlorine concentrations in a cooling tower. The electrochemical measurements show the corrosion resistance of TTA prior to the addition of chlorine. When chlorine is introduced at 4 ppm, the ability of TTA to protect copper surfaces is reduced by approximately 40 percent. When increased to 8 ppm, corrosion inhibition is reduced by approximately 60 percent.

In contrast and under the same conditions, HST initially has a higher potential for copper corrosion inhibition (Figure 4). Both trials were dosed with the same azole concentration. When chlorine was added at 4 and 8 ppm respectively, a reduction of approximately 5 percent was demonstrated. In the presence of 8 ppm free chlorine, HST showed greater performance than TTA prior to chlorine addition.

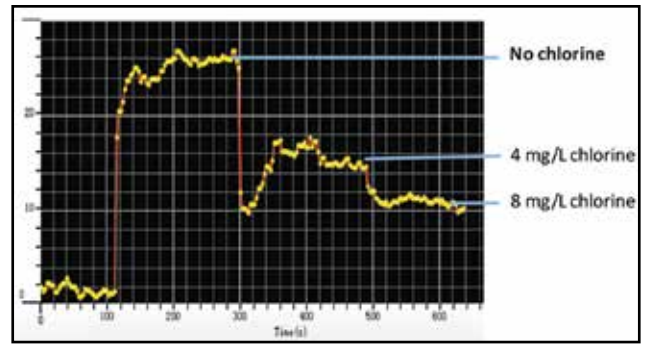


Figure 3. Stability of TTA in the presence of high chlorine concentration

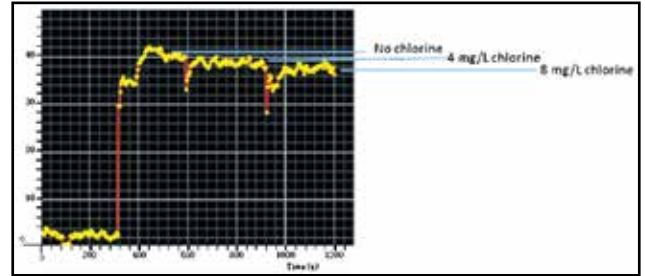


Figure 4. Stability of HST in the presence of high chlorine concentration

Figure 5 shows the corrosion rates using HST versus TTA both before and after chlorination. Prior to chlorine addition, corrosion rates with HST were measured around 0.2 mpy, while TTA took much longer to form a protective film and eventually achieved a corrosion rate of 0.6 mpy. After a shot feed of chlorine, corrosion rates with TTA immediately rose to 1.5 mpy. Eventually, the protective film reformed, and corrosion rates fell back to 0.6 mpy. With HST, corrosion rates remained relatively unchanged throughout the trial.

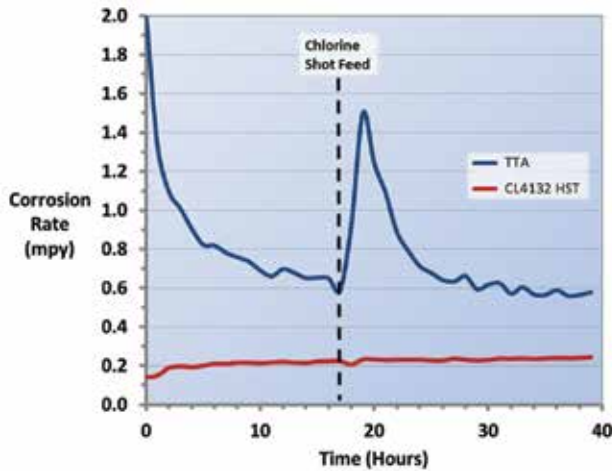
HST has an additional advantage: it will fluoresce at a specific wavelength. Fluorescence is a common technique for controlling water treatment chemicals for cooling water systems. Several commercially-available dyes, such as fluorescein and p-Toluenesulfonic acid (PTSA), are commonly used. These are often added to water treatment formulations in known quantities and measured with on-line and hand-held fluorometers to measure and control cooling water chemistry.

A new fluorometer, available in both hand-held and on-line models, has been developed to measure and control HST in cooling water systems. Using an HST and a fluorometer, accurate testing can be conducted on-site, and in-situ HST concentrations can be controlled. Better HST control equates to lower chemical treatment costs and decreased copper corrosion rates. Excellent correlation between on-site testing with both the hand-held and on-line meters and with laboratory testing using HPGC was found with less than a 5 percent deviation. Field testing also shows little interference in cooling water systems using reclaimed water as a makeup water source.

Conclusions

Copper corrosion can be challenging because of a variety of factors that influence corrosion rate and corrosion inhibition. Among these, are the type of azole used, control and monitoring techniques, halogen concentration, and organophosphates. To better control yellow metal corrosion, a new halogen-stable triazole has been developed. HST is more effective than the more common TTA in forming a stable, corrosion-resistant film on yellow metals such as copper. Film formation is also much faster with HST than TTA. Corrosion resistance with HST is augmented as a result of its halogen resistance. HST corrosion inhibition is minimally affected in the presence of halogens at higher-than-normal concentrations in cooling water systems.

HST feed and control is superior to traditional methods used for other azoles in cooling water systems. Introducing real-time measurement of



HST concentrations in-situ and having a rapid, accurate hand-held meter will enable cooling tower owners and operators to ensure proper treatment levels are maintained. Excellent correlation was found between the new fluorometers and laboratory test methods. Correlation between previous field test methods and laboratory methods was poor and affected not only by the type of azole used, but also by variations

in product quality. Increased ability to monitor and control HST, combined with superior performance, will enhance cooling water treatment programs and reduce azole feed.

Bibliography

1. Cooling Water Treatment for Control of Scaling, Fouling, Corrosion, Strauss and Puckorius, Power, June 1984
2. Improved Calcium Phosphate Control for Stressed Systems, Geiger and Sui, CTI Journal, Vol. 29, No 2., 2008
3. Development and Application of Phosphorous Free Cooling Water Treatment, Post, Tribble, Kalakodimi, CTI Journal Vol 35, No. 2, 2014
4. A Synergistic Combination of Advanced Separation and Chemical Scale Inhibitor Technologies for Efficient Use of Impaired Water in Cooling Towers, Gill and Lin, CTI Journal Vol 34, No. 1, 2013
5. Improve System Performance and Reduce System Corrosivity Using a Novel Biocide for Cooling Towers, Barron and Hammond, CTI Journal Vol 37, No. 1, 2016
6. Film Formation, Stability and Corrosion Inhibition of Surface Deposited Film Inhibitors, Cohen, Becker, Parmelee, CTI Journal Vol. 34, No. 2, 2013
7. New Corrosion Inhibitor Resists Chlorine, May, Cheng, Given and Higginbotham, Power Engineering, Vol. 102, Issue 7, 1998

FRP Panels for Cooling Tower Industry

Resolite Fiberglass Casing & Louvers

Since 1951, RESOLITE has provided high strength and corrosion resistant panels for the cooling tower industry. Designed to withstand the extremely corrosive environments often associated with cooling tower markets, Resolite panels are engineered specifically for use as louvers, stair enclosures and exterior casing.

FEATURES

- > Fire Retardant, with UL Fire Rating Classification
- > Corrosion Resistant
- > Outstanding Resistance to Weathering

BENEFITS

- > Unmatched, Long-Lasting Performance



Resolite

A DIVISION OF STABILIT AMERICA

285 Industrial Drive
 Moscow, TN 38057
 ph. 888-737-6548
 fx. 901-877-1388
 email. sales@resolite.com



EXHIBIT SPONSOR

GEAR UP
FOR FEW

WHERE ETHANOL
PRODUCERS MEET

LOCK IN YOUR 2018 EXHIBIT SPACE & SPONSORSHIP

Limited Number of Sponsorships Available.
Don't Wait, Become a Sponsor Today

**Surround Yourself with
Ethanol Decision Makers**
Don't Wait, Get Your Premium Booth Now

By purchasing a booth you are surrounding yourself
with industry professionals who are looking
for solutions to their challenges.

866-746-8385 | service@bbiinternational.com

#FEW18 @ethanolmagazine

Produced By Ethanol #BBI

WORLD'S LARGEST ETHANOL EVENT

34th ANNUAL
INTERNATIONAL
FEW
FUEL ETHANOL
WORKSHOP® & EXPO

June 11-13, 2018

CenturyLink Center Omaha
Omaha, Nebraska

FuelEthanolWorkshop.com


**ADVANCED
BIOFUELS
CONFERENCE**

Co-located Event

June 11-13, 2018

CenturyLink Center Omaha
Omaha, Nebraska

AdvancedBiofuelsConference.com



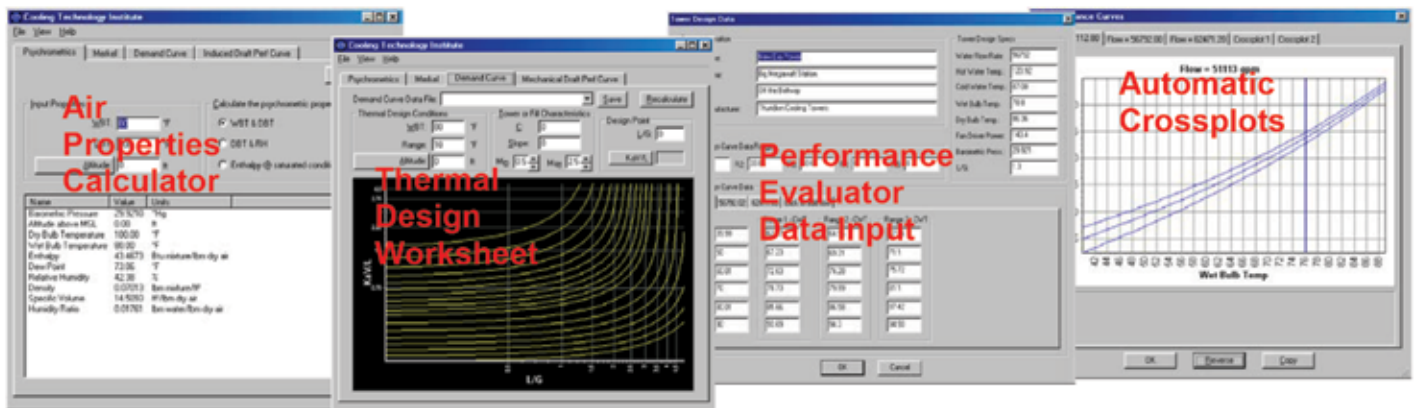
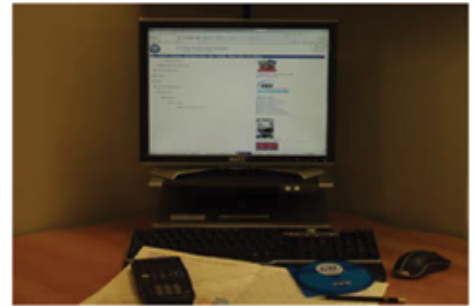
CTI Toolkit Version 3.2

...now Windows 10 compatible

A great opportunity to upgrade your CTI Blue Book Version 1.0 and CTI Toolkit Version 2.0 Software

Key Features of CTI Toolkit Version 3.2:

- **Air Properties Calculator**; fully ASHRAE Compliant psychrometrics. Interactive.
- **Thermal Design Worksheet** in the "Demand Curve" Tab which can be saved to file and retrieved for later review. Now with printable and exportable graphs.
- **Performance Evaluator** in the "Performance Curve" Tab to evaluate induced draft or forced draft, crossflow or counterflow cooling tower performance. Now calculates percent performance or leaving water temperature deviation. Data can be entered manually or with an input file. Automatic Cross-Plotting. Now with printable and exportable graphs.
- **New and Improved Help Files** guide you through the software, explain performance evaluation techniques and offer tips for use.



Now works with Microsoft Windows 10 and all earlier Windows Operating Systems back to Windows 95
16 MB ram recommended, and 3 MB free disk space required.

Upgrade Now! Only \$25/per upgrade from 3.0 for CTI Members (\$40 for Non-Members)

To Order, Call (281) 583-4087 or visit CTI's Website www.cti.org

8/8/08



Order Today
Call 281-583-4087

"The Performance Curve method is widely recognized as a more accurate method of determining tower capability from measured test data. The new CTI ToolKit Tab Application provides a quick and easy method for anyone to evaluate a performance test using this more accurate method."

- Rich Harrison, Jr. ATC-105 Task Group Chairman

Bill to: _____

Phone: _____ Fax: _____

Email Address: _____

Ship to: _____

Phone: _____ Fax: _____

Email Address: _____

Charges can be made to Visa, MasterCard or American Express

Card No.: _____ Expiration Date: _____

Signature: _____ CVV; CVC; CID Code: _____

Product	Unit Price	Quantity	Total
CTI ToolKit Version 3.2 (single user license)			
CTI Member	\$395		
Non-member	\$450		
CTI ToolKit Version 3.2 (Upgrade from V1.0 and V2.0)			
CTI Member	\$ 95		
Non-member	\$120		
CTI ToolKit Version 3.2 (Upgrade from V3.0)			
CTI Member	\$ 25		
Non-member	\$ 40		
Shipping for Flash Drive (from Texas): <i>Priority mail \$6; 2nd Day Air \$18; Overnight Domestic \$28; / International (DHL) TBA</i>			

System Requirements:
 Microsoft Windows®
 95/98, 2000, XP, and
 Windows 10



Multi-user site licenses and educational institution pricing available on request

Phone: 281.583.4087
 Fax: 281.537.1721
 Web: <http://www.cti.org>



Cooling Technology Institute Sound Testing



Cooling towers are used extensively wherever water is used as a cooling medium or process fluid, ranging from HVAC to a natural draft cooling tower on a power plant. Sound emanating from a cooling tower is a factor in the surrounding environment and limits on those sound levels, and quality, are frequently specified and dictated in project specifications. The project specifications are expected to conform to local building codes or safety standards. Consequently, it may be in the interest of the cooling tower purchaser to contract for field sound testing per CTI ATC-128 in order to insure compliance with specification requirements associated with cooling tower sound.

Licensed CTI SoundTesting Agencies

Clean Air Engineering
 7936 Conner Rd
 Powell, TN 37849
 800.208.6162 or 865.938.7555
 Fax 865.938.7569
 www.cleanair.com
 khennon@cleanair.com
Contact: Kenneth (Ken) Hennon

McHale Performance
 4700 Coster Rd
 Knoxville, TN 37912
 865.588.2654
 Fax 865.934.4779
 www.mchaleperformance.com
 jacob.faulkner@mchaleperformance.com
Contact: Jacob Faulkner

Cooling Technology Institute Certification Program STD-201 for Thermal Performance



As stated in its opening paragraph, CTI Standard 201... "sets forth a program whereby the Cooling Technology Institute will certify that all models of a line of water cooling towers offered for sale by a specific Manufacturer will perform thermally in accordance with the Manufacturer's published ratings..." By the purchase of a "certified" model, the User has assurance that the tower will perform as specified, provided that its circulating water is no more than acceptably contaminated-and that its air supply is ample and unobstructed. Either that model, or one of its close design family members, will have been thoroughly tested by the single CTI-licensed testing agency for Certification and found to perform as claimed by the Manufacturer.

CTI Certification under STD-201 is limited to thermal operating conditions with entering wet bulb temperatures between 12.8°C and 32.2°C (55°F to 90°F), a maximum process fluid temperature of 51.7°C (125°F), a cooling range of 2.2°C (4°F) or greater, and a cooling approach of 2.8°C (5°F) or greater. The manufacturer may set more restrictive limits if desired or publish less restrictive limits if the CTI limits are clearly defined and noted in the publication.

Those Manufacturers who have not yet chosen to certify their product lines are invited to do so at the earliest opportunity. You can contact Virginia A. Manser, Cooling Technology Institute at 281.583.4087, or vmanser.cti.org or PO Box 681807, Houston, TX 77268 for further information

Licensed CTI Thermal Certification Agencies

Agency Name / Address	Contact Person / Website / Email	Telephone / Fax
Clean Air Engineering 7936 Conner Rd Powell, TN 37849	Kenneth (Ken) Hennon www.cleanair.com khennon@cleanair.com	800.208.6162 or 865.938.7555 (F) 865.938.7569
Cooling Tower Test Associates, Inc. 15325 Melrose Dr. Stanley, KS 66221	Thomas E. (Tom) Weast www.cttai.com cttakc@aol.com	913.681.0027 (F) 913.681.0039
Cooling Tower Technologies Pty Ltd PO Box N157 Bexley North NSW 2207 Australia	Ronald Rayner coolingtwrtech@bigpond.com	+61.2.9789.5900 +61.2.9789.5922
DMT Gmbh & Co. KG Am Technologiepark 1 45307 Essen, Germany	Dr. Ing. Meinolf Gringel www.dmt-group.de meinolf.gringel@dmt-group.de	+49.201.172.1164
McHale Performance 4700 Coster Rd Knoxville, TN 37912	Jacob Faulkner www.mchaleperformance.com ctitesting@mchaleperformance.com	865.588.2654 (F) 865.934.4779



Cooling Technology Institute Licensed Testing Agencies

For nearly thirty years, the Cooling Technology Institute has provided a truly independent, third party, thermal performance testing service to the cooling tower industry. In 1995, the CTI also began providing an independent, third party, drift performance testing service as well. Both these services are administered through the CTI Multi-Agency Tower Performance Test Program and provide comparisons of the actual operating performance of a specific tower installation to the design performance. By providing such information on a specific tower installation, the CTI Multi-Agency Testing Program stands in contrast to the CTI Cooling Tower Certification Program which certifies all models of a specific manufacturer's line of cooling towers perform in accordance with their published thermal ratings.

To be licensed as a CTI Cooling Tower Performance Test Agency, the agency must pass a rigorous screening process and demonstrate

a high level of technical expertise. Additionally, it must have a sufficient number of test instruments, all meeting rigid requirements for accuracy and calibration.

Once licensed, the Test Agencies for both thermal and drift testing must operate in full compliance with the provisions of the CTI License Agreements and Testing Manuals which were developed by a panel of testing experts specifically for this program. Included in these requirements are strict guidelines regarding conflict of interest to insure CTI Tests are conducted in a fair, unbiased manner.

Cooling tower owners and manufacturers are strongly encouraged to utilize the services of the licensed CTI Cooling Tower Performance Test Agencies. The currently licensed agencies are listed below.



Licensed CTI Thermal Testing Agencies

*License Type A, B**

Clean Air Engineering

7936 Conner Rd, Powell, TN 37849

800.208.6162 or 865.938.7555

Fax 865.938.7569

www.cleanair.com / khennon@cleanair.com

Contact: Kenneth (Ken) Hennon

Cooling Tower Technologies Pty Ltd

PO Box N157, Bexley North, NSW 2207

AUSTRALIA

+61.2.9789.5900 / (F) +61.2.9789.5922

coolingtwrtech@bigpond.com

Contact: Ronald Rayner

Cooling Tower Test Associates, Inc.

15325 Melrose Dr., Stanley, KS 66221

913.681.0027 / (F) 913.681.0039

www.cttai.com / cttakc@aol.com

Contact: Thomas E. (Tom) West

DMT GmbH & Co. KG

Plant & Product Safety division

Am Technologiepark 1, 45307 Essen, Germany

+49.201.172.1164

www.dmt-group.de / meinolf.gringel@dmt-group.com

Dr. -Ing. Meinolf Gringel

McHale Performance

4700 Coster Rd, Knoxville, TN 37912

856.588.2654 / (F) 865.934.4779

www.mchaleperformance.com

ctitesting@mchaleperformance.com

Contact: Jacob Faulkner



Licensed CTI Drift Testing Agencies

Clean Air Engineering

7936 Conner Rd, Powell, TN 37849

800.208.6162 or 865.938.7555

Fax 865.938.7569

www.cleanair.com / khennon@cleanair.com

Contact: Kenneth (Ken) Hennon

McHale Performance

4700 Coster Rd, Knoxville, TN 37912

856.588.2654 / (F) 865.934.4779

www.mchaleperformance.com

ctitesting@mchaleperformance.com

Contact: Jacob Faulkner

* Type A license is for the use of mercury in glass thermometers typically used for smaller towers.

Type B license is for the use of remote data acquisition devices which can accommodate multiple measurement locations required by larger towers.

Cooling Towers Certified by CTI Under STD-201

As stated in its opening paragraph, CTI Standard STD-201 "...sets forth a program whereby the Cooling Technology Institute will certify that all models of a line of evaporative heat rejection equipment offered for sale by a specific Manufacturer will perform thermally in accordance with the Manufacturer's published ratings..."

By the purchase of a **CTI Certified** model, the Owner/Operator has assurance that the tower will perform as specified*.

**Performance as specified when the circulating water temperature is within acceptable limits and the air supply is ample and unobstructed. CTI Certification under STD-201 is limited to thermal operating conditions with entering wet bulb temperatures between 10°C and 32.2°C (50°F to 90°F), a maximum process fluid temperature of 51.7°C (125°F), a cooling range of 2.2°C (4°F) or greater, and a cooling approach of 2.8°C (5°F) or greater. The manufacturer may set more restrictive limits if desired or publish less restrictive limits if the CTI limits are clearly defined and noted in the publication.*



For each certified line, all models have undergone a technical review for design consistency and rated performance. One or more representative models of each certified line have been thoroughly tested by a CTI Licensed testing agency for certification and found to perform as claimed by the Manufacturer.

The CTI STD-201 Thermal Performance Certification Program has grown rapidly since its' inception in 1983 (see graphs that follow). A total of 61 cooling tower manufacturers are currently active in the program. In addition, 11 of the manufacturers also market products as private brands through other companies.

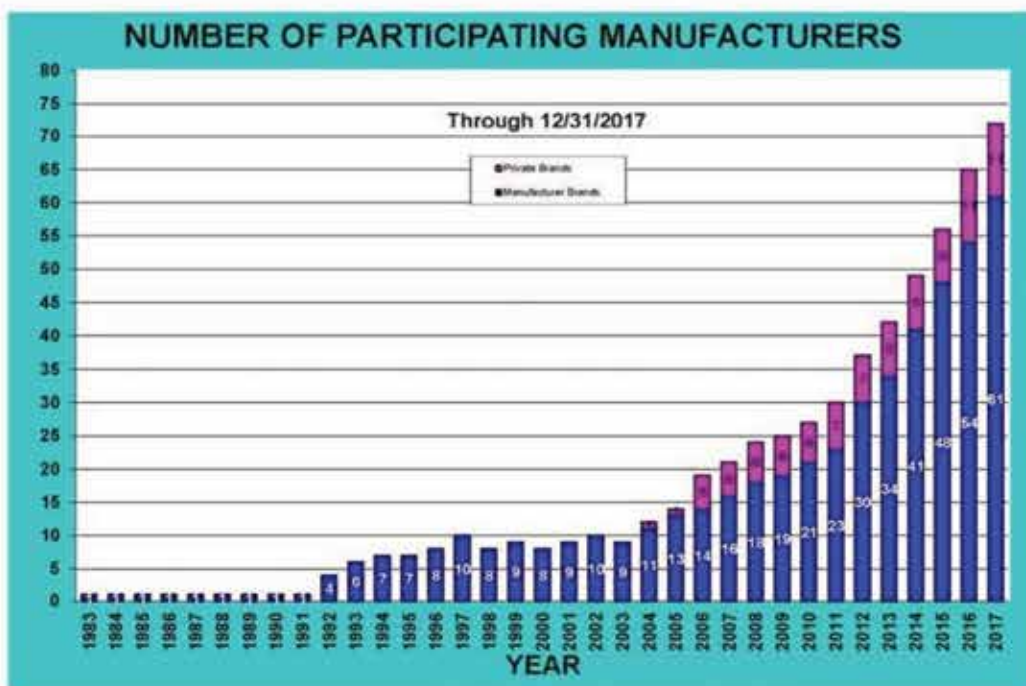
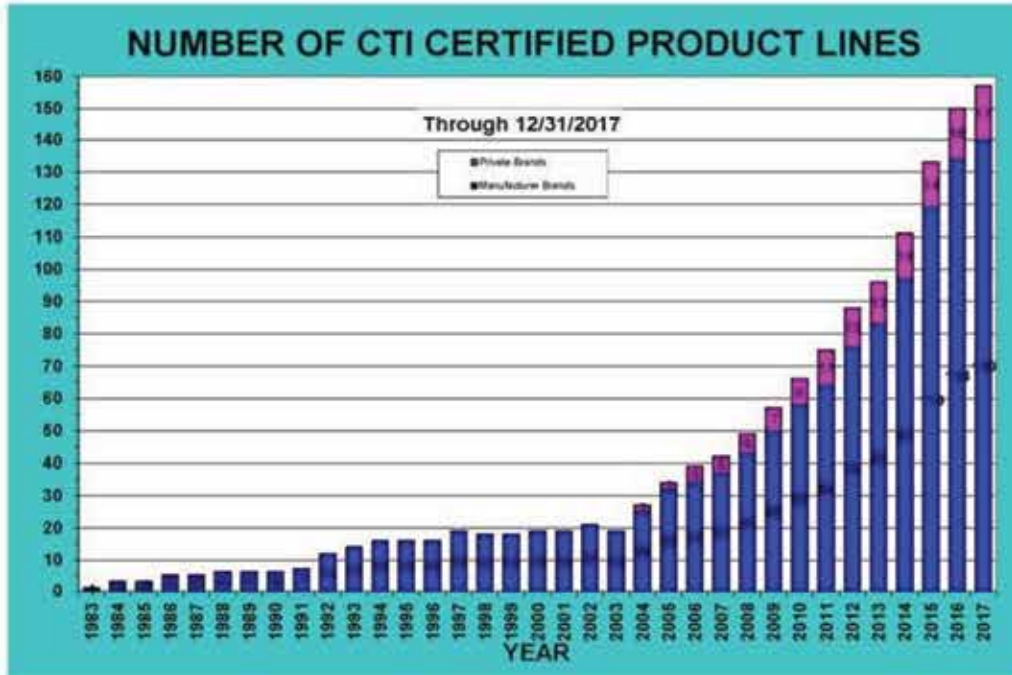
While in competition with each other, these manufacturers benefit from knowing that they each achieve their published performance capability and distinguish themselves by providing the Owner/Operator's required thermal performance. The participating manufacturers currently have 140 certified product lines plus 17 product lines marketed as private brands which result in approximately 32,000 CTI Certified cooling tower models to select from.

For a complete listing of certified product lines, and listings of all CTI Certified models, please see:

<http://www.cti.org/certification.php>

Those Manufacturers who have not yet chosen to certify their product lines are invited to do so at the earliest opportunity. Contact the CTI Administrator at vmanser@cti.org for more details.

Thermal Performance Certification Program Participation Through December 31, 2017



Current Program Participants

(as of December 31, 2017)

Program Participants and their certified product lines are listed below. Only the product lines listed here have achieved CTI STD-201 certification. For the most up-to-date information and a complete listing of all CTI Certified models please visit:

<http://www.cti.org/certification.php>

Current Certified Model Lists are available by clicking on the individual line names beneath the Participating Manufacturer name.

Catalog information and product selection data are also available by clicking on the links beneath each listed line.

A

Advance GRP Cooling Towers, Pvt.,Ltd.

Advance 2020 Series A Validation No. C31A-07R03

Aggreko Cooling Tower Services

AG Line Validation No. C34A-08R02

Amcot Cooling Tower Corp.

Series R-LC Validation No. C11E-11R02

AONE E&C Corporation, Ltd.

ACT-C Line Validation No. C28B-09R01

ACT-R/ACT-RU Line Validation No. C28A-05R04

Approach Engineering Co., Ltd.

NS Line Validation No. C76A-16R00

Axima (China) Energy Technology Co., Ltd.

EWX Line Validation No. C72A-15R02

EWK Line Validation No. C72C-17R00

ACC Line Validation No. C72B-15R01

B

Baltimore Aircoil Company, Inc.

FXT Line Validation No. C11A-92R02

FXV Line Validation No. C11J-98R10

PF Series Validation No. C11P-12R02

PT2 & PTE Series Validation No. C11L-07R05

Series V Closed VF1 & VFL Validation No. C11K-00R02

Series V Open VT0,VT1,VTL &VTL-E

Validation No. C11B-92R06

Series 1500 Validation No. C11H-94R09

Series 3000 A,C,D,E, Compass & Smart

Validation No. C11F-92R18

Bell Cooling Tower Pvt, Ltd

BCTI Line Validation No. C43A-12R02

C

CenK Endüstri Tesisleri Imalat Ve Taahüt A.Ş.

LEON Line Validation No. C89A-17R00

LISA Line Validation No. C89B-17R00

Cool Water Technologies

RTAi Line Validation No. C52A-13R02

RTi Line Validation No. C52B-13R01

Composite Cooling Solutions, Inc.

PLC Line Validation No. C79A-17R00

D

Delta Cooling Tower, Inc.

TM Series Validation No. 02-24-01

Decsa

RCC Series Validation No. C42C-14R00

TMA-EU Validation No. C42C-17R00

Dongguan Ryoden Cooling Equipment Co., Ltd

RT-L&U Series Validation No. C71A-15R02

RTM-L Series Validation No. C71B-15R00

E

Elendoo Technology (Beijing) Co., Ltd.

EL Line Validation No. C50C-15R02

ELN Line Validation No. C50D-17R00

ELOP Line Validation No. C50B-14R02

Ebara Refrigeration Equipment & Systems Co.

CDW Line *Validation No. C53A-13R03*

CXW Line *Validation No. C53B-14R01*

Evapco, Inc.

AT Series *Validation No. C13A-99R18*

ATWB Series *Validation No. C13F-09R08*

AXS Line *Validation No. C13K-15R03*

ESWA & ESWB Series *Validation No. C13E-06R09*

L Series Closed *Validation No. C13G-09R04*

L Series Open *Validation No. C13C-05R03*

G

Genius Cooling Tower Sdn Bhd

MT Series *Validation No. C67A-16R00*

MX Series *Validation No. C67B-16R00*

Guangdong Feiyang Industry Group Co., Ltd

LK Line *Validation No. C77A-17R00*

Guangdong Zhaorin Industrial Co., Ltd

SRN Series *Validation No. C95A-17R00*

Guangzhou Goaland Energy Conservation Tech Co., Ltd.

GLH Series *Validation No. C96A-17R00*

GLN Series *Validation No. C96B-17R00*

Guangzhou Laxun Technology Exploit Company, Ltd.

HMK Line *Validation No. C45A-12R04*

LMB Line *Validation No. 12-45-02*

PL Line *Validation No. C45E-16R01*

LC Line *Validation No. C45F-16R00*

PG Line *Validation No. C45G-17R00*

Guntner U.S. LLC

ECOSS Line *Validation No. C84A-17R00*

H

Hon Ming (Guang Dong) Air Conditioning Equipment Company, Ltd.

MK Series *Validation No. C66A-15R02*

Hunan Yuanheng Technology Company, Ltd.

YHA Line *Validation No. C40A-11R03*

YHD Line *Validation No. C40B-15R00*

YCF-H Line *Validation No. C40C-16R00*

HVAC/R International, Inc.

Therflow Series TFC *Validation No. C28B-09R01*

Therflow Series TFW *Validation No. C28A-05R04*

I

Industrial Mexicana, S.A. de C.V.

Series 1000 *Validation No. C60A-15R00*

Series 2000 *Validation No. C60B-16R00*

Series 6000 *Validation No. C60C-15R00*

J

Jacir

KS Line *Validation No. 12-46-01*

KSF Line *Validation No. C46B-15R00*

VAP Line *Validation No. C46C-16R00*

Jiangxi Ark Fluid Science Technology Co., Ltd.

FKH Line *Validation No. C83A-17R00*

Jiangsu Dayang Cooling Tower Co., Ltd.

HLT Line *Validation No. C94A-14R02*

Jiangsu i-Tower Cooling Technology Co., Ltd.

TMH Series *Validation No. C75A-16R00*

REH Series *Validation No. C75B-16R00*

Ji'Nan Chin-Tech Thermal Technology Co., Ltd.

CTNX Line *Validation No. C91D-16R00*

CTHX Line *Validation No. C91E-16R00*

K

Kelvion B.V.

Polacel CF Series *Validation No. C25A-04R02*

Polacel XF Series *Validation No. 13-25-02*

KIMCO (Kyung In Machinery Company, Ltd.)

CKL Line *Validation No. C18B-05R03*

Endura Cool Line *Validation No. C18A-93R08*

King Sun Industry Company, Ltd.

HKB Line *Validation No. C35A-09R04*

HKD Line *Validation No. C35B-09R04*

KC Line *Validation No. C35-11R01*

KFT Line *Validation No. C35D-16R00*

Korytko Systems, Ltd.

KDI Line *Validation No. C70A-16R01*

Kuken Cooling Tower Co.,Ltd.

GXE Series *Validation No. C81A-16R00*

GXC Series *Validation No. C81B-16R00*

L

Liang Chi Industry Company, Ltd.

Series C-LC *Validation No. C20B-09R02*

Series D-LC *Validation No. C20F-14R02*

Series R-LC *Validation No. C11E-11R03*

Series U-LC *Validation No. C20D-10R04*



Liang Chi Industry Company, Ltd. (con't)

Series V-LC *Validation No. C20C-10R01*

LCTR Line *Validation No. C20H-17R00*

TLC Line *Validation No. C20G-16R00*

M

Marley (SPX Cooling Technologies)

Aquatower Series *Validation No. 01-14-05*

AV Series *Validation No. C14D-98R03*

MCW Series *Validation No. 06-14-08*

MD Series *Validation No. C14L-08R04*

MHF Series *Validation No. C14G-04R08*

NC Series *Validation No. C14A-92R20*

Quadraflow Line *Validation No. 92-14-02*

NX Series *Validation No. C14M-15R01*

DTW Series *Validation No. C14N-16R01*

LW Series *Validation No. C14P-16R01*

Mesan Cooling Tower, Ltd.

MCC Series *Validation No. C26G-12R03*

MFD Series *Validation No. C26J-16R01*

MXC Series *Validation No. C26H-12R01*

MXR-KM, MXL, MXH Series *Validation No. C26C-08R08*

MITA S.r.l.

PM Series *Validation No. C56B-16R00*

N

NIBA Su Sogutma Kulerleri San, ve Tic, A.S.

HMP-NB Line *Validation No. C55A-14R00*

Nihon Spindle Manufacturing Company, Ltd.

KG Line *Validation No. C33B-12R04*

O

OTT Company, Ltd.

OTTC Line *Validation No. C44A-12R02*

OTTX Line *Validation No. 12-44-02*

OTTC-C Line *Validation No. C44C-14R00*

OTTX-C Line *Validation No. C44D-14R00*

Ocean Cooling Tower Sdn Bhd

YC Series *Validation No. C86A-17R00*

P

Paharpur Cooling Tower, Ltd.

CF3 Line *Validation No. C51A-13R01*

OXF-30K Line *Validation No. C51B-14R00*

Protec Cooling Towers, Inc.

FRS Series *Validation No. 05-27-03*

FWS Series *Validation No. 04-27-01*

Q

Qingdao VOFAT Air Conditioning Equipment Co., Ltd.

MF Series *Validation No. C82A-16R00*

R

Reymisa Cooling Towers, Inc. (Fabrica Mexicana de Torres, SA de CV)

HFC Line *Validation No. C22F-10R4*

RT & RTM Series *Validation No. C22G-13R04*

Rosemex, Inc.

RC (RSC/D) Series *Validation No. C54A-13R03*

RO (ROS/D) Series *Validation No. C94A-14R02*

RSD Cooling Towers

RSS Series *Validation No. 08-32-01*

Ryowo (Holding) Company, Ltd.

FCS Series *Validation No. 10-27-04*

FRS Series *Validation No. 05-27-03*

FVS Series *Validation No. 12-27-06*

FWS Series *Validation No. 04-27-01*

S

Shangdong Grad Group Co., Ltd.

GAT Series *Validation No. C88A-17R00*

Shanghai ACE Cooling Refrigeration Technology Col, Ltd.

AC Line *Validation No. C80A-17R00*

Shanghai Baofeng Machinery Manufacturing Co., Ltd.

BTC Line *Validation No. C49A-12R01*

Shanghai Liang Chi Cooling Equipment Co., Ltd.

LCM Line *Validation No. C62A-14R00*

LNCM Line *Validation No. C62B-16R00*

LRS Line *Validation No. C62C-16R00*

Shanghai Wanxiang Cooling Equipment Co., Ltd.

FBH/HL Line *Validation No. C54A-13R03*

FKH/FKHL Series *Validation No. C94A-14R02*

Sinro Air-Conditioning (Fogang) Company, Ltd.

CEF-A Line *Validation No. C37B-11R02*

Sung Ji Air-Conditioning Technology Co., Ltd.

SJMO Series *Validation No. C74A-16R00*

SJCO Series *Validation No. C74B-16R00*

T

Ta Shin F.R.P. Company, Ltd.

TSS Series *Validation No. 08-32-01*

The Cooling Tower Company, L.C

Series TCIA *Validation No. C29B-15R00*

Thermal-Cell sdn bhd

TYH Line *Validation No. C40A-11R03*

Tower Tech, Inc. a div. of CPK Manufacturing, LLC

TTXL Line *Validation No. C17F-08R04*

TTXR Line *Validation No. C17F-15R00*

Truwater Cooling Towers, Inc.

EC-S Series *Validation No. C41A-12R03*

EX-S Series *Validation No. C41B-12R04*

VXS Series *Validation No. C41C-13R01*

W

Wuxi Ark Fluid Science Technology Co., Ltd.

FBF Line *Validation C78A-16R00*

Wuxi Fangzhou Water Cooling Equipment Co., Ltd.

FKH Line *Validation C64A-14R00*

FNB Line *Validation C64B-15R01*

Y

York (By Johnson Controls)

AT Series *Validation No. C13A-99R18*

LSTE Line *Validation No. C13G-09R03*

Z

Zhejiang Dongjie Cooling Tower Co., Ltd.

DMNC Line *Validation No. C63A-15R00*

DHC Line *Validation No. C63B-15R00*

Zhejiang Haicold Cooling Technology Co., Ltd

SF Line *Validation No. C76A-16R00*

Zhejiang Jinling Refrigeration Engineering Co.,Ltd.

JFT Series *Validation No. C28C-16R00*

JNC Series *Validation No. C28B-09R01*

JNT Series *Validation No. C28A-05R04*

Zhejiang Shangfeng Cooling Tower Co., Ltd.

SFB Line *Validation No. C73A-15R01*

Zhejiang Wanxiang Science and Technology Company, Ltd.

WBH Line *Validation No. C96A-17R00*

WBN Line *Validation No. C96B-17R00*

Always look for the CTI Certified Label with Validation Number on Your Equipment



Index to Advertisers

Aggreko Cooling Tower Services	36-37
Amarillo Gear Company.....	IBC
Amarillo Gear Service	45
AMSA, Inc.	5
Arvind Composites.....	15
Bailsco Blades & Castings, Inc.....	6
Bedford Reinforced Plastics	41
Brentwood Industries	49
ChemTreat, Inc.....	3
CTI Certified Towers.....	66-71
CTI License Testing Agencies.....	64-65
CTI Owners/Operators.....	47
CTI Sound Testing/Thermal Performance	79
CTI ToolKit	62-63
Denso.....	43
Dynamic Fabricators	11
EvapTech, Inc.....	42
Fuel Ethanol	61
Hewitech.....	22
Hudson Products Corporation	IFC
IWC	57
KIMCO Cooling Towers	25
Kipcon	33
Midwest Cooling Towers	51
Mist Cooling.....	50
North Street Cooling Towers	53
OxiKing.....	56
PT,NTI Composites	14
Research Cottrell Cooling.....	2
Resolite.....	60
Rexnord Industries.....	17
C.E. Shepherd Company, LP	23
Simpson Strong-Tie	7
SPX Cooling Technologies.....	OBC
Tower Performance, Inc.....	29 & 72
Walchem (Iwaki America).....	19

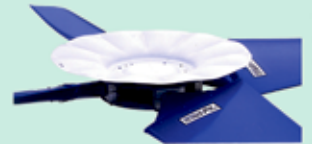
TPI Tower Performance, Inc. Cooling Tower Specialists

Since 1964, Tower Performance, Inc., has been providing full service to the utility, cogeneration, chemical, petrochemical, and related industries by constructing new cooling towers and upgrading and repairing all makes and models of existing cooling towers.



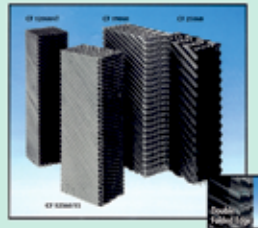
New Cooling Towers:

- Counterflow • Crossflow
- Wood • FRP



Professional Services Include:

- Cooling Tower Evaluations
- Bid Preparations • Wood Analysis
- Thermal Engineering



Field Services Include:

- Repair & Overhaul
- Scheduled Maintenance
- Inspection & Evaluations
- Emergency Service



Nationwide Service

New Jersey Office:

Toll Free: (800) 631-1196
 NJ: (973) 966-1116
 NY: (212) 355-0746
 Fax: (973) 966-5122

Arkansas Office:

Ph: (504) 236-3629
 Fax: (870) 862-2810
 E-Mail ctowers@tpila.com

Pennsylvania Office:

Ph: (215) 778-6027
 Fax: (215) 938-8900
 E-Mail smorris@towerperformance.com

E-Mail: stefanguetzov@towerperformance.com

Parts Sales:

Toll Free: (800) 314-1695
 Ph: (970) 593-8637
 Fax: (970) 472-1304

E-Mail: jfritz@towerperformance.com



Texas Office:

Toll Free: (800) 324-0691
 Ph: (713) 643-0691
 Fax: (713) 643-0310

E-Mail: ctowers@tpitx.com



OVER 100 YEARS QUALITY BUILT HERE

AMARILLO[®]

Gear Company has built a worldwide reputation for building quality gear drives and composite drive shaft assemblies during its 95 year history. While others farm-out and piecemeal, Amarillo still designs and manufactures its gears and builds them in Amarillo, Texas.

Amarillo is ISO 9001:2008 quality certified and stands behind their extensive line of right angle spiral bevel cooling tower fan drives, including single and double reduction models.

They also 100% manufacture the high quality A Series drives for drop-in replacement of other manufacturer's models, complete with the backing of Amarillo's warranty.



Tested. Proven. Amarillo.[®]

Want to know more? Please contact our staff of sales representatives or gear engineers for a quick response to your fan drive needs.

www.amarillogear.com (806) 622-1273
info@amarillogear.com

Amarillo[™]
Gear
Company LLC



A Marmon Water/Berkshire Hathaway Company





HIGHEST COOLING CAPACITY

OF ANY COUNTERFLOW COOLING TOWER

IN THE WORLD*



MD EVEREST™

HIGHEST CAPACITY

The MD Everest tower offers greater than 85% more cooling capacity per cell compared with other preassembled counterflow towers. At 2500 tons, the MD Everest tower is an ideal one-to-one match for some of the largest chillers.

INSTALLATION SAVINGS

The MD Everest tower's design minimizes piping and electrical connections to reduce installation costs.

HIGHEST VALUE

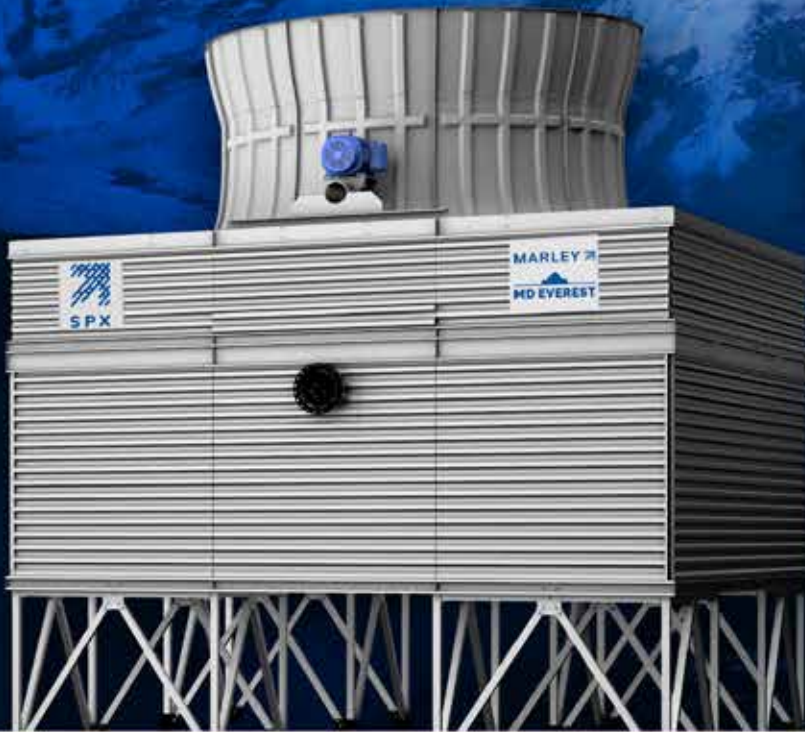
The MD Everest tower offers significant advantages compared with other counterflow towers, including unmatched cooling capacity, energy efficiency, fewer components, and lower maintenance costs.

LOWER DRIFT RATE

The MD Everest tower achieves a low drift rate, down to 0.0005 percent of circulating water flow, so less water escapes the tower.

FASTER DELIVERY & INSTALL

Compared with field-erected alternatives, the MD Everest tower delivers 60% sooner and installs 80% faster.



Take Cooling To A Higher Level – spxcooling.com/MDEverest

*Compared to other single-cell, pre-assembled counterflow cooling towers.

**Pending CTI final approval and notification.

COPYRIGHT © 2018 SPX Cooling Technologies, Inc. All rights reserved.



MARLEY®

